

# **Interface stability of granular filter structures**

**desk study**

Henk Verheij, Gijs Hoffmans, Henk den Adel and Gert Jan Akkerman and Sanjay Giri



Prepared for:  
CUR Building & Infrastructure

# **Interface stability of granular filter structures**

**desk study**

Henk Verheij, Gijs Hoffmans, Henk den Adel and Gert Jan  
Akkerman and Sanjay Giri

Report

October 2009



<b>Client</b>	CUR Building & Infrastructure						
<b>Title</b>	Interface stability of granular filter structures						
<b>Abstract</b>							
<p>A desk study has been carried out regarding interface stability of granular filter structures. Actually, the project focuses on two particular aspects:</p> <ul style="list-style-type: none"> <li>(1) interface stability as function of the thickness of the filter layer consisting of standard armourstone gradings, and</li> <li>(2) interface stability of gravel mixtures with a wide gradation</li> </ul> <p>The objective of the study is to present an overview of the existing design formulas for interface stability for the above mentioned aspects, including remarks which formulas need improvement or are even missing. On the basis of the inventory recommendations are presented for future research including a list of priorities and quick wins.</p> <p>First, an overview of the existing filter criteria has been made. Secondly, a new formula has been derived. The formula includes the influence of the grading width as well as interface stability as a function of filter layer thickness. It is recommended to validate the new filter design formula in a hydraulic model.</p>							
<b>References</b>			CUR order 6401 dated March 19, 2008-09-04 (proposal ZWS29497/Q4541.95/up dated January 31, 2008) and June 2009				
Ver	Author	Date	Remarks	Review	Approved by		
5	Henk Verheij et al	19 October 2009	draft	Frans vd Knaap	T. Segeren		
<b>Project number</b>		1002029					
<b>Keywords</b>		granular filters, interface stability, armouring, internal stability					
<b>Number of pages</b>		96					
<b>Classification</b>		None					
<b>Status</b>		preliminary					



## Contents

### List of Symbols

<b>1</b>	<b>Introduction</b> .....	<b>1</b>
<b>2</b>	<b>Literature search</b> .....	<b>3</b>
2.1	Introduction.....	3
2.2	Permanent flow conditions.....	4
2.2.1	Traditional filter criteria.....	4
2.2.2	Hydrodynamically sand-tight filter criteria.....	5
2.2.3	Transport filters.....	7
2.3	Wide-graded filter material.....	9
2.4	Other hydraulic conditions.....	13
2.4.1	Non-permanent conditions.....	13
2.4.2	Wave conditions.....	13
<b>3</b>	<b>New granular filter criteria</b> .....	<b>17</b>
3.1	Introduction.....	17
3.2	Hydraulic principles and incipient motion.....	18
3.2.1	Turbulence.....	18
3.2.2	Flow in filters.....	20
3.2.3	Incipient motion.....	21
3.3	Derivation new criteria for interface stability of open granular filters.....	23
3.3.1	Introduction.....	23
3.3.2	Horizontal filters without bed turbulence.....	23
3.3.3	Horizontal filters influenced by bed turbulence.....	26
3.4	Sensitivity analysis.....	35
3.5	Conclusions and recommendations.....	47
<b>4</b>	<b>Overview of knowledge gaps and quick wins</b> .....	<b>48</b>
4.1	Summary of design methods.....	48
4.2	Knowledge gaps.....	50
4.2.1	Non-uniform flow.....	51
4.2.2	Wide-graded material.....	52
4.2.3	Damping of turbulence.....	52
4.3	Quick wins.....	52
4.4	Hydraulic modelling.....	53
4.5	Evaluation.....	53
4.6	Possible approach to estimate the thickness (reduction) of wide-graded layers.....	53

---

5	<b>QW-3: Adjustment of Wörman for a bed protection.....</b>	<b>57</b>
6	<b>QW-5: Design of a thick bed protection consisting of wide-graded material .....</b>	<b>62</b>
7	<b>Conclusions and recommendations.....</b>	<b>69</b>
8	<b>Literature.....</b>	<b>71</b>
	<b>Paper presented at the Fourth International Conference on Scour and Erosion, ICSE-4, Tokyo, 5-7<sup>th</sup> November 2008 .....</b>	<b>75</b>
	<b>REFERENCES.....</b>	<b>84</b>

## List of Symbols

Symbol	Unit	Description
$A$	$m^2$	cross section area of filter
$A_e$	$m^2$	erosion area
$a$	$s/m$	coefficient in Forchheimer equation
$b$	$s^2/m^2$	coefficient in Forchheimer equation
$C$	$m^{1/2}/s$	Chézy coefficient
$C_f$	$m^{1/2}/s$	coefficient representing the resistance in the filter layer
$C_i$	$m^2/s^2$	parameters
$C_0$	-	turbulence parameter
$C_U$	-	uniformity coefficient, $C_U = d_{60}/d_{10}$
$D$	$m$	resulting layer thickness
$D_F$	$m$	thickness of filter layer
$D_0$	$m$	initial layer thickness
$D_*$	-	dimensionless diameter $[= d_{50}(\Delta g/\nu^2)^{1/3}]$
$d_i$	-	particle diameter in the filter layer for which $i\%$ of the particles is finer than $d_i$ ,
$d_{pore}$	$m$	pore diameter
$d_{50}$	$m$	median particle diameter
$E_f$	$m^2/s^2$	mean turbulent kinetic energy in filter
$E_0$	$m^2/s^2$	depth-averaged turbulent kinetic energy
$e$	-	coefficient
$g$	$m/s^2$	acceleration due to gravity
$F_s$	$N/m$	seepage resistance per unit width
$G$	-	grading width, $G = d_{85}/d_{15}$
$H_{rms}$	$m$	root mean square wave height
$H_S$	$m$	significant wave height
$H_1$	$m$	flow level upstream of filter
$H_2$	$m$	flow level downstream of filter
$h$	$m$	water depth
$k$	$m/s$	permeability
$L$	$m$	length of the filter
$N_{od}$	-	stability number (number of displaced elements)
$N$	-	number of waves
$n$	-	porosity
$O$	-	order of magnitude
$P$	-	ratio $d_{90}/d_{10}$
$p_m$	$N/m^2$	pressure peak (or maximum under water pressure)
$Q$	$m^3/s$	discharge
$r_0$	-	relative depth-averaged turbulence intensity in channel flow
$r_{0,f}$	-	mean relative turbulence intensity in granular filter
$Re$	-	Reynolds number in open channel flow $[= RU_0/\nu]$
$Re_f$	-	Reynolds number in granular filter $[= d_{50} u_f/\nu]$
$R_h$	-	hydraulic radius
$S$	-	mean energy slope $[= (H_1 - H_2)/L]$
$S_b$	-	bed slope
$S_{rms}$	-	root mean square value of the gradient parallel to the slope
$T$	$s$	wave period at the toe of the structure

$u$	m/s	flow velocity
$u_b$	m/s	velocity in the base material
$u_{bf}$	m/s	velocity at the transition of filter and base material
$u_f$	m/s	filter velocity
$u_s$	m/s	filter velocity at $z = D_F$ (at the transition with the flow)
$u^*$	m/s	bed shear velocity
$u^*,bf$	m/s	shear velocity at transition of filter and base layer
$U_0$	m/s	depth-averaged flow velocity
$v_p$	m/s	velocity of the particles in the pores
$V_G$	-	variation coefficient representing the non-uniformity of the filter material
$V_0$	-	variation coefficient representing the bed turbulence in uniform flow
$z$	m	vertical co-ordinate
$\alpha_i$	-	coefficient
$\alpha_{lam}$	$s^2/m^2$	coefficient
$\alpha_{tur}$	$s^2/m^2$	coefficient
$\gamma$	-	transport parameter
$\Delta$	-	under water relative density [ $=\rho_s/\rho - 1$ ]
$\xi$	-	damping parameter
$\zeta$	-	ratio between measurements and calculations
$\eta$	-	turbulence parameter
$\kappa$	-	constant of Von Kármán
$\mu$	-	average value in a Gaussian distribution
$\mu$	-	number of particles at rest (in a transport filter approach)
$\nu$	$m^2/s$	kinematic viscosity
$\nu$	$s^{-1}$	frequency
$\nu_1$	$s^{-1}$	probability per second to bring in motion an individual particle
$\nu_t$	$m^2/s$	turbulent viscosity (or eddy viscosity)
$\rho$	-	total number of particles (in a transport filter approach)
$\rho$	$kg/m^3$	density of water
$\rho_s$	$kg/m^3$	density of sediment
$\sigma_G$	$N/m^2$	standard deviation of the critical instantaneous bed shear stress
$\sigma_0$	$N/m^2$	standard deviation of the instantaneous bed shear stress
$\tau'$	$N/m^2$	instantaneous bed shear stress
$\tau_{bf}$	$N/m^2$	mean shear stress at the transition of the filter-base layer
$\tau_c$	$N/m^2$	critical mean bed shear stress according to Rouse
$\tau_{c,k}$	$N/m^2$	critical characteristic shear stress in filter
$\tau_f$	$N/m^2$	mean shear stress in granular filter
$\tau_G$	$N/m^2$	critical mean bed shear stress according to Grass
$\tau_{G,k}$	$N/m^2$	critical characteristic bed shear stress
$\tau_k$	$N/m^2$	characteristic shear stress in filter
$\tau_m$	$N/m^2$	maximum bed shear stress
$\tau_0$	$N/m^2$	mean bed shear stress
$\tau_{0,k}$	$N/m^2$	characteristic bed shear stress
$\chi$	-	damping parameter

$\psi$	-	Shields parameter
Subscripts		
$b$	-	base layer
$c$	-	critical
$f$	-	filter layer
$lam$	-	laminar
$tur$	-	turbulent



# 1 Introduction

On March 19, 2008 CUR Building & Infrastructure commissioned Deltares to carry out a desk study regarding interface stability of granular filter structures. Actually, the project focuses on two particular aspects of the interface between filter layer and base material:

- (1) interface stability as function of the thickness of the filter layer consisting of standard armourstone gradings, and
- (2) interface stability of gravel mixtures with a wide gradation.

The reason for the study is two-fold:

- In the past many protective structures have been built using granular material, for example around bridge piers and spur dikes. In general, the structures consist of one or more layers. The filter structure should prevent erosion of base material and, therefore, sand tightness is required. This means that the internal stability (within the filter layer) as well as the interface stability (at the interfaces between the layers) has to be guaranteed. Due to larger design loads than assumed in the past, the interface stability is in some instances no longer guaranteed. Increasing the layer thickness might solve this problem.
- Large amounts of wide-graded gravel mixtures will become available on the market in the near future because of various projects in the flood plains of rivers. These mixtures may be useful to be applied in (bed) protection structures. However, the strength against currents is known insufficiently, viz in the armouring phenomenon in relation to the layer thickness.

For both typical situations it is assumed that the resistance of the material in the top layer – i.e. the armour layer stability – against the erosive forces of the flow velocities is sufficient.

The objective of the study is to present an overview of the existing design formulas for interface stability for the above mentioned aspects, including remarks which formulas need improvement or are even missing. On the basis of the inventory recommendations are presented for future research including a list of priorities and quick wins.

The approach is as follows:

1. **Overview of existing and derivation of new design formulas for interface stability**  
The emphasis is on formulas for permanent current attack, however, formulas for non-permanent and short term hydraulic attack (e.g. by propeller jets), wave attack (on offshore structures, breakwaters) and transport filters are mentioned. Obviously, the applicability ranges of the formulas are mentioned.
2. **Determination of priorities and quick wins for design formulas for permanent current attack**

The study was carried out by Mr. Henk Verheij, dr. Gijs Hoffmans and dr. Henk den Adel of Deltares, and Mr. Gert Jan Akkerman of Royal Haskoning. Mr. Henk Verheij was responsible for the project management.

Mr. Frans van der Knaap of Deltares was responsible for the QA.



## 2 Literature search

### 2.1 Introduction

Literature has been searched for:

- (1) permanent flow conditions
  - a geometrically-closed and open filters and transport filters (section 2.2)
  - b wide-graded filters (section 2.3)
- (2) other hydraulic conditions (section 2.4)
  - a non-permanent and short duration hydraulic loads
  - b waves

Starting point for the literature search are the CUR report 161 “Filters in de Waterbouw” (CUR, 1993) and the paper by Hoffmans, Den Adel and Verheij “Shear stress concept in granular filters” presented in Melbourne (Hoffmans et al, 2000).

The following types of filters can be distinguished (based on the two criteria enabling erosion: (1) Base material can pass the pores in the filter material, and (2) Hydraulic load is higher than threshold value):

- *Geometrically closed (sand-tight)* filters: no transport of base material is possible
- *Stable Geometrically-open sand-tight* filters, also called hydrodynamically sand tight filters: the hydraulic load is less than the threshold value
- *Instable Geometrically-open or transport filters*: the hydraulic load is occasionally larger than the threshold value

Note: the design method for transport filters differs from that for the other two. Relevant is the total amount of eroded material as function of the hydraulic load (duration and magnitude) during the life time of the filter structure.

In Figure 2.1 definitions are presented.

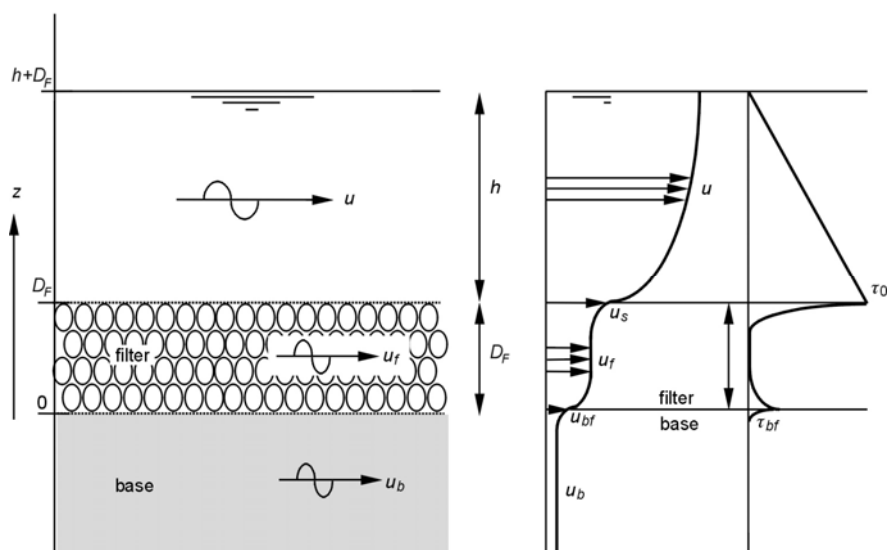


Figure 2.1 Overview of definitions for a one-layer filter structure

## 2.2 Permanent flow conditions

### 2.2.1 Traditional filter criteria

#### *General*

The requirements of granular filters are four-fold. First, the filter layer material that covers the base material should be sufficiently fine to control erosion of the base layer. Secondly, both the filter and the base layer should be permeable enough to permit adequate drainage of seepage water. Thirdly both the filter and base layer should be internally stable to avoid suffusion or internal erosion (e.g. washing out of the finer particles through the voids associated with the larger ones) and to eliminate the occurrence of piping and heave. Finally, granular filters must be installed in accordance with the practical requirements regarding the layer thickness.

#### *Retention criterion*

The eroded material of the base layer passes through the filter layer either by outgoing flow perpendicular to the filter-base interface or by flow parallel to the interface. Particles that are transported by seepage flow between the larger particles in the filter may be washed out. Retention criteria in engineering practice are based on experiments performed with various combinations of filter and base materials. Based on Bertram's experiments with nearly uniformly graded filter materials and vertical flow, Terzaghi and Peck (1948) specified:

$$d_{f15} / d_{b85} < 4 \quad (2.1)$$

where  $d_{f15}$  is the particle (or grain) diameter in the filter layer for which 15% of the mass of the particles is smaller than  $d_{f15}$  [m],  $d_{b85}$  is the particle (or sand) diameter in the base layer for which 85% of the mass of the particles is smaller than  $d_{b85}$  [m]. The U.S. Army Corps of Engineers (Heibaum, 2004) performed tests with narrowly graded sand and grain size distributions for the filters (defined as  $p < 5$  with  $p = d_{90}/d_{10}$ ). Based on these experiments, the following criteria have been developed:

$$d_{f15} / d_{b85} < 5 \quad (2.2)$$

$$d_{f50} / d_{b50} < 25 \quad (2.3)$$

where  $d_{f50}$  and  $d_{b50}$  are the median particle sizes of the filter and base layer respectively [m].

#### *Permeability criterion*

Progressive accumulation of fines in the pores of a filter layer leads to clogging, which may lead to instability of the protection layers caused by uplifting. If the thickness of the filter and base layer is decreased by erosion, settlement of the filter structure occurs with local differences in the level of the top layer and as a consequence of these differential settlement local scour might occur. To reduce the load across the filter layer and thus to prevent uplifting this layer should be sufficiently permeable. An accepted permeability criterion originally derived for vertical flow direction is (Terzaghi and Peck, 1948):

$$d_{f15} / d_{b15} > 4 \quad (2.4)$$

Equation 2.4 is valid for uniform filter and base materials. For materials where filter and base material have approximately the same  $d_{15}$ , the filter may thus be prone to clogging in the long term.

It should be noted here that uplifting may be prevented then by applying a sufficiently thick filter layer.

#### *Internal stability criterion*

Suffusion or internal erosion occurs in filters that are internally unstable. Such filters typically have a wide gradation ( $d_{60}/d_{10} > 6$ ) and may result in washout of finer particles by seepage or turbulent flow. The criteria for internal stability for vertical flow in the direction of gravity are (Kenney and Lau, 1985):

$$d_{10}/d_5 < 4 \quad \text{and} \quad d_{20}/d_{10} < 4 \quad \text{and} \quad d_{30}/d_{15} < 4 \quad \text{and} \quad d_{40}/d_{20} < 4 \quad (2.5)$$

Internal erosion results in compaction and is less likely to lead to a rapid failure, than piping and heave. Piping starts at the exit point of seepage and develops in the base layer by backward erosion. When the pipe reaches approximately halfway the seepage length a sudden breakthrough may occur (Sellmeijer 1988). Heave is defined as the situation in which vertical effective stresses in the base layer fall away under the influence of vertical groundwater flow, also called fluidisation or the forming of quicksand.

#### *Filter thickness*

To be practically effective, filter layers should have a minimum thickness of at least two to three times the diameter of the larger particles of the base layer. For controlled construction the thickness of a gravel filter layer should be at least 0.20 m, and sand filter layers should be at least 0.10 m thick (Pilarczyk 1990, 1998). In underwater placement, to ensure that bed irregularities are completely covered, the thickness of the top layer should be at least two to three times the size of the larger particles used in the layer, but never less than 0.30 m thick.

### 2.2.2 Hydrodynamically sand-tight filter criteria

Hydrodynamically sand-tight filters, or geometrical-open sand-tight filters, are characterized by the condition that the hydraulic load is less than the threshold value. In other words: the strength is larger than the load, and consequently no erosion of base material will occur.

Bakker et al. (1994) discussed a filter model that includes near-bed pressure fluctuations:

$$\frac{d_{f15}}{d_{b50}} = \frac{2.2}{C_0 e^2} \frac{R_h}{d_{f50}} \frac{\Psi_{cb}}{\Psi_{cf}} \frac{\Delta_b}{\Delta_f} \quad (2.6)$$

where  $C_0$  is a turbulence coefficient [-] that varies from 6 (when using the time- and space-averaged bed shear stress  $\tau_0$ ) to 100 (when using the maximum bed shear stress  $\tau_m$ ) with a commonly applicable value of 15; the variable  $e$  [-] is a coefficient that takes into account the difference between the flow in granular filters and open channels (with an average value of  $e = 0.24$ );  $\Psi_{cb}$  and  $\Psi_{cf}$  are the critical Shields parameters for the base and the filter material respectively [-], and  $\Delta_b$  and  $\Delta_f$  are the relative density for the base and the filter material respectively [-].

Although the prediction capacity of Equation 2.6 is reasonable for the experiments investigated, this relationship is not useful for non-uniform flow conditions as it depends on the ratio  $R_f/d_{f50}$  with  $R_h$  is the hydraulic radius. The reason for this is that at locations with high turbulence, for example, downstream backward facing steps, the hydraulic radius is not the most appropriate parameter to take into account the correct flow conditions.

On the basis of Equation 2.6 a simplified design equation was recommended in CUR report 161 (CUR, 1993):

$$\frac{d_{f15}}{d_{b50}} = \frac{\alpha}{C_0} \frac{R_h}{d_{f50}} \tag{2.7}$$

Where  $\alpha = 9.5$  for base material with a  $d_{b50}$  in the range of 0.15 to 5 mm and  $\alpha = 19$  for base material with a  $d_{b50}$  larger than 5 mm, and  $C_0 \sim 15$ .

Hoffmans et al. (2000) discussed a shear stress approach in a horizontal one-layer filter with a thickness ( $D_F$ ) above the base material in open channel flow. Equations for granular filters based on the Navier Stokes equation for uniform flow, Forchheimer’s equation and the hypothesis of Boussinesq have been combined. The hypothesis of Grass has been used to analyse the influence of gradation and armouring in a qualitative way. Subsequently, the mean turbulence in granular filters has been discussed (Figure 2.2).

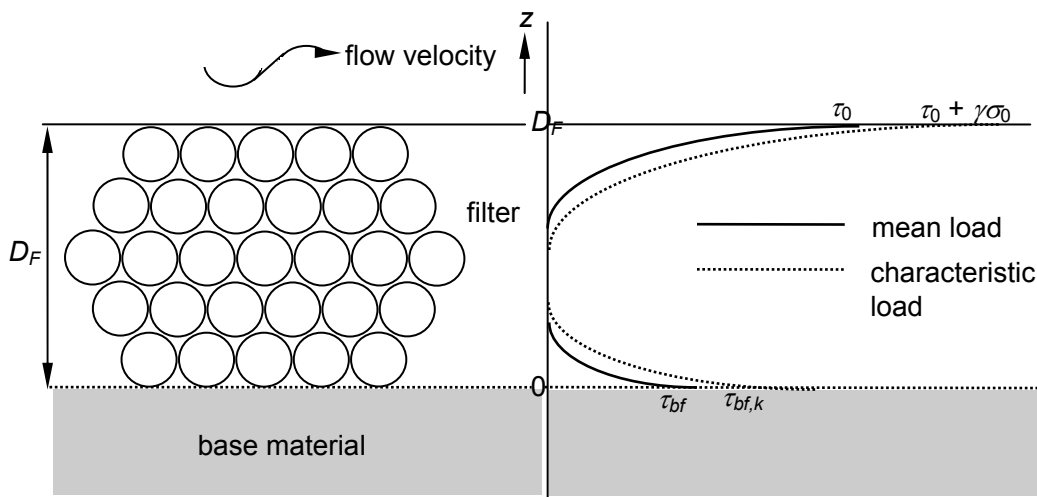


Fig. 2.2 Distribution of the mean and characteristic load

The paper by Hoffmans et al. (2000) is based on various desk studies at Delft Hydraulics in the period 1998 to 2000: Verheij (1999, 2000, 2003). It resulted for instance in an equation for the filter velocity  $u_f(z)$  (Verheij et al., 2000):

$$u_f(z) = \sqrt{C_1 e^{z\zeta} + C_2 e^{-z\zeta} + S_b/b} \tag{2.8}$$

where  $C_1 = \frac{(u_s^2 - S_b/b) - e^{-\zeta D_F} (u_{bf}^2 - S_b/b)}{(e^{\zeta D_F} - e^{-\zeta D_F})}$

$$C_2 = \frac{e^{\xi D_F} (u_{bf}^2 - S_b/b) - (u_s^2 - S_b/b)}{(e^{\xi D_F} - e^{-\xi D_F})}$$

$$\xi = \sqrt{\frac{2gb}{\alpha_v d_{f15}}} \approx \frac{5.5}{d_{f15}}$$

where  $u_s$  is the filter velocity at  $z = D_F$  [m/s];  $u_{bf}$  is the flow velocity at the transition between base and filter material [m/s],  $\alpha_v$  (= 0.9) is a coefficient,  $\xi$  is a damping factor [-],  $D_F$  is the filter thickness [m],  $C_1$  and  $C_2$  are parameters [-],  $S_b$  is the bed slope [-],  $b$  is a coefficient in the Forchheimer formula; and  $z$  is the vertical co-ordinate [m].

For non-uniform flow conditions at bridge piers Wörman (1989) has investigated granular filters. Based on accepted theories he arrived at the following relationship for a single layer bed protection:

$$\frac{D_F}{d_{f15}} = 0.16 \frac{\Delta_f}{\Delta_b} \frac{n_f}{1 - n_f} \frac{d_{f85}}{d_{b85}} \quad (2.9)$$

where  $n_f$  is the porosity of the filter material [-].

Note: In CUR report 161 an equation is presented with  $d_{f50}$  in stead of  $d_{f85}$ . Wörman used a factor 1.25 between the two characteristic diameters and applying this factor results in a coefficient with a value 0.133 or 1/7.5 as shown in CUR report 161.

Wenka et al (2007) carried out simultaneous pressure and 3D flow measurements in the pores of a granular layer. Filter thicknesses of 0.04 m, 0.1 m and 0.20 m with filter size  $d_{f50} = 10$  mm ( $d_{60}/d_{10} = 1.25$ ) and base material size  $d_{b50} = 1$  mm were tested with flow velocities in the range of 0.31 m/s to 0.86 m/s.

The data can be interesting for validating other formulas.

### 2.2.3 Transport filters

Transport filters are not subject of this study, but in short the principles will be explained. A more elaborate description of the model can be found in Den Adel et al (1994).

The transport model for filtration is a mathematical description of physical processes that occur in geometrically open filter structures. The model has been validated for water flow parallel to the interface between filter and base material. The model describes a bi-state situation: particles can be either at rest or moving.

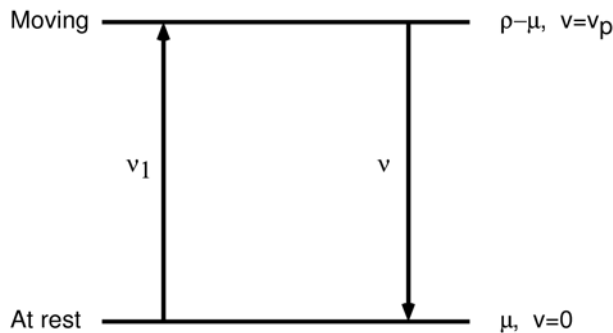


Figure 2.3 The basics of the transport model

The total number of particles is expressed by  $\rho$ , whereas  $\mu$  is the number of particles at rest. All moving particles are assumed to be in motion with the same velocity,  $v_p$ . Particles at rest can be brought into motion by hydraulic forces. Their corresponding frequency is  $\nu_1$ , see Figure 2.3. The frequency  $\nu$  describes the probability per second to stop moving particles. For geometrically open filters this frequency,  $\nu$ , is not that relevant, so can be neglected.

The frequency  $\nu_1$  – the probability per second to bring in motion an individual particle – consists of two parts: (i) the probability that a particle is brought in motion, and (ii) the conversion of this probability into a frequency [1/s]:

- (i) The first part describes the probability for a particle to be brought into motion. This probability is determined by the balance between strength of the particles and loading by the current. Both are considered to be probabilities, since the strength of the particles varies considerably; the same is true for the loading on the particles. Some particles are clamped between or shielded by other particles and are thus not exposed to the full extent of the loading. On the other hand, the water velocity in the filter varies with time and location. The resulting probability is determined by the material parameters of the base and filter (strength), the averaged value of the water velocity (loading) and a combined variance (strength and loading). The variance is found to be constant. The strength of the particles is converted into an effective water velocity at which ‘to some degree’ erosion will occur. The effective water velocity is directly related to the critical filter velocity as determined by Klein Breteler (1992).
- (ii) The second part converts the probability into a frequency. For this process a time scale is needed. The approach followed is to estimate the time scale of small vortices within the filter. This has led to a relationship that includes the particle size and the water velocity within the pores.

The model developed is therefore a combination of both loading and strength, each of which expressed in terms of frequency,  $\nu_1$  [1/s].

This model has been used to predict transport as measured in 3D laboratory experiments. The model has been validated for base material, ranging from fine sand (0.1 mm) to gravel (10 mm), and for filter material, ranging from fine gravel (2 mm) to boulders (300 mm).

Locke et al (2001) published also an article on time-dependent particle transport through granular filters for perpendicular flow. In their method a finite difference model is needed in order to make predictions. The ideas presented by Silveira (1965) formed the basis for the method proposed by Locke et al (2001). It should be noted that the Silveira method is sound, but incomplete. The model overestimates the amount of material transported.

Laboratory tests and simulations of these tests are similar to the results as obtained in the filter research program of Rijkswaterstaat.

The laboratory tests have been performed on coarse material: coarse sand (1 mm) and gravel (20 mm). The ratio  $F = d_{f15}/d_{b85}$  varied: 4, 7, 10 and 12. When  $F = 12$ , and the flow conditions are stronger than a certain threshold value, the vertical filter is (of course) not sufficient to retain the base material.

### 2.3 Wide-graded filter material

Based on practice two gradations or grading widths of filter material (and armour stone) are distinguished within the framework of granular filter structures:

standard gradation	$d_{85}/d_{15} < 2.5$
(wide) graded mixtures	$d_{85}/d_{15} > 2.5$

The standard grading width is in accordance with the European standard EN-13383 for armourstone. All recommended armourstone gradings show a grading width less than 2.01 (except for 45/180 mm).

In addition, it should be mentioned that gravel from the Meuse River can be characterised by a uniformity coefficient  $C_U$  ( $C_U = d_{60}/d_{10}$ ) of 6 to 10. This means that Meuse gravel belongs to the (wide) graded mixtures.

The Rock Manual gives a different definition for the gradations of material (CUR/CIRIA/CETMEF, 2007):

Narrow graded mixtures	$d_{85}/d_{15} < 1.5$
Wide graded mixtures	$1.5 < d_{85}/d_{15} < 2.5$
Very wide graded mixtures	$d_{85}/d_{15} > 2.5$

**Note:** The main reason to apply rather narrow-graded armourstone gradings in coastal engineering is the stability against waves: small stones in a very wide graded armour layer may result in 'rocking' and thus damage. According to the Rock Manual nearly all armourstone gradings belong to the wide-graded mixtures, except for the gradings larger than 40-200 kg.

In CUR report 161 (CUR, 1993) some remarks are made about wide-graded filters. For normally graded filter materials the pore diameter  $d_{pore}$  is about  $0.2 \cdot d_{f15}$  ( $d_{pore}$  is the characteristic diameter of the pores (m); for wide-graded soils the factor 0.2 decreases to for instance 0.1. In fact, the value of  $d_{pore}$  is not related anymore to  $d_{f15}$ , but to a smaller particle. A factor 0.1 means a geometrically sand tight criterion of  $d_{f15}/d_{b85} \leq 10$  instead of  $d_{f15}/d_{b85} \leq 5$  for normally graded filter materials. Thus, the existing criteria are too conservative for wide-graded filters.

In CUR report 161 it is recommended to apply filter thicknesses that are at least  $10 \cdot d_{f50}$ .

Heibaum (2004) has presented the German method for designing granular filters, see Figure 2.4. The method is applicable for both narrow-graded and wide-graded mixtures.

Note: A more commonly used definition of the gradation than the factor  $p = d_{90}/d_{10}$  is either the grading width (= gradation),  $G = d_{85}/d_{15}$ , or the coefficient of uniformity,  $C_U = d_{60}/d_{10}$ .

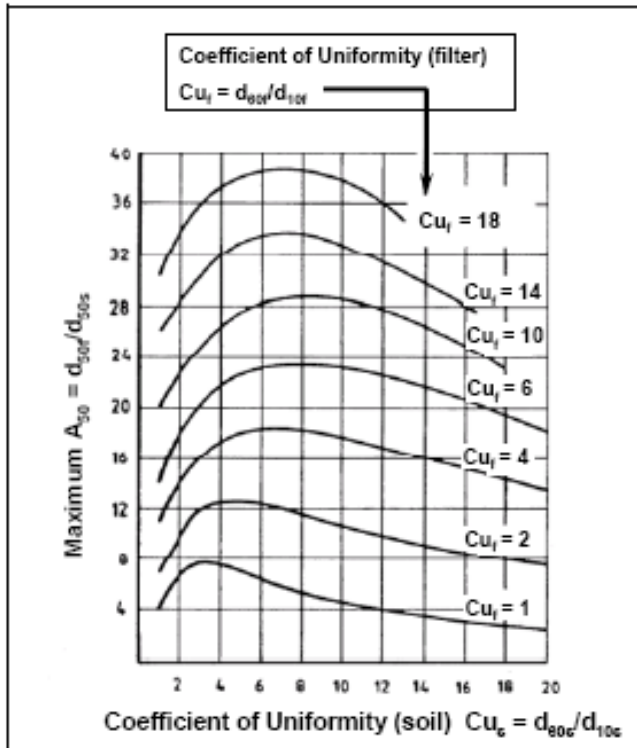


Figure 2.4 Granular filter design chart according to Cistin and Ziems (Heibaum, 2004)

Grading affects the value of the critical Shields factor. Egiazaroff (1965) presented a modified  $\Psi_{cf}$  as follows:

$$\Psi_{cf} = 0.1 \log^{-2} (19d_{f15} / d_{f50}) \tag{2.10}$$

There is still some discussion in literature about this formula that in essence has been derived to compute sediment transport of wide-graded sand-gravel mixtures.

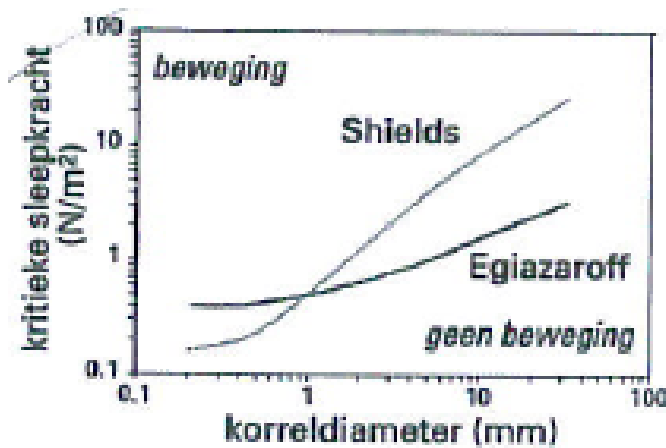


Figure 2.5 Comparison between critical shear forces of Shields and Egiazaroff

Figure 2.5 gives a graphic comparison between the Egiazaroff equation and the Shields equation. The graph looks to be in contradiction with the formula, Equation 2.10. However, one should keep in mind that in the case of wide-graded material the small

particles are hiding in the shelter of large particles and that is the reason that the critical shear force is higher compared with Shields.

It is recommended to investigate whether Equation 2.10 can be useful in the framework of this study.

For filter structures with an armoured upper part Chin et al (1994) determined a value for the critical shear stress on the basis of tests:

$$\Psi_{ca} = 0.05 \left( 0.4 \left( \frac{d_{50a}}{d_{50}} \right)^{-0.5} + 0.6 \right)^2 \quad (2.11)$$

where  $d_{50a}$  is the median particle size of the material in the top of the armour layer (m), and  $d_{50}$  is the median diameter of the original filter material (m).

It is recommended to compare the formulas 2.10 and 2.11.

Within the framework of the Eastern Scheldt works research was carried out to the stability of the edge of the bed protection on the scour hole. In memo 22RABO-N-82009 (Deltadienst, 1982) a short overview was presented on armouring based on research by Harrison (1950) and Gessler (1970). This resulted in the following findings:

- The characteristic material diameter is  $d_{85}$  for mixtures with a value of the ratio  $d_{85}/d_{15}$  of about 10
- The thickness of the layer reduces with about 1 to 5 times  $d_{85}$  before armouring is fully realized

Based on these findings the minimum thickness is set at 6 times  $d_{85}$ .

Research carried out at Delft Hydraulics with sea gravel (M1048, 1972) showed a smaller transport of uniform material than graded material with equal  $d_{50}$ . However, the difference was small. Also the value of the critical flow velocity hardly differed. In addition, the model tests showed that at flow velocities just above the critical velocity a smaller amount of larger particles and a larger amount of finer particles are present in the transported material than in the original material.

Research has also been carried out regarding sediment in rivers with armoured beds, in particular the River Meuse (Klaassen, 1990) and the Allier (Kleinhans et al, 2000). From the model tests at Delft Hydraulics followed that the destruction of the armour layer was caused by the occurrence of isolated dunes and not by increasing instability of armour layer particles; see Figure 2.6. The tests showed that after the passage of the flood the armour layer re-formed again, although at a lower level.

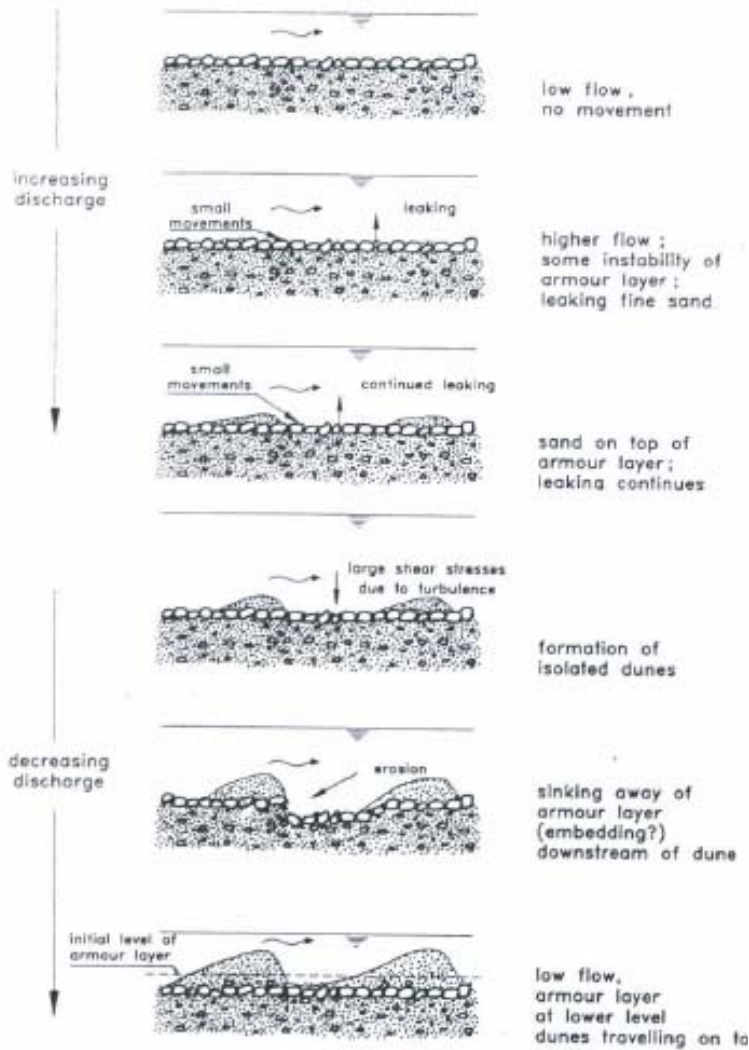


Figure 2.6 Schematic indication of breaking up of armour layer during passage of a flood

Kleinhans et al (2000) describes in detail the options what happens during a flood with the armour layer. Two situations can be distinguished: a static armour layer that will be stable during a flood or a dynamic armour layer where particles will be transported during a flood. A static armour layer is characteristic for rivers without upstream gravel supply as is the situation downstream reservoir dams. The Meuse has a river bed with a static armour layer, while the river bed of the Allier has a dynamic armour layer.

Recently, information was found about the required minimum thickness of an armour layer that would prevent washing out of base material. Sumer et al (2001) and Dixen et al (2008) have presented experimental data on suction removal of sediment from between armour blocks due to currents and waves.

Finally, Van den Berg (2004) carried out tests at the Delft University with top layers with and without a granular joint filling (gjf). The tests showed clearly that the stability of a single top layer of cubes as armour layer, expressed by the relative damage Nod (number of displaced elements) increased significantly when granular joint filling was applied; see Figure 2.7.

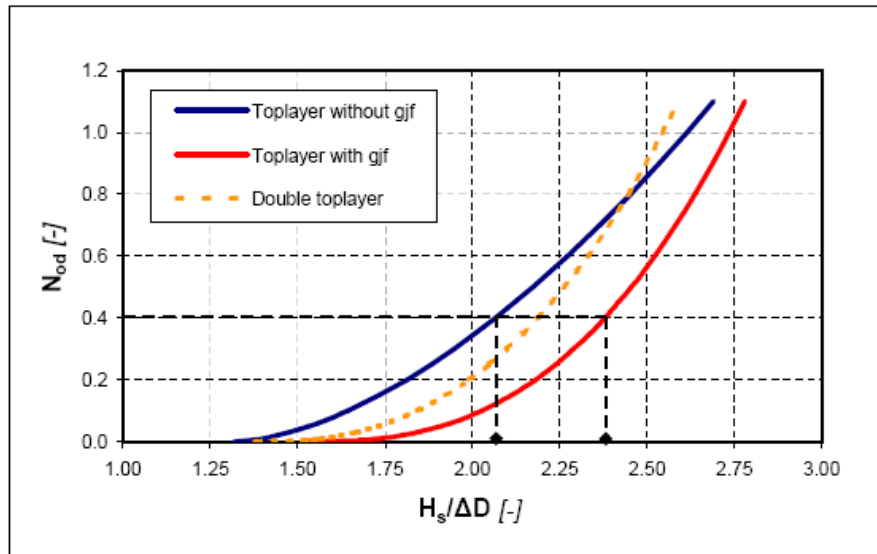


Figure 2.7 Stability of single top layers and a double top layer  
(Note:  $N_{od}$  is the relative damage, i.e. is the number of displaced elements)

For non-uniform conditions Bezuijen and Köhler (1998) have examined the stability of revetment structures, which is governed by the interaction between pore water on the one hand, and the top layer, filter layer and base layer on the other hand. Based on theoretical considerations they derived an exponential function for the pressure decrease, which is here expressed in terms of relative turbulence intensities:

$$r_{0,f}^2 = r_0^2 \exp\left(-\frac{\chi D_F}{d_{f15}}\right) \quad (2.12)$$

where  $\chi$  is a damping parameter [-] with a value in the order of  $\chi = O(0.1)$ . Equation 2.12 will be used in section 3.3.3 in deriving a new filter equation.

## 2.4 Other hydraulic conditions

### 2.4.1 Non-permanent conditions

No literature was found regarding the stability at interfaces during non-permanent and short hydraulic loads, induced for example by jets of ship propulsion systems.

### 2.4.2 Wave conditions

Breakwaters experience the forces of waves. Since breakwaters have a slope the filter is subjected to horizontal and vertical gradients. In the following vertical filters and filters in breakwaters will be discussed.

#### *Vertical filters*

With perpendicular flow, there is a serial system where the flow through base and filter layer has to be the same, causing a much larger gradient  $S$  in the base layer, because of the greater permeability of the filter layer. When the transport of particles is upwards in the vertical direction, erosion of the base layer will take place due to fluidisation (Figure

2.8). This situation is found when there is seepage through a body of sand. Usually a geometrically closed filter is applied when the flow is downwards directed.

Van der Meulen (1983) carried out 38 experiments to investigate the principle working of vertical filters. In all these tests the filter consisted of two layers, a base layer below a filter layer in which the flow direction was upwards. Three different base materials were analysed ( $d_{b50}$  varied from 150  $\mu\text{m}$  to 460  $\mu\text{m}$ ) and the ratio between  $d_{f15}$  and  $d_{b85}$  was in the range of 2 to 20. The flow conditions were laminar since in all tests  $Re_f$  was smaller than 1000. The experiments confirmed Terzaghi's filter equation as well as Darcy's law (or Equation 3.9 using  $b = 0$ ), so if  $d_{f15}/d_{b85} < 5$  no particle erosion was observed. The experiments also showed that the critical mean energy slope ( $S_c$ ) decreases if  $d_{f15}/d_{b85}$  increases until a lower limit that is reached when the uplift force of the flow is greater than the weight of the fines. When the flow is directed upwards the failure mechanism heave can be given by the following expression:

$$\rho g S_c = (1 - n_f)(\rho_s - \rho)g \quad \text{or} \quad S_c \approx 1 \tag{2.13}$$

For  $d_{f15}/d_{b85} > 5$  and  $S_c > 1$ , the tests indicated that the filter could be stable and no washout of fines would occur, which can probably be ascribed to the formation of arches (De Graauw et al., 1983). Arches are defined as fines that are trapped (pre-stressed) between the larger ones. When fines are transported from the base to the filter layer they arrive in larger pores with lower pore velocities. Hence, the resulting force on these fines decreases enormously. Tests show that if  $S$  lies in the range of 1 to 3, the trapped fines dance in the pores of the filter layer. However, in case of cyclic flow the arches will disappear.

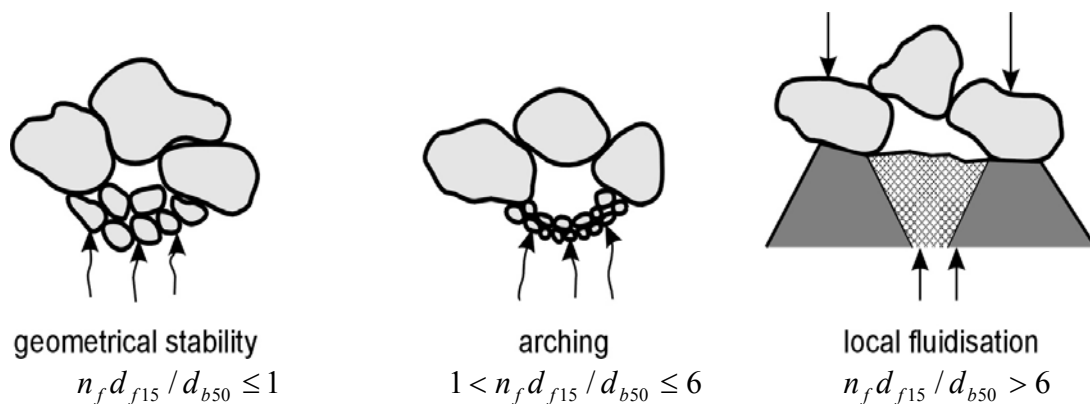


Figure 2.8 Different filter mechanism (De Graauw et al., 1983)

**Breakwaters**

Uelman (2006) investigated a breakwater with an unstable geometrically open filter (i.e. transport filter) that allows an acceptable and a predictable loss of core material of sand. He carried out wave flume experiments with different layer thicknesses and filter stone sizes. The transport of core material was governed by sheet flow transport (= bed load transport) and suspension transport. Thick filters and small filter stone sizes showed sheet flow transport. Decreasing thickness and increasing filter stone size resulted in an increase in transport and a change to suspension transport. An S-shaped profile developed.

The total erosion, the erosion depth and the erosion area depend on the ratio of filter thickness  $D_F$  and filter stone size  $d_{f50}$ . Increasing this ratio means decreasing erosion.

Ockeloen (2007) continued the research started by Uelman. He developed a best fit formula for the non-dimensional erosion area on the basis of tests:

$$\frac{A_e}{H_{rms} L_f} = 0.21 \left( S_{rms} \frac{N}{D_F / d_{f50}} \right)^{0.2} - 0.4 \quad (2.14)$$

where  $A_e$  is erosion (or damaged) area [ $m^2$ ],  $H_{rms}$  is the root mean square wave height in front of the structure [m],  $S_{rms}$  is the root-mean-square value of the gradient parallel to the slope [-],  $L_f$  is the fictitious wave length [m], defined as:  $(g/2\pi)T^2$ ,  $T$  is the wave period at the toe of the structure [s], and  $N$  is the number of waves [-].

It was observed that mostly suspended transport occurred due to the strong accelerations in wave run-up and wave rundown. The hydraulic gradient parallel to the interface was the driving force for the erosion of core material.

The shortcomings of the deduced formula are that the gradient along the interface is difficult to determine, and that the grain size of the core material is not included.



### 3 New granular filter criteria

#### 3.1 Introduction

In this chapter new filter criteria for interface stability for geometrically-open sand-tight filters will be derived in section 3.2 and 3.3. This is rather complicated. A concise version can be found in Appendix A with a paper presented at the ICSE-4 conference in Tokyo, 2008. Before the derivation, however, first the two research questions are illustrated. The two questions are:

**Q1: Relationship between layer thickness of a standard armourstone grading and the interface stability**

If for a particular reason (for example a higher flow velocity) a structure is no longer sand tight and erosion is a real threat, adequate measures have to be taken. One option is to replace the complete structure by a new bed protection, this is however costly. An alternative option is to repair the structure by making it sand tight again by increasing the layer thickness. In Figure 3.1 the issue is shown for a bed protection around a bridge pier.

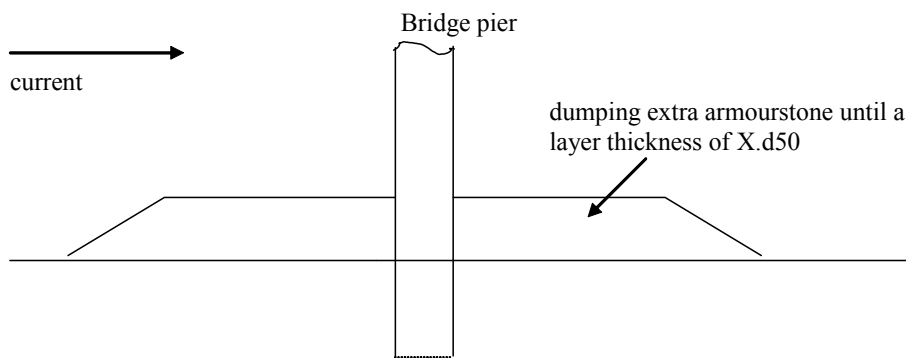


Figure 3.1 Riprap bed protection around a bridge pier

A thicker layer means a smaller hydraulic load at the interface between filter and base (see Figure 3.2). The effect of eddies is reduced because of the increased thickness. The (horizontal) flow velocity, which is the driving force for erosion also reduces. Turbulence and loading duration are crucial aspects regarding the interface stability, but also characteristic properties of the base material such as grading and cohesion.

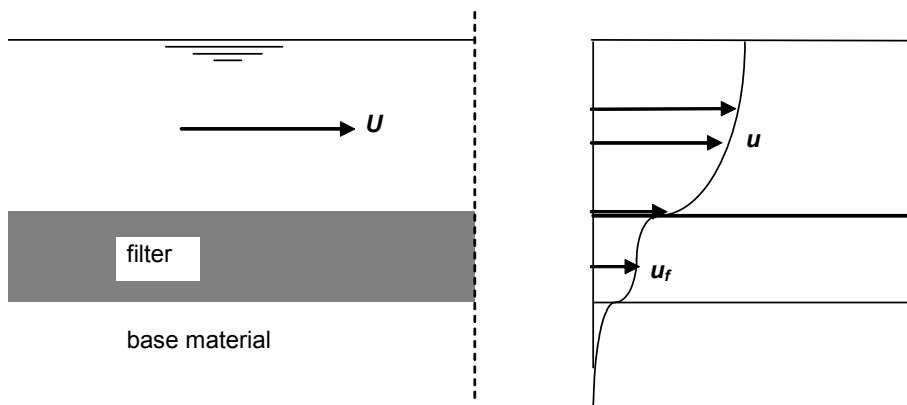


Figure 3.2 Flow velocity as driving force in a one-layer filter structure

**Q2: Interface stability when applying wide-graded (gravel) mixtures**

This phenomenon can be described as follows (Figure 3.3): the water flow causes erosion of fine particles in the case of wide-graded gravel bed material and creates a dynamic equilibrium with an outer armour layer of stable larger stones. In principle, wide graded mixtures also enable the creation of an armour layer. However, there is very limited knowledge about such armour layers. For instance, what is the resulting layer thickness, what are the dimensions of the armour layer and the composition of it related to the base material.

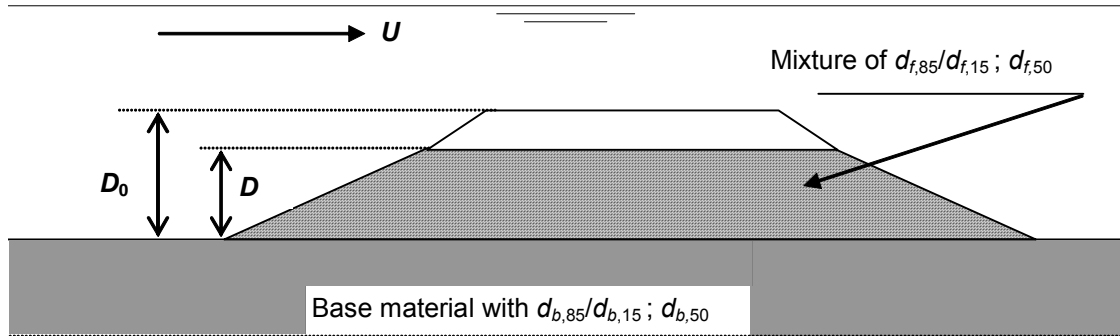


Figure 3.3 Definitions of armouring and relevant parameters

The problem is illustrated in Figure 3.4 for the situation of a pipeline cover. The cover layer is eroded partly after a river bed lowering and the stability of the pipeline is endangered.

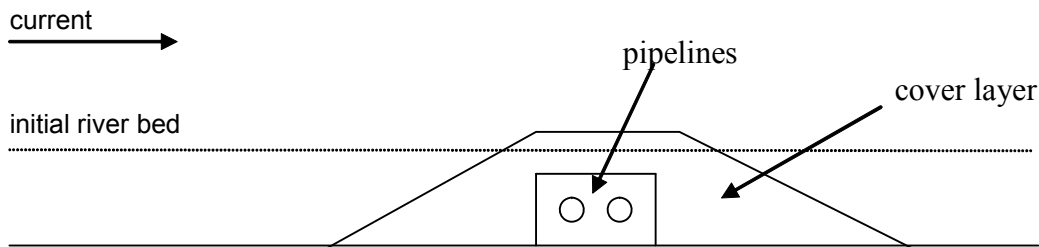


Figure 3.4 Cover layer of pipelines

**3.2 Hydraulic principles and incipient motion**

**3.2.1 Turbulence**

The Reynolds number ( $Re$ ) relates the inertial forces to the viscous forces and specifies the type of the flow (laminar or turbulent). Laminar flow occurs at  $Re < 500$ , where viscous forces are dominant. This flow domain is characterized by smooth, constant fluid motion. Turbulent flow, on the other hand, occurs at  $Re > 2000$  and is dominated by inertial forces, which tend to produce random eddies, vortices and other turbulent flow fluctuations. The Reynolds number  $Re$  is defined as:

$$Re = R_h U_0 / \nu \quad (3.1)$$

where  $R_h$  is the hydraulic radius [m],  $U_0$  is the depth-averaged flow velocity in open channel flow [m/s], and  $\nu$  is the kinematic viscosity [m<sup>2</sup>/s].

For  $500 < Re < 2000$  the transition flow could be either turbulent or laminar (e.g. Graf, 1998). Replacing  $R_h$  by  $d_{\#50}$  and  $U_0$  by the filter velocity ( $u_f$ ), the Reynolds number in granular filters ( $Re_f$ ) could be given by :

$$Re_f = d_{\#50} u_f / \nu \quad (3.2)$$

Turbulence in uniform open channel flow is generated close to the bed. In non-uniform flow conditions, turbulence is also caused by the geometry of hydraulic structures. The blunter the hydraulic structure and the rougher the bed, the higher the bed turbulence is. The definition of the relative depth-averaged turbulence intensity ( $r_0$ ) has been given by (Hoffmans 1993):

$$r_0 = \sqrt{E_0} / U_0 \quad (3.3)$$

where  $E_0$  is the depth-averaged turbulent kinetic energy in open channel flow [m<sup>2</sup>/s<sup>2</sup>]. For uniform flow Equation 3.3 reads:

$$r_0 = 1.21 \sqrt{g} / C \quad (3.4)$$

where  $C$  is the Chézy coefficient [m<sup>1/2</sup>/s] and  $g$  is the acceleration due to gravity [m/s<sup>2</sup>].

In granular filters water flows through open spaces and when the flow reattaches, small mixing layers occur that generate turbulence. The vortices in these open spaces are much smaller than the vortices in open channel flow and thus contain less energy. However, if the filter thickness ( $D_F$ ) is  $D_F = 2$  to  $3d_{\#50}$ , the turbulence intensity in both flows is assumed to have the same order of magnitude  $O(x)$ , which is a conservative assumption compared to an exponential decrease:

$$O(r_0) = O(r_{0,f}) \quad \text{or} \quad \sqrt{E_0} / U_0 \approx \sqrt{E_f} / u_f \quad (3.5)$$

where  $E_f$  is the mean turbulent kinetic energy in the filter layer [m<sup>2</sup>/s<sup>2</sup>] and  $r_{0,f}$  is the mean turbulence intensity in the filter layer [-].

Combining the definition of the mean bed shear stress,  $\tau_0 = \rho u_*^2$ , where  $u_*$  is the bed shear velocity (m/s), the Chézy equation  $u_* = U_0 g^{1/2} / C$  and Equation 3.3 for uniform flow,  $\tau_0$  can be rewritten as:

$$\tau_0 = \rho U_0^2 g / C^2 = 0.7 \rho (r_0 U_0)^2 \quad (3.6)$$

Following a similar approach for the filter layer, and assuming that  $u_{*bf} = u_f g^{1/2} / C_f$ ,  $u_f = u_*$  and  $r_{0,f} = 1.21 \sqrt{g} / C_f$  (where  $u_{*bf}$  is the shear velocity at the transition of the filter and the base layer and  $u_f$  is the mean filter velocity (m/s)), the shear stress at the interface,  $\tau_{bf}$ , is:

$$\tau_{bf} = \rho u_{*bf}^2 = \rho u_f^2 g / C_f^2 = 0.7 \rho (r_{0,f} u_*)^2 \quad (3.7)$$

Hence, the parameter ( $\eta$ ) that represents the relative turbulence in the filter layer, is given by:

$$\eta = \frac{\tau_{bf}}{\tau_0} = \left( \frac{r_{0,f} u_*}{r_0 U_0} \right)^2 = 0.7 r_{0,f}^2 \quad (3.8)$$

For thick filter layers the relative turbulence can be estimated using Equation 2.12.

### 3.2.2 Flow in filters

#### *Darcy's Law*

Darcy laid the foundation of the theory of the flow through filters. Based on his classic experiments he stated that the discharge ( $Q$ ) through a filter is proportional to the area ( $A$ ) of the filter and to the mean energy slope ( $S = (H_1 - H_2)/L$ ) where  $(H_1 - H_2)$  is the head over the filter and  $L$  is the length of the filter. Darcy's law reads:

$$Q = AkS \quad \text{or} \quad u_f = kS \quad (3.9)$$

where  $k$  is the permeability of the filter [m/s], which is determined by the geometric properties of the filter such as porosity, shape and size of the particles and the kinematic viscosity. Darcy's law assumes laminar flow, which implies that the dynamic forces resulting from acceleration and deceleration in the flow are neglected in comparison with the classical Navier-Stokes equations.

#### *Forchheimer's equation*

Forchheimer developed a relationship between the gradient  $S$  and the filter velocity  $u_f$ , which is non-linear for sufficiently high flow velocities. This non-linearity increases with increasing values of  $u_f$  and is caused by turbulence effects of the flow in the filter. The Forchheimer equation reads:

$$S = au_f + bu_f^2 \quad (3.10)$$

where  $a$  [s/m] and  $b$  [s<sup>2</sup>/m<sup>2</sup>] are dimensional coefficients. The Forchheimer equation assumes that Darcy's law is still valid. However, an additional term is added to account for the increased value of  $S$ . Based on measurements in permeable filters Den Adel (1986) deduced the following formulas for the coefficients  $a$  and  $b$ :

$$a = 160 \frac{\nu (1 - n_f)^2}{g n_f^3 d_{f15}^2} \quad \text{and} \quad b = \frac{2.2}{g n_f^2 d_{f15}} \quad (3.11)$$

where  $n_f$  is the porosity of the filter and  $\nu$  is the kinematic viscosity. The predictability of  $u_f$  in Equation 3.10 applying the expressions for  $a$  and  $b$ , lies in the range of  $\frac{1}{3} < \zeta < 3$  where  $\zeta$  represents the ratio of the measured and calculated value of the filter velocity  $u_f$ .

### 3.2.3 Incipient motion

#### General

Particle transport occurs when the load exceeds the strength. When the load is less than some critical value, particles remain motionless and can be considered as fully stable. But when load exceeds its critical value, particle motion begins. The initiation of motion is difficult to define, which can mainly be ascribed to phenomena that are random in time and space. In the modified Shields (1936) diagram (Figure 3.5), the influence of the instantaneous bed shear stresses ( $\tau'$ ) is not directly specified. Although the distribution of  $\tau'$  is unknown, there are indications that this distribution must be asymmetrical due to sweeps and ejections (Lu and Willmarth, 1973).

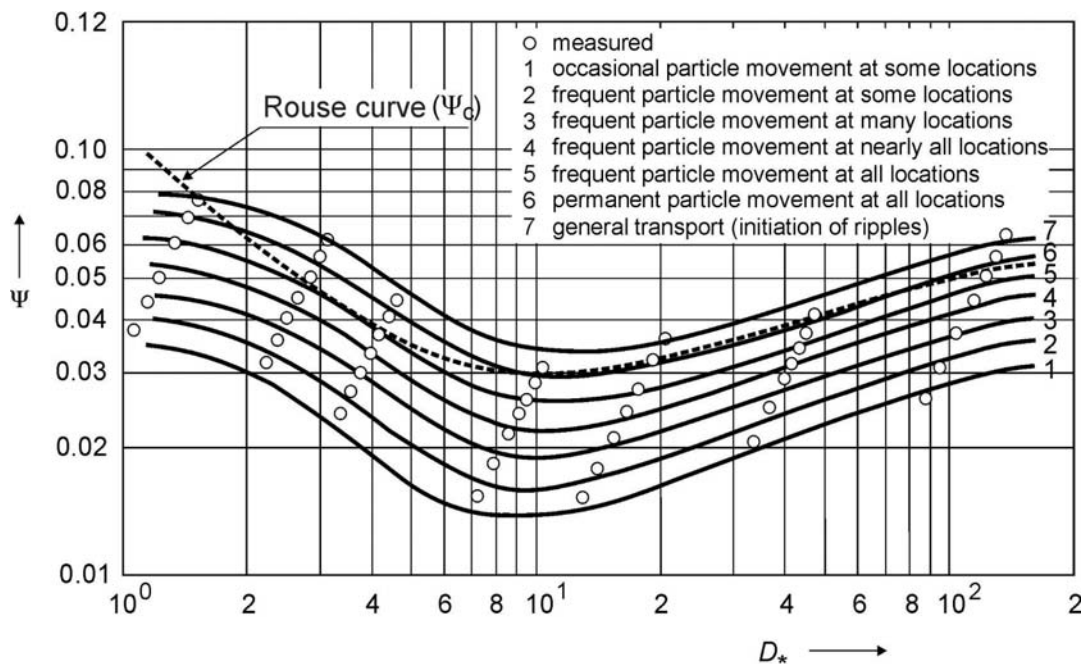


Figure 3.5 Modified Shields diagram;  $\Psi$  as function of  $D^* = d_{50}(\Delta g/v^2)^{1/3}$

When dealing with particle stability in granular filters, the determination of the exact shape of the distribution of both load and strength can be avoided because a characteristic shear stress ( $\tau_k$ ) can be defined, this being a mean (or time and space-averaged) value and a fluctuating term that originates from the turbulence near the bed. In addition to the random nature of load, another random parameter in the process of initial instability is determined by the strength ( $\tau_{c,k}$ ) of the particles.

#### Hypothesis of Grass

Based on statistical assumptions for both the characteristic bed shear stress ( $\tau_{0,k}$ ) and the critical characteristic bed shear stress ( $\tau_{G,k}$ ), Grass (1970) defined (Figure 3.6):

$$\tau_{0,k} = \tau_0 + \gamma\sigma_0 \quad (3.12)$$

$$\tau_{G,k} = \tau_G - \gamma\sigma_G \quad (3.13)$$

where  $\gamma$  is determined by an allowable transport of the bed material [-],  $\sigma_0$  is the standard deviation of the instantaneous bed shear stress [ $\text{N/m}^2$ ],  $\sigma_G$  is the standard deviation of the critical instantaneous bed shear stress [ $\text{N/m}^2$ ], and  $\tau_G$  is the critical mean bed shear stress as given by Grass.

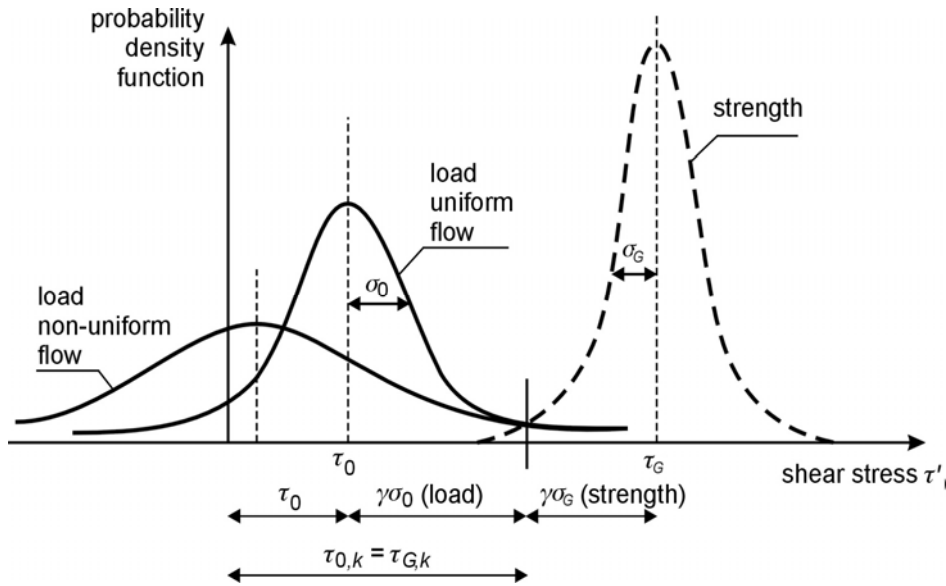


Figure 3.6 Probability functions of the load and strength (Grass 1970)

Before continuing some remarks are made about uniform and non-uniform flow. Uniform flow means that the flow does not change in the flow direction. Obviously, this is not the situation downstream of a hydraulic structure or near a bridge pier. The flow characteristics will change at such locations. At least the turbulence level will be higher, but it also possible that even negative flow velocities occur (see Figure 3.6). The consequence for the design of bed protections is that the maximum load, mean velocity plus turbulence, will be decisive for the dimensions of the protection.

The critical situation (loading equals strength) can be described by  $\tau_{0,k} = \tau_{G,k}$ ; see also Figure 3.6, with  $\sigma_0 = V_0 \tau_0$  ( $V_0$  is the variation coefficient representing the bed turbulence and  $\sigma_G = V_{Gf} \tau_G$  ( $V_{Gf}$  is the variation coefficient representing the non uniformity of the top layer and variation in strength), where  $\tau_G = \Psi_{Gf} \Delta_f \rho g d_{f50}$  (analogous to Shields), a general relationship for the top layer can be derived, as follows:

$$\Delta_f d_{f50} = \frac{\tau_0 + \gamma \sigma_0}{\Psi_{Gf} \rho g (1 - V_{Gf} \gamma)} \tag{3.14}$$

where  $\Delta_f (= \rho_s / \rho - 1)$  is the relative density of the top material [-],  $\rho$  is the density of the water [ $\text{kg/m}^3$ ],  $\rho_s$  is the density of the top material [ $\text{kg/m}^3$ ] and  $\Psi_{Gf}$  [-] is related to the critical Shields parameter  $\Psi_c$ .

A specific transport will occur if  $\tau_{0,k} = \tau_{G,k}$ . For uniform flow,  $V_0 \approx 0.4$ , Grass found that for sand with  $V_{Gf} \approx 0.3$ , was completely stable for  $\gamma = 1$  and for  $\gamma = 0$  a significant transport of sediment particles was observed. Based on his experiments, he reported that for  $\gamma = 0.625$  the criterion of Shields (or Rouse curve in Figure 3.5) was met for the initial movement of sands up to a size of  $250 \mu\text{m}$ . Note that  $\tau_G \approx 1.5 \tau_c$  where  $\tau_c$  is the critical mean bed shear stress according to Rouse.

### 3.3 Derivation new criteria for interface stability of open granular filters

#### 3.3.1 Introduction

Typically, granular filter elements (stone, gravel and sand) are sustainable and robust and give a good contact interface with the base layers (PIANC 1987, 1992). Granular filters could smoothen bed irregularities and thus provide a more uniform construction base. Moreover, they are easy to repair and, to some extent, they are self-healing. The major disadvantage of granular filters is the difficulty of assuring construction procedures underwater as to obtain the required thickness of the filter layers. In addition, conventional filters with several layers may be very expensive, especially in the Netherlands.

Granular filters protect the underlying soil, i.e. the base layer, from erosion by flow induced loads (static and fluctuating components from turbulence). The approach flow velocity or water level difference produces the static load over hydraulic structures, whereas the fluctuating load reflects the turbulence caused by the geometry of the structures or by the roughness of the top layer. The erosion resistance (or strength) of granular filters is mainly characterised by the geometrical properties of the materials used.

Hereafter existing and new approaches to designing horizontal filters, that are influenced by laminar or by turbulent flow are discussed together with the ranges of validity.

#### 3.3.2 Horizontal filters without bed turbulence

##### *General*

Below hydraulic structures such as breakwaters and weirs, horizontal filters can be found. In this situation no water flow is present above the filter. Subsequently, bed turbulence does not play a role. The flow in the filter is driven by the water head difference over the structure.

Obviously, the water flows parallel to the interface, and thus the gradient,  $S$ , in both layers is about the same, causing  $u_f$  in the filter layer to be much higher than in the base layer, because of the greater permeability. At the interface there will be a velocity gradient, inducing a shear stress at the upper fines in the base layer. Van der Meulen (1984), Klein Breteler (1989) and Broekens (1991) conducted experiments in which the flow was parallel to the filter and base layer. In these tests the flow was laminar as well as turbulent and no open channel flow above the filter was considered.

**Note:** obviously, turbulence in the filter is included, but as no channel flow above the filter was modelled, the bed turbulence in the flow above the filter is not included.

##### *Modelling*

De Graauw et al. (1983) proposed an empirical relation between the critical value of the mean energy slope  $S_c$  and the critical bed shear velocity ( $u_{*c,bf}$ ) at the interface of filter and base layer:

$$S_c = (\alpha_{lam} + \alpha_{tur}) u_{*c,bf}^2 \quad \text{where} \quad u_{*c,bf} = \sqrt{\Psi_{cb} \Delta_b g d_{b50}}$$

$$\alpha_{lam} = \frac{0.06}{n_f^3 (d_{f15})^{4/3}} \quad \text{and} \quad \alpha_{tur} = \frac{n_f^{5/3} (d_{f15})^{1/3}}{1000 (d_{b50})^{5/3}} \quad (3.15)$$

where  $\alpha_{lam}$  [ $\text{m}^{-2} \text{s}^2$ ] and  $\alpha_{tur}$  [ $\text{m}^{-2} \text{s}^2$ ] are coefficients that represent laminar and turbulent flow conditions respectively. Rewriting Equation 3.15 gives the dimensionless gradient:

$$S_{c,lam} \approx \frac{d_{b50}}{(d_{f15})^{4/3}} \quad \text{and} \quad S_{c,tur} \approx \frac{(d_{f15})^{1/3}}{(d_{b50})^{2/3}} \quad (3.16)$$

According to Koenders (1985),  $S_c$  is in the low and high gradient range proportional to:

$$S_{c,lam} \approx \frac{(d_{b50})^{2/3}}{(d_{f15})^{5/3}} \quad \text{and} \quad S_{c,tur} \approx \frac{d_{b50}}{(d_{f15})^{1/3}} \quad (3.17)$$

Since the above mentioned approaches result in significantly different equations, the modelling of  $S_c$  is here reconsidered hereafter. The critical filter velocity ( $u_{c,f}$ ) is a function of filter characteristics on the one hand and the critical shear velocity  $u_{*c,bf}$  on the other hand. Analogous to channel flow,  $u_{c,f}$  can be written as:

$$u_{c,f} = \frac{C_f}{\sqrt{g}} u_{*c,bf} \quad \text{with} \quad C_f = \alpha_{15} \sqrt{g} \left( \frac{d_{f15}}{d_{b50}} \right)^{1/6} \quad (3.18)$$

where  $C_f$  is a coefficient [ $\text{m}^{1/2}/\text{s}$ ] representing the resistance in the filter layer and comparable with the Chézy coefficient,  $\alpha_{15}$  is a coefficient [-],  $\Delta_b$  is the relative density related to the base layer material [-] and  $\Psi_{cb}$  is the critical Shields parameter related to  $d_{b50}$  [-]. Combining Equations 3.10, 3.11 and 3.18 and considering laminar flow (thus  $Re_f < 500$  and  $b = 0$  in Equation 3.10) yields:

$$S_{c,lam} = \alpha_L \frac{(1 - n_f)^2 v \sqrt{\Delta_b} (d_{b50})^{1/3}}{n_f^3 \sqrt{g} (d_{f15})^{13/6}} \quad \text{with} \quad \alpha_L = 160 \alpha_{15} \sqrt{\Psi_{cb,lam}} \approx 65 \quad (3.19)$$

The value of  $\alpha_L \approx 65$  has been derived from Figure 3.7 with  $S_{c,lam}$  on the vertical axis and the right hand term of Equation 3.19 on the horizontal axis.

Substituting Equation 3.18 in Equation 3.10 with  $a = 0$ , Equation 3.10 reads for turbulent flow (thus  $Re_f > 2000$ ):

$$S_{c,tur} = \alpha_T \frac{\Delta_b}{n_f^2} \left( \frac{d_{b50}}{d_{f15}} \right)^{2/3} \quad \text{with} \quad \alpha_T = 2.2 \alpha_{15}^2 \Psi_{cb,tur} \approx 0.1 \quad (3.20)$$

The value of  $\alpha_T \approx 0.1$  has been derived from Figure 3.8 with  $S_{c,tur}$  on the vertical axis and the right hand term of Equation 3.20 on the horizontal axis.

The modified Shields diagram (see Figure 3.5) shows that for laminar flow or for fines smaller than 0.1 mm,  $\Psi_{cb,lam}$  could reach values up to 0.1. Assuming that  $\Psi_{cb,lam} = 0.1$  and using Equation 3.19,  $\alpha_{15} = 65 / (160 \cdot \sqrt{0.1}) = 1.28$ . Substitution of  $\alpha_{15} = 1.28$  into

Equation 3.20,  $\Psi_{cb,tur} = 0.1/(2.2 \cdot 1.28^2) = 0.03$ , which is in agreement with turbulent flow observations.

Although Koenders used a completely different approach of solving the equilibrium of particles in granular filters, the proposed equations for  $S_c$  (Equations 3.19 and 3.20) correspond quite well with his findings (Equation 3.17). Figures 3.7 and 3.8 show the results of 43 experiments in which the initiation of motion was investigated in the base layer of the horizontal filter. The vertical axis represents  $S_c$  and the horizontal axis represents the strength of both the filter and base layer. The scatter in the results can mainly be described to the complexity of the description of the incipient motion, see also Figure 3.5.

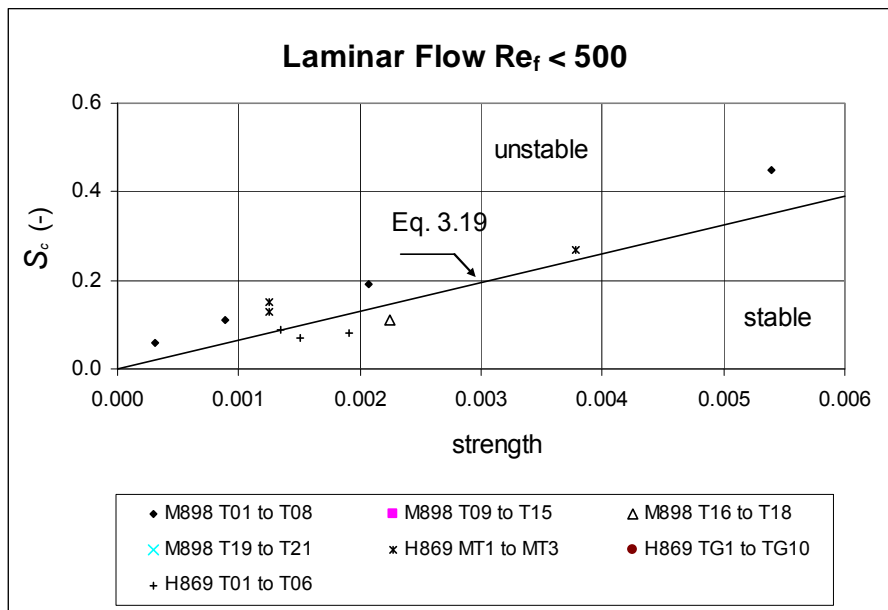


Figure 3.7 The critical mean energy slope,  $S_c$ , as function of strength; see Equation 3.19

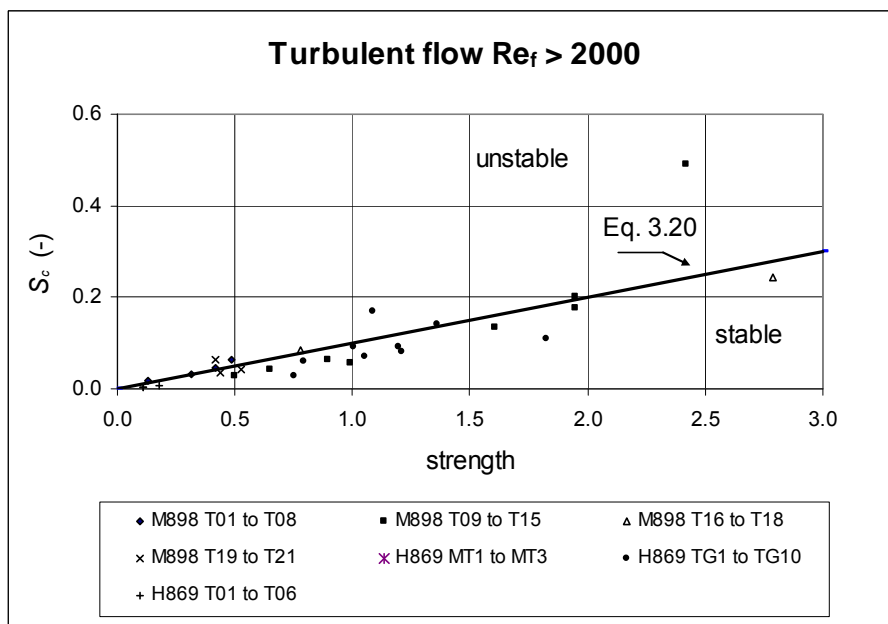


Figure 3.8 The critical mean energy slope,  $S_c$ , as function of strength; see also Equation 3.20

Klein Breteler (1992) related the critical and actual filter velocity. It is recommended to compare his results with those results from Equation 3.20.

### 3.3.3 Horizontal filters influenced by bed turbulence

#### General

Filter structures with a flowing water layer above the structure, for example bed protections, experience the bed turbulence exerted by the flow. The stability of the filter structure has been examined below.

Figure 3.9 gives an impression about the type of structures with high turbulence and non-uniform flow.

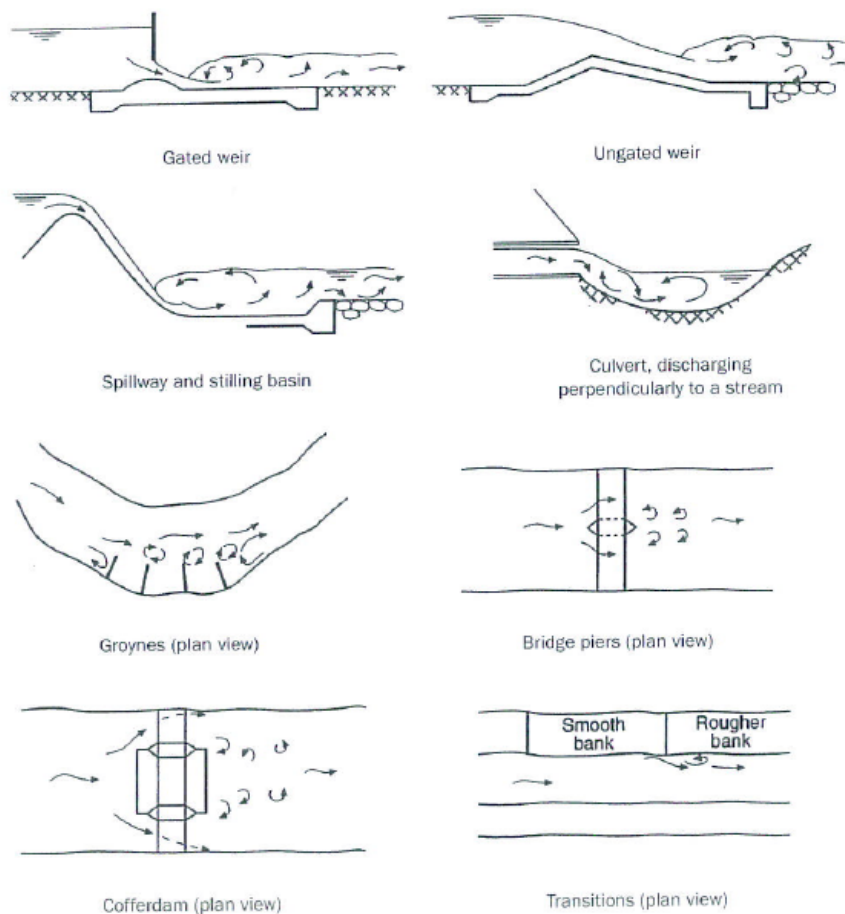


Figure 3.9 Examples of situations with high turbulence

Hoffmans et al. (2000) discussed a shear stress approach in a horizontal one-layer filter with a thickness ( $D_F$ ) above the base material in open channel flow (Figure 3.10). Equations for granular filters based on the Navier Stokes equation for uniform flow, Forchheimer's equation and the hypothesis of Boussinesq are combined. The hypothesis of Grass was used to analyse the influence of gradtion and armouring in a qualitative way. Subsequently, the mean turbulence in granular filters is included (see also section 3.2.1). The decrease of turbulence, which is relevant for thick filter layers, is simulated by the exponential relation as proposed by Bezuijen and Köhler (1998). Finally, experiments are applied to verify the proposed method in relation to the design equation of Wörman (1989).

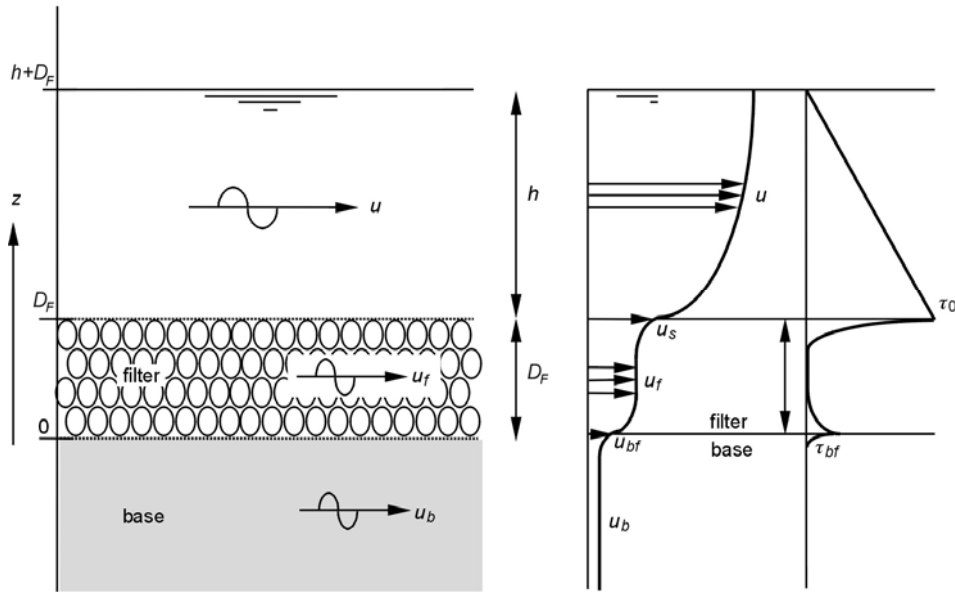


Figure 3.10 Overview of definitions for a one-layer filter

#### Shear stress approach

Considering uniform flow, the shear stress distribution is linear and the mean flow velocity as function of the vertical coordinate ( $z$ ) is approximately logarithmic. In a granular filter the balance of forces acting on a control volume are (e.g. Shimizu et al., 1990):

$$\frac{d\tau_f}{dz} + F_s + \rho g S_b = 0 \quad \text{with} \quad F_s = -\rho g (a u_f + b u_f^2) \quad (3.21)$$

in which  $F_s$  is the seepage resistance per unit width ( $\text{N/m}^3$ ),  $S_b$  ( $\approx S$ ) is the bed slope (-) and  $\tau_f$  is the mean shear stress in the filter layer ( $\text{N/m}^2$ ), which is not the same as the definition of the mean shear stress in open channel flow. The first term in Equation 3.21 represents the momentum transfer from the free surface flow to the filter bed. Using the hypothesis of Boussinesq the expression for  $\tau_f$  reads:

$$\tau_f = \rho \nu_t \frac{du_f}{dz} \quad (3.22)$$

where  $\nu_t$  is the turbulent viscosity (or eddy viscosity), which relates  $u_f$  to  $\tau_f$ . Most of the turbulence-model-development and application work has been carried out in the field of mechanical and aeronautical engineering. In the early 80's Rodi (1984) has assessed the applicability of turbulence models to hydraulic flow problems. However, these models have not been extensively validated for flow in porous media such as granular filters. Therefore some assumptions have been made for  $\nu_t$ . For example,  $\nu_t$  is related to a representative length scale and to a representative flow velocity. The length scale has been determined by the open space or by the particle sizes:

$$\nu_t = \alpha_v u_f d_{f15} \quad (3.23)$$

where  $\alpha_v$  ( $\approx 0.9$ ) is a constant. Combining Equations 3.21, 3.22 and 3.23 and assuming turbulent flow conditions ( $a = 0$  in Equation 3.10) the exact mathematical distribution of  $u_f$  as function of  $z$  in a one layer filter using the boundary conditions  $u_f(0) = u_{bf}$  and  $u_f(D_f) = u_s$ , is (Verheij et al., 2000) as follows:

$$u_f(z) = \sqrt{C_1 e^{z\xi} + C_2 e^{-z\xi} + s_b/b} \quad (2.8)$$

with  $\xi = \sqrt{\frac{2gb}{\alpha_v d_{f15}}} \approx \frac{5.5}{d_{f15}}$

$$C_1 = \frac{(u_s^2 - s_b/b) - e^{-\xi D_f} (u_{bf}^2 - s_b/b)}{(e^{\xi D_f} - e^{-\xi D_f})}$$

$$C_2 = \frac{e^{\xi D_f} (u_{bf}^2 - s_b/b) - (u_s^2 - s_b/b)}{(e^{\xi D_f} - e^{-\xi D_f})}$$

where  $u_{bf}$  is the mean pore velocity at the transition of filter and base layer [m/s],  $u_s$  is the mean near bed velocity [m/s] and  $\xi$  is a damping parameter [-]. The exact mathematical solution for the shear stress  $\tau$  in the filter layer is (Verheij et al., 2000) as follows:

$$\tau_f(z) = \frac{1}{2} \alpha_v \rho \xi d_{f15} (C_1 e^{z\xi} - C_2 e^{-z\xi}) \quad (3.24)$$

which can be approximated by:

$$\tau_f(z) = \tau_{bf} e^{-z\xi} + \tau_0 e^{\xi(z-D_f)} \quad (3.25)$$

For laminar flow conditions, Verheij et al. (2000) derived similar equations for both the filter velocity  $u_f$  and the shear stress in the filter  $\tau_f$ . The damping parameter for laminar flow is approximately 6 times greater than for turbulent flow ( $\xi = 30/d_{f15}$ ). An analytical solution can also be obtained for a two-layer filter. Tables 3.1 to 3.3 show computed distributions of  $u_f(z)$  and  $\tau_f(z)$  using Equations 2.8 and 3.24 for a uniform flow at prototype scale and additional information about input and output parameters.

So far, this study shows that the application of the hypothesis of Boussinesq yields satisfactory results with respect to the distribution of the filter velocities in granular filters. Moreover, the shear-stress approach yields a prediction of the shear stress at the interface base layer – filter layer  $\tau_{bf}$ , which is of interest for modelling the stability of the base layer. This analysis also demonstrates that the value of the damping factor  $\xi$  is extremely high, so the computed  $du_f/dz$  is very large both in the near bed zone and at the transition to the base layer. In the filter layer itself the computed  $du_f/dz \approx 0$ , resulting in a zero shear-stress (Figure 3.10). Since the flow accelerates and decelerates in the open spaces of the filter, turbulence is generated and thus shear stresses will act on particles. Therefore, the hypothesis of Boussinesq does not represent the shear stress distribution in filter layers adequately.

Table 3.1 Input parameters for the calculation of flow velocities using shear stress approach

Symbol	Name	Value	Remarks
$b$	Forchheimer parameter	$9 \text{ s}^2/\text{m}^2$	calculated using Eq. 3.11
$C$	Chézy coefficient	$32 \text{ m}^{0.5}/\text{s}$	calculated
$d_{f15}$	15% filter stone size	0.15 m	-
$d_{f50}$	median filter stone size	0.30 m	-
$D_F$	filter thickness	0.50 m	-
$h$	water depth	3.0 m	-
$r_0$	relative turbulence intensity	0.12	calculated using Eq. 3.3
$S_b$	gradient	0.0013	$S_b = (U_0)^2/(h C^2)$
$u_s$	flow velocity at bed	0.12 m/s	estimated by trial and error
$u_{bf}$	interface velocity	0.0005 m/s	-
$u_f$	mean filter velocity	0.0115 m/s	calculated using Eq. 3.10
$U_0$	depth averaged flow velocity	2.0 m/s	-
$\xi$	damping parameter	$37 \text{ m}^{-1}$	calculated using Eq. 2.8

Table 3.2 Computational results using Equations 2.8 and 3.24 (see also Table 3.1)

$z$ (m)	$u_f(z)$ (m/s)	$\tau(z)$ (N/m <sup>2</sup> )
0.50	0.1200	35.29567
0.45	0.0492	5.643063
0.40	0.0224	0.902212
0.35	0.0141	0.144246
0.30	0.0122	0.023068
0.25	0.0119	0.003723
0.20	0.0118	0.000814
0.15	0.0118	0.001499
0.10	0.0116	0.008801
0.05	0.0108	0.054955
0.00	0.0005	0.343713

Table 3.3 Output parameters from shear stress approach

Output parameters		
symbol	value	remarks
$u^*$	0.188 m/s	$u^* = (\tau_f(0.5)/\rho)^{1/2}$
$u^*_{bf}$	0.019 m/s	$u^*_{bf} = (\tau_f(0)/\rho)^{1/2}$
$u_f$		See Table 3.2
$\eta$	0.01	$\eta = \tau_f(0)/\tau_f(0.5)$

**Influence of the gradation**

Measurements of Klar (2005) showed that the local turbulence energy ( $k_f$ ) in the filter layer decreases with depth. Based on Klar’s uniform flow tests,  $k_f$  is here approximated by an exponential function

$$k_f(z) = k_{ref} \exp(z / \ell_d) \quad \text{with} \quad \ell_d = \alpha_\chi d_{f15} \tag{3.26}$$

where  $k_f [= (r_f u_f)^2]$ ,  $r_f$  is the local relative turbulence intensity in the filter layer,  $k_{ref} [= \alpha_{ref} (u^*)^2]$  is the turbulence energy at a reference level close to the bed,  $\alpha_{ref}$  and  $\alpha_\chi$  are coefficients and  $\ell_d$  is a length scale. In  $k$ - $\varepsilon$ -models,  $\alpha_{ref} = \chi_k = 3.3$  at  $z^+ = 70$  where  $z^+ [= zu^*/\nu]$  is the dimensionless

vertical coordinate (see also Chapter 2). In the viscous sub layer  $\alpha_{ref}$  could reach values up to 5.6 (e.g. Hinze 1975). In the upper part of the filter layer, that is, for  $-1 < z/d_{f15} < 0$ , Eq. 6.22 yields satisfactory results by using  $\alpha_\chi = 0.2$  and  $\alpha_{ref} = 5.6$  (Fig. 6.7). In the lower part, i.e., for  $-8 < z/d_{f15} < -1$ , the calculated  $k_f$  is adequate provided  $\alpha_\chi = 2$  and  $\alpha_{ref} = 2$ .

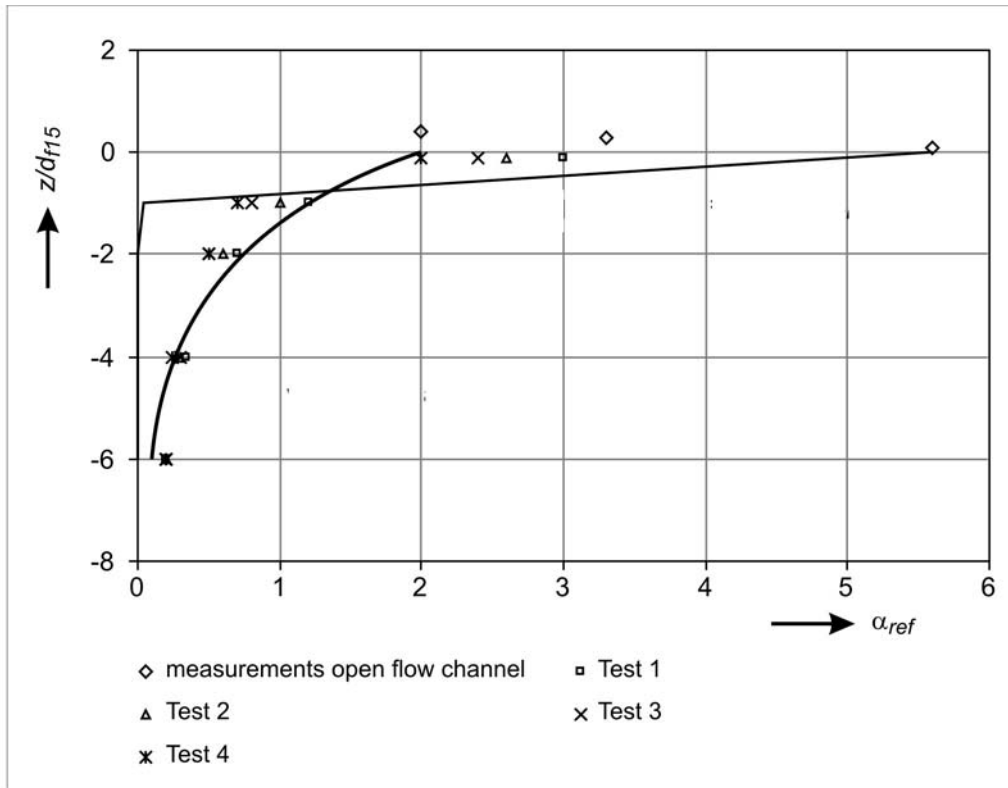


Fig. 3.11  $\alpha_{ref}$  versus  $z/d_{f15}$ ; experimental data of Klar (2005)

— Eq. 3.26 with  $\alpha_\chi = 0.2$  and  $\alpha_{ref} = 5.6$

— Eq. 3.26 with  $\alpha_\chi = 2$  and  $\alpha_{ref} = 2$

By applying the hypothesis of Boussinesq,  $\tau_{bf}$  is

$$\tau_{bf} = \rho v_{t,bf} \left( \frac{du}{dz} \right)_{bf}$$

with  $v_{t,bf} = \frac{1}{2} \alpha_k (u_{f,bf} + u_{b,bf}) d_{f15}$ ,  $\left( \frac{du}{dz} \right)_{bf} = \frac{u_{f,bf} - u_{b,bf}}{d_{f15}}$  (3.27)

in which  $\alpha_k$  is a coefficient and  $v_{t,bf}$  is the local eddy viscosity near the interface of the filter-base layer. For uniform flow conditions, Klar (2005) found  $O(r_f) = 1$ . Combining Eqs. 3.26, 3.27 and the definition of  $\tau_0 = \rho(u_*)^2$  and assuming that  $u_{b,bf} \ll u_{f,bf}$  with  $\alpha_\chi = 2$ ,  $\alpha_{ref} = 2$  and  $r_f = 1$ , the relative load ( $\eta$ ) at the transition of the filter base layer is ( $z = -D_F$ )

$$\eta = \tau_{bf} / \tau_0 = \alpha_k \exp(-\frac{1}{2} D_F / d_{f15})$$
 (3.28)

If  $\tau_0$  increases or if  $D_F/d_{f15}$  decreases,  $\tau_{bf}$  increases which is in agreement with observations. In a similar way,  $\eta$  can also be derived using the characteristic load ( $\tau_{bf,k}$ ). The reason for this is the hiding effect, see also section 2.3.

Applying the hypothesis of Grass, the characteristic shear stress ( $\tau_{bf,k}$ ) and the critical characteristic shear stress ( $\tau_{c,bf,k}$ ) at  $z = 0$  are (see also Figure 2.2):

$$\tau_{bf,k} = \eta(\tau_0 + \gamma\sigma_0) \quad (3.29)$$

$$\tau_{c,bf,k} = \tau_{Gb} - \gamma\sigma_{Gb} = \Psi_{Gb} \Delta_b \rho g d_{b50} (1 - \gamma V_{Gb}) \quad (3.30)$$

Combining the Equations 3.14, 3.29 and 3.30 and substituting  $\Psi_{Gb}/\Psi_{Gf} = \Psi_{cb}/\Psi_{cf}$  in Equation 3.14, gives for geometrically open filters the following expression:

$$\frac{d_{f50}}{d_{b50}} = \frac{1 - \gamma V_{Gb}}{\eta (1 - \gamma V_{Gf})} \frac{\Psi_{cb}}{\Psi_{cf}} \frac{\Delta_b}{\Delta_f} \quad (3.31)$$

With Equation 3.31 the influence of the gradation on the stability of the base material can be explained in a qualitative way. For example, when the base material has a wider gradation than the filter material, thus  $V_{Gb} > V_{Gf}$ , the required ratio  $d_{f50}/d_{b50}$  is less than the value in situations where base and filter materials do have the same gradation. If only the filter material is wide-graded, thus  $V_{Gb} < V_{Gf}$ , the maximum value of  $d_{f50}/d_{b50}$  is higher than for similarly graded materials. These predictions correspond with observations in flume experiments. Wide-graded base material has more fines than a less wide-graded material. The material in the filter layer has to prevent the erosion of the fines. This can only be achieved by reducing  $u_f$  or by putting more fines into the filter layers. Wide-graded material in the filter layer has relatively more fines, which reduces  $u_f$  and so  $\tau_{bf}$ . Hence, the wide-graded filter material is allowed to have a  $d_{f50}$  that is larger than for narrow-graded or uniform material. Rewriting Equation 3.31, using  $\Psi_{cb} = 0.06$ ,  $\gamma = 0.625$  and  $V_{Gb} = 0$ , and assuming  $d_{f50}/d_{b50} = 1/\eta$  (see also Equation 3.34), gives:

$$\Psi_{cf} = \frac{0.06}{1 - \gamma V_{Gf}} = \frac{0.06}{0.375 + 0.625 d_{f15}/d_{f50}} \quad (3.32)$$

Consequently, for  $0.5 < d_{f15}/d_{f50} < 1$ , the use of Equations 3.31 and 3.32 gives similar results.

Note: The derivation of Equation 3.32 is an attempt to present a formula that, in analogy with Egiazaroff (see Equation 2.10), shows the influence of the gradation. Some of the assumptions can be disputed or are not fully in line with some others; however, starting with the Grass method Equation 3.32 shows the influence. It is recommended to study this aspect in future studies.

#### Bed turbulence

Bakker et al. (1994) discussed a filter model that includes near-bed pressure fluctuations:

$$\frac{d_{f15}}{d_{b50}} = \frac{2.2}{C_0 e^2} \frac{R_h}{d_{f50}} \frac{\Psi_{cb}}{\Psi_{cf}} \frac{\Delta_b}{\Delta_f} \quad (2.6)$$

where  $C_0$  is a coefficient that varies from 6 (when determined with the average shear stress  $\tau_0$ ) to 100 (when determined with the maximum bed shear stress  $\tau_m$ ) and  $e$  is a coefficient that takes into account the difference between the flow in granular filters and

open channels (with an average value of  $\epsilon = 0.24$ ). The ratio between 100 and 6 is approximately 15, which is in agreement with Emmerling's (1973) findings who found:

$$p_m = 18\tau_0 \quad (3.33)$$

where  $p_m$  represents the pressure peak or the maximum under water pressure caused by velocity differences near the bed. Although the prediction capacity of Equation 2.6 is reasonable for the experiments investigated, the relationship is not useful for non-uniform flow conditions as it depends on the ratio  $R_h/d_{f50}$ , because  $R$  is probably not the most appropriate parameter.

On the basis of Equation 2.6 a simplified design equation has been recommended in CUR report 161:

$$\frac{d_{f15}}{d_{b50}} = \frac{\alpha}{C_0} \frac{R_h}{d_{f50}} \quad (2.7)$$

where  $\alpha = 9.5$  for base material with a  $d_{b50}$  in the range of 0.15 to 5 mm and  $\alpha = 19$  for base material larger than 5 mm, and  $C_0 \sim 15$ .

Using Equation 2.10 and assuming that  $V_{Gb} = V_{Gf}$ ,  $\Delta_b = \Delta_f$  and  $\Psi_{cb} = \Psi_{cf}$ , Equation 3.31 simplifies, thus  $r_{0,f} = r_0$  to:

$$\frac{d_{f50}}{d_{b50}} = \frac{1}{\eta} = \frac{1}{0.7r_0^2} \quad (3.34)$$

For uniform equilibrium and non-uniform gradually varied flows,  $r_0$  ranges typically from  $r_0 = 0.042$  (or  $\eta = 0.0012$ ) to  $r_0 = 0.126$  (or  $\eta = 0.0111$ ). For steep channel flow and non-uniform flow when  $0.2 < r_0 < 0.5$ , the value of  $\eta$  lies in the range of 0.028 to 0.18. Consequently, for very high turbulence intensities, say  $r_0 > 0.25$  (or  $\eta > 0.04$ , see also Equation 2.3) geometrically closed filters are required.

Van Huijstee et al. (1991) conducted experiments with bed turbulence above the top layer in which a distinction was made between simultaneous instability of base and top layer and instability of either top or base layer. In all these tests  $D_F/d_{f50}$  varied from 1.5 to 4.5 and the critical value of  $d_{f50}/d_{b50}$  ranged from 40 to 415. Equation 3.35 gives the relationship between the computed ratio of the median grain sizes and the ratio of the critical Shields parameters,  $\Psi_c$  (-), together with the inverse of the relative turbulence intensity,  $r_0$  (-). Figure 3.12 shows the critical value of  $[d_{f50}/d_{b50}]_{\text{measured}}$  when erosion occurs versus the critical value of  $[d_{f50}/d_{b50}]_{\text{computed}}$ :

$$\left[ \frac{d_{f50}}{d_{b50}} \right]_{\text{computed}} = \frac{1}{0.7r_0^2} \frac{\Psi_{cb}}{\Psi_{cf}} \quad \text{where } r_0 = 1.21 \frac{\sqrt{g}}{C} = 1.21\kappa \left( \ln \frac{12R_h}{2d_{f50}} \right)^{-1} \quad (3.35)$$

with  $\kappa$  is 0.4, the Von Kármán constant. Since most of the experiments consisted of situations with thin filter layers, 100% of the measurements lie in the range of  $0.5 < \zeta < 2$ , where  $\zeta$  is the ratio between the measured and computed value of  $d_{f50}/d_{b50}$ .

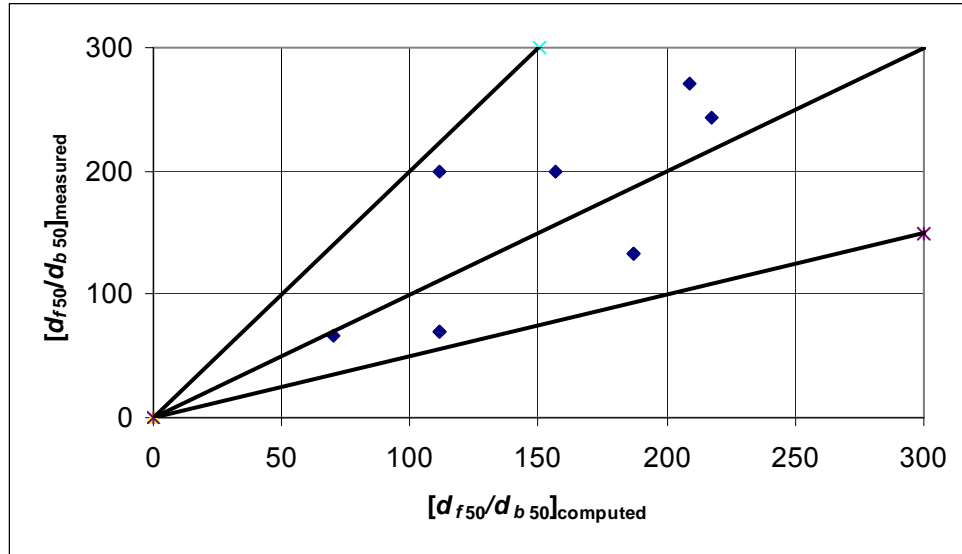


Figure 3.12 Critical values of  $[d_{f50}/d_{b50}]_{\text{measured}}$  versus values of  $[d_{f50}/d_{b50}]_{\text{computed}}$  (see also Eq. 3.35); Erosion occurred simultaneously in filter and base layer (Van Huijstee et al., 1991)

Wörman (1989) investigated granular filters at bridge piers. Based on accepted theories he arrived at the following relationship for a single layer bed protection under non-uniform flow conditions:

$$\frac{D_F}{d_{f15}} = 0.16 \frac{\Delta_f}{\Delta_b} \frac{n_f}{1-n_f} \frac{d_{f85}}{d_{b85}} \quad (2.9)$$

For nearly narrowly-graded materials when  $d_{b85}/d_{b50} = d_{f85}/d_{f50} = d_{f50}/d_{f15} \approx 1.25$ ,  $n_f = 0.4$ , and  $\Delta_b = \Delta_f$ , Equation 2.9 can be rewritten as:

$$\frac{D_F}{d_{f50}} = \alpha_W \frac{d_{f50}}{d_{b50}} \quad \text{with} \quad \alpha_W = 0.086 \quad (3.36)$$

According to Wörman (1989) Eqs. 2.9 and 3.36 do not include any safety factor. When Eq. 3.34 can be approximated by

$$\frac{d_{f50}}{d_{b50}} = \frac{1}{\eta} \quad (3.34)$$

and combining Eqs. 3.28 and 3.34 gives with  $d_{f50}/d_{f15} \approx 1.25$  for both uniform and non-uniform flow

$$\frac{D_F}{d_{f50}} = 1.6 \ln \left( \frac{\alpha_k d_{f50}}{d_{b50}} \right) \quad (3.37)$$

Consequently, Eqs. 3.36 and 3.37 are similar, since in both equations  $D_F$  depends on the ratio of  $d_{f50}$  and  $d_{b50}$ . Figure 3.13 shows Wörman's equation (Eq. 3.36), Eq. 3.37 as a best guess predictor with  $\alpha_k = 0.05$  (low turbulence) and an envelop curve by using  $\alpha_k = 0.5$  (high turbulence) as first approximations. In addition, experimental data is plotted for both uniform flow (Van Huijstee and Verheij 1991) and non-uniform flow (Wörman

1989). The interesting region for designing and assessing geometrically open filters in non-uniform flow is the stable part that lies above Eq. 6.31 and adjacent to the zone representing geometrically closed filters.

The differences between Eqs. 3.36 and 3.37 is the increase of  $D_F$  with respect to  $d_{f50}/d_{b50}$ . Wörman assumed that the decrease of the turbulence is under non-uniform flow

$$\eta_W = \tau_{bf} / \tau_0 = \alpha_W d_{f50} / D_F \tag{3.38}$$

Substituting Eq. 3.38 into Eq. 3.34, Eq. 3.36 is obtained, which results for large values of  $d_{f50}/d_{b50}$  in a more robust design. Since Wörman did not measure the local flow velocities and turbulence intensities in the open spaces of the filter layer, it is recommended to carry out experiments to validate the turbulence penetration under non-uniform flow.

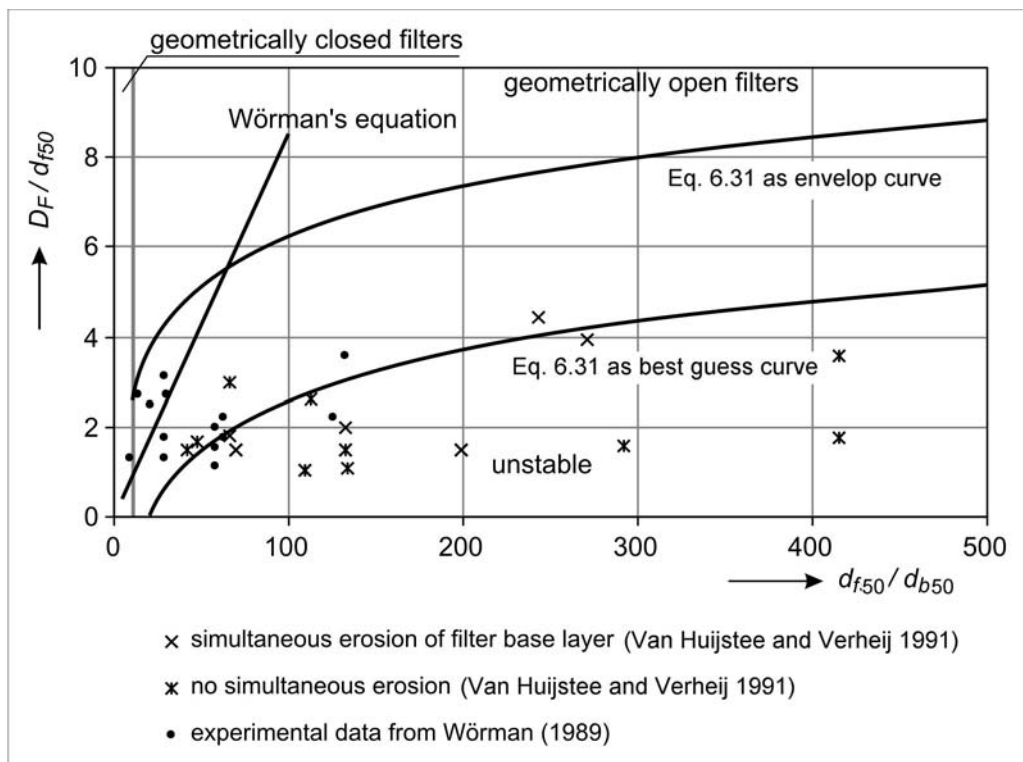


Fig. 3.13  $D_F/d_{f50}$  versus the critical  $d_{f50}/d_{b50}$ . Eq. 3.37 as best guess curve ( $\alpha_k = 0.05$ ; low turbulence); Eq. 3.37 as envelop curve ( $\alpha_k = 0.5$ ; high turbulence)

*example*

The Dordtsche Kil is a Dutch waterway near Rotterdam in which the bed gradually erodes. As a result, the fixed bed protection above tunnels and gas and water pipelines roughens the bed owing to sills, which gives extra turbulence in the river. To prevent the deepening of the scour holes and to protect the primary water defences against the failure mechanism liquefaction, Deltares proposed to fill the scour holes and to construct a geometrically open filter at the critical locations.

For design conditions, the soil and hydraulic parameters are:  $d_{b50} = 0.25$  mm,  $h = 10$  m,  $U_0 = 1.7 + 0.3 = 2$  m/s (0.3 m/s is a correction for shipping);  $r_0 = 0.18$  and is approximated by:

$$r_0 = \sqrt{0.0225 \left(1 - \frac{D}{h}\right)^{-2}} \quad (3.39)$$

in which  $D$  ( $= 1.5$  m) is the height of the sill.

The stability and the dimensions of the top layer are calculated by using Eqs. 6.15 and 6.37 with  $\Psi_c = 0.03$  and  $\alpha_k = 0.5$  giving  $d_{f50} = 0.2$  m and a required thickness  $D_{F,req} = 1.9$  m. To optimise costs, Deltares advised a two-layered system: a top layer with  $d_{f50} = 0.2$  m, a minimum thickness of  $D_{F,1} = 2d_{f50}$  and a filter layer with  $d_{f50} = 0.08$  m. The top and filter layer form a geometrically closed filter since the ratio between  $d_{f50}$  and  $d_{b50}$  is  $0.2/0.08 = 2.5$ . However,  $d_{f50}/d_{b50} = 0.08/0.00025 = 320$  thus the filter and base layer are geometrical open. By using Eq. 6.37 with  $d_{f50}/d_{b50} = 320$  and  $\alpha_k = 0.5$  yields  $D_{F,2} = 0.6$  m. Hence,  $D_{F,req}$  reduces from 1.9 m to  $D_{F,req} = D_{F,1} + D_{F,2} = 0.4 + 0.6 = 1.0$  m.

### 3.4 Sensitivity analysis

A sensitivity study has been conducted in order to evaluate the new design criteria for geometrically-open sand-tight filter structures. Basically the sensitivity of two equations, namely 3.31 and 3.37, has been evaluated within the scope of this work. A First Order Reliability Method (FORM) was used to evaluate the contribution of each parameter to the output. The method, also referred to as First Order Second Moment, can be used to estimate the mean (first moment) and the variance (second moment) of model output by computing the derivative of the model at a single point (Yen et al., 1986). This method is often used to evaluate the uncertainty propagation but it can also be used to evaluate the relative contribution of each parameter to the standard deviation of the model output, i.e. model sensitivity to input parameters. Such study could be of use to set up the priority for further investigations.

The first step in the FORM analysis is to approximate the system output solution of interest in Taylor series form. In the simplest form, a first-order Taylor series approximation requires computing the model output at a single point and determining the derivative, i.e. change of model output due a change in model input.

#### Equation 3.31

A reliability function in Taylor series is used by taking into account only the linear term. For instance, the reliability function based on Equation 1.1 can be expressed as:

$$Z = R - S = d_{f50\_acceptable} - d_{f50\_actual} \quad (2.1)$$

$$Z = d_{b50} \frac{1}{\eta} \frac{1 - \gamma V_{Gb}}{1 - \gamma V_{Gf}} \frac{\Psi_{cb}}{\Psi_{cf}} \frac{\Delta_b}{\Delta_f} - d_{f50\_actual} \quad (2.2)$$

where  $d_{b50}$  and  $d_{f50}$  are the median diameters of base and filter layer material respectively;  $\eta$  is the turbulence parameter for the filter layer;  $\gamma$  is the transport parameter;  $V_{Gb}$  and  $V_{Gf}$  are the variation coefficients for base and filter layer material respectively;  $\Psi_{cb}$  and  $\Psi_{cf}$  are the Shields parameters for base and filter layer material respectively;  $\Delta_b$  and  $\Delta_f$  are the relative densities of base and filter layer material respectively.

The first step is to find the derivative of the function Z for each variable. These should be independent from other variables in the function.

NOTE: Considering precisely, the value of  $V_{Gb}$  also depends somewhat on the  $d_{b50}$  value; however, this fact is ignored here to avoid the complication. It is assumed that it has no significant effect, as this parameter includes  $d_{b85}$  and  $d_{b15}$ , both of which are also unknown and have to be assumed for the analysis.

The derivative of the function Z (Equation 2.2) for each variable can be expressed as follows:

$$\frac{\partial Z}{\partial d_{b50}} = \frac{1}{\eta} \frac{1 - \gamma V_{Gb}}{1 - \gamma V_{Gf}} \frac{\Psi_{cb}}{\Psi_{cf}} \frac{\Delta_b}{\Delta_f} \quad (2.3)$$

$$\frac{\partial Z}{\partial \eta} = -\frac{1}{\eta^2} \frac{1 - \gamma V_{Gb}}{1 - \gamma V_{Gf}} \frac{\Psi_{cb}}{\Psi_{cf}} \frac{\Delta_b}{\Delta_f} = -\frac{1}{\eta} \frac{\partial Z}{\partial d_{b50}} \quad (2.4)$$

$$\frac{\partial Z}{\partial \gamma} = d_{b50} \frac{1}{\eta} \frac{V_{Gf} - V_{Gb}}{(1 - \gamma V_{Gf})^2} \frac{\Psi_{cb}}{\Psi_{cf}} \frac{\Delta_b}{\Delta_f} = \frac{d_{b50}(V_{Gf} - V_{Gb})}{(1 - \gamma V_{Gb})(1 - \gamma V_{Gf})} \frac{\partial Z}{\partial d_{b50}} \quad (2.5)$$

$$\frac{\partial Z}{\partial V_{Gb}} = -d_{b50} \frac{1}{\eta} \frac{\gamma}{1 - \gamma V_{Gf}} \frac{\Psi_{cb}}{\Psi_{cf}} \frac{\Delta_b}{\Delta_f} = -\frac{\gamma d_{b50}}{1 - \gamma V_{Gb}} \frac{\partial Z}{\partial d_{b50}} \quad (2.6)$$

$$\frac{\partial Z}{\partial V_{Gf}} = d_{b50} \frac{1}{\eta} \frac{\gamma(1 - \gamma V_{Gb})}{(1 - \gamma V_{Gf})^2} \frac{\Psi_{cb}}{\Psi_{cf}} \frac{\Delta_b}{\Delta_f} = \frac{\gamma d_{b50}}{(1 - \gamma V_{Gf})} \frac{\partial Z}{\partial d_{b50}} \quad (2.7)$$

$$\frac{\partial Z}{\partial \Psi_{cb}} = d_{b50} \frac{1}{\eta} \frac{1 - \gamma V_{Gb}}{1 - \gamma V_{Gf}} \frac{1}{\Psi_{cf}} \frac{\Delta_b}{\Delta_f} = \frac{d_{b50}}{\Psi_{cb}} \frac{\partial Z}{\partial d_{b50}} \quad (2.8)$$

$$\frac{\partial Z}{\partial \Psi_{cf}} = -d_{b50} \frac{1}{\eta} \frac{1 - \gamma V_{Gb}}{1 - \gamma V_{Gf}} \frac{\Psi_{cb}}{\Psi_{cf}^2} \frac{\Delta_b}{\Delta_f} = -\frac{d_{b50}}{\Psi_{cf}} \frac{\partial Z}{\partial d_{b50}} \quad (2.9)$$

$$\frac{\partial Z}{\partial \Delta_b} = d_{b50} \frac{1}{\eta} \frac{1 - \gamma V_{Gb}}{1 - \gamma V_{Gf}} \frac{\Psi_{cb}}{\Psi_{cf}} \frac{1}{\Delta_f} = \frac{d_{b50}}{\Delta_b} \frac{\partial Z}{\partial d_{b50}} \quad (2.10)$$

$$\frac{\partial Z}{\partial \Delta_f} = -d_{b50} \frac{1}{\eta} \frac{1 - \gamma V_{Gb}}{1 - \gamma V_{Gf}} \frac{\Psi_{cb}}{\Psi_{cf}} \frac{\Delta_b}{\Delta_f^2} = -\frac{d_{b50}}{\Delta_f} \frac{\partial Z}{\partial d_{b50}} \quad (2.11)$$

$$\frac{\partial Z}{\partial d_{f50\_actual}} = -1 \quad (2.12)$$

The next step is to calculate the value of each derivative for the mean value of each parameter. Consequently we need to assess the mean value of each parameter and also the standard deviation of each parameter to calculate the overall standard deviation (precisely saying, the variance) of the function  $F$ , which reads as:

$$\sigma_F^2 = \sum_{i=1}^P \left( \frac{\partial Z}{\partial X_i} \sigma(X_i) \right)^2 \quad (2.13)$$

where  $P$  is the number of input parameters;  $X_i$  is input parameter and  $\sigma(X_i)$  is the standard deviation of each parameter.

The contribution of each parameter to the standard deviation of the function can be calculated by using Equation (2.13) .

The specific data are not available for all parameters in order to calculate the mean value and the standard deviation, so we calculated them based on some tentative maximum and minimum values for each parameter as shown here:

$$X_{max} = X_{mean} + n \sigma(X_i) \quad (2.14)$$

$$X_{min} = X_{mean} - n \sigma(X_i) \quad (2.15)$$

According to so called empirical or three-sigma rule in statistics,  $n$  can be taken from 1 to 3. For a Gauss distribution, almost all values lie within three standard deviations from the mean value. In this case, we took  $n = 2$ ; i.e. within the range of twice the standard deviation, which implies that 95% of the values are within the range (considering Gauss distribution). This is generally accepted level, and thus appears to be appropriate for our sensitivity analysis in the absence of real data set. Then, the range of the values and thereby the expected standard deviation can be defined as:

$$Range = X_{max} - X_{min} = 4 \sigma(X_i) \quad (2.16)$$

$$\sigma(X_i) = (X_{max} - X_{min})/4 \quad (2.17)$$

We calculated the model sensitivity for four different cases selected from the available data for filter material:

- Case 1: filter material according to 10-60 kg with  $d_{f50\_actual} = 0.28$  m
- Case 2: filter material according to 63-180 mm with  $d_{f50\_actual} = 0.115$  m
- Case 3: filter material according to 40-100 mm with  $d_{f50\_actual} = 0.075$  m  
(minimum = 0.062 m and maximum = 0.088 m)
- Case 4: wide graded filter material with  $d_{f50\_actual} = 0.0375$  m  
(minimum = 0.025 m and maximum = 0.050 m).

For other inputs, we basically use universal (if available) or tentative values, and some parameters were related to the values of filter material. For example, data for  $d_{f50}$ ,  $d_{f15}$  and  $d_{f85}/d_{f15}$  of the filter material are available. We used them to define other variables

like  $d_{b50}$  (considering the retention criterion, namely  $d_{f50}/d_{b50} < 25$  (we used  $d_{f50}/d_{b50} = 25$ ). Similarly, we used available data  $d_{f50}$ ,  $d_{f15}$  and  $d_{f85}/d_{f15}$  to define  $V_{Gf}$ , and  $V_{Gb}$  was assumed to be 25% less than  $V_{Gf}$  as a criterion to reduce the mobility of fine material in the filter layer. Other parameters were assumed to be within tentative range as reported previously. Table 3.1 to

<b>Parameters</b>	<b>Xmax</b>	<b>Xmin</b>	<b>Xmean (<math>\mu</math>)</b>	<b><math>\sigma</math></b>
<i>db50</i>	0.00035	0.00005	0.00020	0.00010
$\eta$	0.0440	0.0012	0.0070	0.0110
$\gamma$	1	0.250	0.625	0.188
<i>VGb</i>	0.31	0.23	0.26	0.019
<i>VGf</i>	0.39	0.29	0.33	0.024
$\psi_{cb}$	0.057	0.037	0.047	0.005
$\psi_{cf}$	0.047	0.023	0.035	0.006
$\Delta b$	1.66	1.64	1.65	0.005
$\Delta f$	1.71	1.69	1.70	0.005
<i>df50_actual</i>	0.088	0.062	0.075	0.007

Table 3.4 give the values that were used for the various parameters in the calculations (for all four cases).

Table 3.1 Input parameters for case 1 – light armourstone 10-60 kg

<b>Parameters</b>	<b><math>X_{max}</math></b>	<b><math>X_{min}</math></b>	<b><math>X_{mean} (\mu)</math></b>	<b><math>\sigma</math></b>
$d_{b50}$	0.00035	0.00005	0.00020	0.00010
$\eta$	0.0440	0.0012	0.0070	0.0110
$\gamma$	1	0.250	0.625	0.188
$V_{Gb}$	0.19	0.15	0.16	0.011
$V_{Gf}$	0.24	0.18	0.20	0.014
$\psi_{cb}$	0.057	0.037	0.047	0.005
$\psi_{cf}$	0.047	0.023	0.035	0.006
$\Delta_b$	1.66	1.64	1.65	0.005
$\Delta_f$	1.71	1.69	1.70	0.005
$d_{f50\_actual}$	0.30	0.25	0.28	0.013

Table 3.2 Input parameters for case 2 – course grading 63/180 mm

<b>Parameters</b>	<b><math>X_{max}</math></b>	<b><math>X_{min}</math></b>	<b><math>X_{mean} (\mu)</math></b>	<b><math>\sigma</math></b>
$d_{b50}$	0.00035	0.00005	0.00020	0.00010
$\eta$	0.0440	0.0012	0.0070	0.0110
$\gamma$	1	0.250	0.625	0.188
$V_{Gb}$	0.40	0.20	0.28	0.050
$V_{Gf}$	0.50	0.25	0.35	0.063
$\psi_{cb}$	0.057	0.037	0.047	0.005
$\psi_{cf}$	0.047	0.023	0.035	0.006
$\Delta_b$	1.66	1.64	1.65	0.005
$\Delta_f$	1.71	1.69	1.70	0.005
$d_{f50\_actual}$	0.140	0.090	0.115	0.013

Table 3.3 Input parameters for case 3 – course grading 40/100 mm

<b>Parameters</b>	<b><math>X_{max}</math></b>	<b><math>X_{min}</math></b>	<b><math>X_{mean} (\mu)</math></b>	<b><math>\sigma</math></b>
$d_{b50}$	0.00035	0.00005	0.00020	0.00010
$\eta$	0.0440	0.0012	0.0070	0.0110
$\gamma$	1	0.250	0.625	0.188
$V_{Gb}$	0.31	0.23	0.26	0.019
$V_{Gf}$	0.39	0.29	0.33	0.024
$\psi_{cb}$	0.057	0.037	0.047	0.005
$\psi_{cf}$	0.047	0.023	0.035	0.006
$\Delta_b$	1.66	1.64	1.65	0.005
$\Delta_f$	1.71	1.69	1.70	0.005
$d_{f50\_actual}$	0.088	0.062	0.075	0.007



Table 3.4 Input parameters for case 4 - wide-graded material

Parameters	$X_{max}$	$X_{min}$	$X_{mean} (\mu)$	$\sigma$
$d_{b50}$	0.00035	0.00005	0.00020	0.00010
$\eta$	0.0440	0.0012	0.0070	0.0110
$\gamma$	1	0.250	0.625	0.188
$V_{Gb}$	0.28	0.20	0.24	0.020
$V_{Gf}$	0.35	0.25	0.30	0.025
$\psi_{cb}$	0.057	0.037	0.047	0.005
$\psi_{cf}$	0.047	0.023	0.035	0.006
$\Delta_b$	1.66	1.64	1.65	0.005
$\Delta_f$	1.71	1.69	1.70	0.005
$d_{f50\_actual}$	0.050	0.025	0.0375	0.006

The results of the calculations is presented in Figure 3.1: for the given combination of parameters for all cases, the trend is similar. Analysis shows that the most sensitive parameter appears to be the turbulence parameter for filter layer  $\eta$ . This can be attributed to the fact that the range of  $\eta$  is rather large due to the large range of relative turbulence intensities (ranging from uniform flow to high turbulence flow).

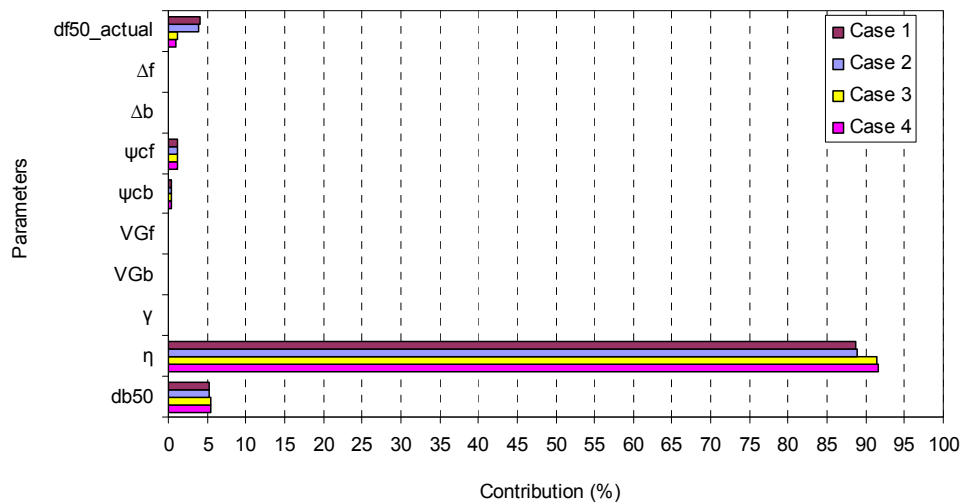


Figure 3.1 Contribution of parameters to the overall standard deviation of Equation 1.1

The sensitivity for  $\eta$  has been evaluated also by changing its value and thus reducing the deviation. The mean value of  $\eta$  has been changed in Case 1 and Case 2 to 0.01 with a standard deviation = 0.006. The results are shown in Figure 3.2 (Case 5 and 6 denotes the cases with changed  $\eta$ ).

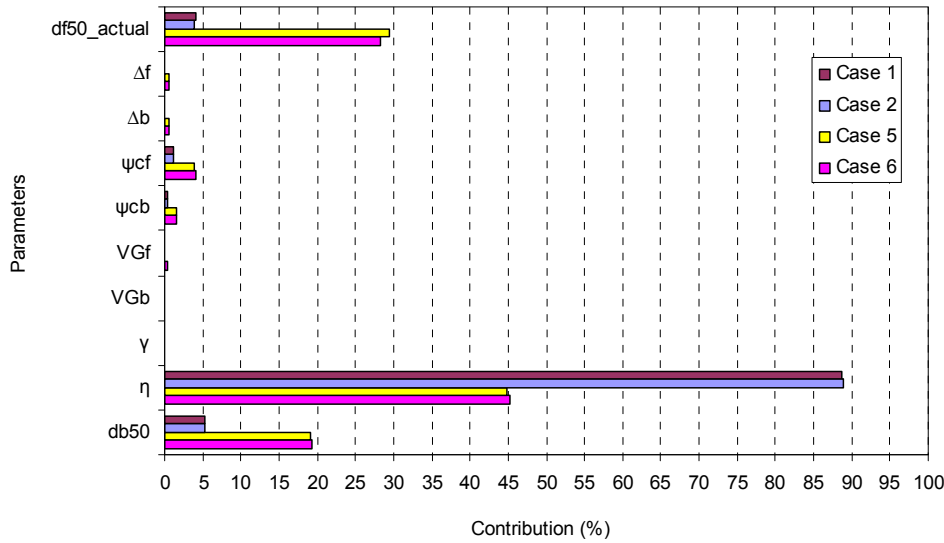


Figure 3.2 Contribution of parameters to the overall standard deviation of Eq. 1.1: Sensitivity of  $\eta$

Note that the above result indicates only that improvements of the accuracy of Equation 1.1 can be obtained by improving the accuracy of  $\eta$ . The result itself will not change as this is related to the absolute mean values of the different parameters in the equation. The range of  $d_{f50}/d_{b50}$  for case 4 (wide graded material) for the most sensitive parameter  $\eta$  is between 30 and 1140 (mean value 190).

**Equation 3.37**

Following the same approach as in section 2.2, the reliability function for Equation 3.37 assume three different filter layer thickness, i.e. 25 times, 10 times and 3 times the median diameter of filter layer material (i.e.  $D_{F\_actual} = n \cdot d_{f50}$ ) can be written as:

$$Z = 2d_{f15} \text{Ln} \left( \frac{\alpha_k d_{f50}}{d_{b50}} \right) - n d_{f50}$$

So, the derivatives of the function Z for each variable are as follows:

$$\frac{\partial Z}{\partial \alpha_k} = \frac{2d_{f15}}{\alpha_k} \tag{1.4}$$

$$\frac{\partial Z}{\partial d_{f50}} = \frac{2d_{f15}}{d_{f50}} - n \tag{1.5}$$

$$\frac{\partial Z}{\partial d_{f15}} = 2 \text{Ln} \left( \frac{\alpha_k d_{f50}}{d_{b50}} \right) \tag{1.6}$$

$$\frac{\partial Z}{\partial d_{b50}} = \frac{2d_{f15}}{d_{b50}} \tag{1.7}$$

We also used a constant value of DF<sub>actual</sub>, for which Eq. (5) has to be rewritten as:

$$\frac{\partial Z}{\partial d_{f50}} = \frac{2d_{f15}}{d_{f50}} \quad (1.5a)$$

with an additional equation:

$$\frac{\partial Z}{\partial D_{F\_actual}} = -1 \quad (1.8)$$

Analysis was conducted for four cases with different filter material for a couple of values for  $\alpha_k$ . (Table 1.1 to 1.4) and two cases with a graded sediment as filter layer (Table 1.5 and 1.6).

Table 1.1: For coarse filter layer material (Case 1)

$Y_i$	<i>max</i>	<i>min</i>	<i>mean</i> ( $\mu$ )	$\sigma(Y_i)$
$d_{f15}$	0.25	0.2	0.23	0.0125
$\alpha_k$	0.07	0.03	0.050	0.010
$d_{f50}$	0.3	0.25	0.28	0.0125
$d_{b50}$	0.00035	0.00005	0.0002	0.0001

Table 1.2: For coarse filter layer material (Case 2)

$Y_i$	<i>max</i>	<i>min</i>	<i>mean</i> ( $\mu$ )	$\sigma(Y_i)$
$d_{f15}$	0.105	0.063	0.084	0.011
$\alpha_k$	0.6	0.4	0.500	0.050
$d_{f50}$	0.14	0.09	0.115	0.0125
$d_{b50}$	0.00035	0.00005	0.0002	0.0001

Table 1.3: For coarse filter layer material (Case 3)

$Y_i$	<i>max</i>	<i>min</i>	<i>mean</i> ( $\mu$ )	$\sigma(Y_i)$
$d_{f15}$	0.25	0.2	0.23	0.0125
$\alpha_k$	0.6	0.4	0.500	0.050
$d_{f50}$	0.3	0.25	0.28	0.0125
$d_{b50}$	0.00035	0.00005	0.0002	0.0001

Table 1.4: For coarse filter layer material (Case 4)

$Y_i$	<i>max</i>	<i>min</i>	<i>mean</i> ( $\mu$ )	$\sigma(Y_i)$
$d_{f15}$	0.105	0.063	0.084	0.011
$\alpha_k$	0.07	0.03	0.050	0.010
$d_{f50}$	0.14	0.09	0.115	0.0125
$d_{b50}$	0.00035	0.00005	0.0002	0.0001

Table 1.5: For filter material with graded sediment (Case 1)

$Y_i$	<i>max</i>	<i>min</i>	<i>mean</i> ( $\mu$ )	$\sigma(Y_i)$
$d_{f15}$	0.0006	0.00025	0.0004	0.0001
$\alpha_k$	0.07	0.03	0.050	0.010
$d_{f50}$	0.02	0.01	0.015	0.003
$d_{b50}$	0.00035	0.00005	0.0002	0.0001

Table 1.6: For filter material with graded sediment (Case 2)

$Y_i$	<i>max</i>	<i>min</i>	<i>mean</i> ( $\mu$ )	$\sigma(Y_i)$
$d_{f15}$	0.0006	0.00025	0.0004	0.000
$\alpha_k$	0.6	0.4	0.500	0.050
$d_{f50}$	0.02	0.01	0.015	0.003
$d_{b50}$	0.00035	0.00005	0.0002	0.0001

Analysis of the cases with coarse filter material shows the sensitivity of the bed and filter materials ( $d_{f15}$ ) for most cases (Figure 1.1-1.3). For the same filter material and two different values of the coefficient  $\alpha_k$  (cases 1 and 3), show that contribution of  $d_{b50}$  is most pronounced for both cases, and also the contribution of finer size ( $d_{f15}$ ) is significant, particularly for case 3 with higher value of  $\alpha_k$ . Moreover, parameter  $\alpha_k$  appears to be somewhat sensitive for case 1. Comparing cases 2 and 4 (coarser material compared to previous cases), it can be seen that the contribution of  $d_{f15}$  is prevalent, particularly for case 2. Analyses were carried out for different value of actual filter layer thickness (3, 10 and 25 times median diameter of filter material respectively). Comparison shows that the sensitivity appears to be shifting towards the  $d_{f50}$  with larger value of actual filter layer thickness.

We analysed all these cases with a constant value of actual filter layer thickness with  $D_{F\_actual} (\mu) = 0.5$  m and  $\sigma (D_{F\_actual}) = 0.1$ . The result (Figure 1.4) shows the contribution of the  $d_{b50}$  and  $d_{f15}$  similar to the case of small filter layer thickness (i.e.  $D_F = 3d_{f50}$ ).

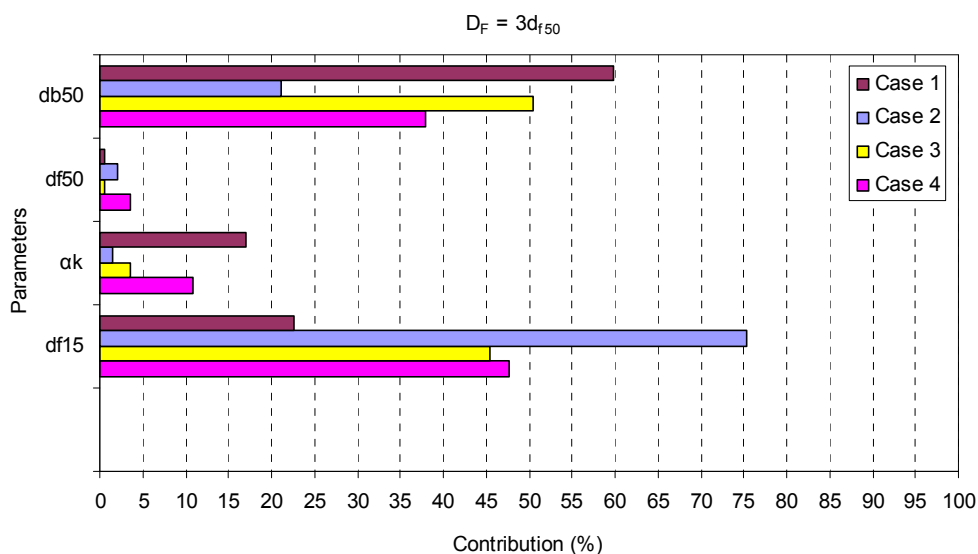


Figure 1.1 Contribution of parameters for different cases ( $D_F = 3d_{f50}$ )

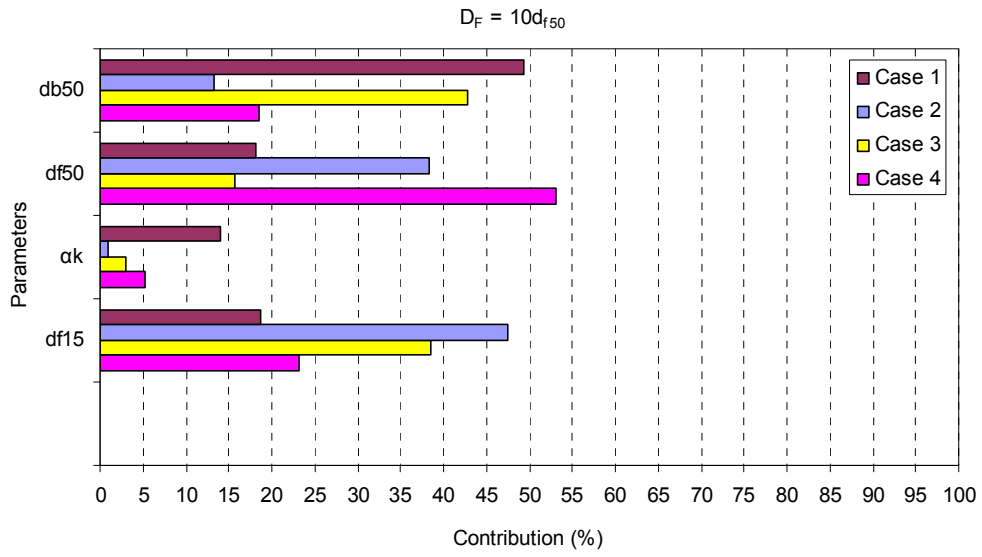


Figure 1.2 Contribution of parameters for different cases ( $D_F = 10d_{f50}$ )

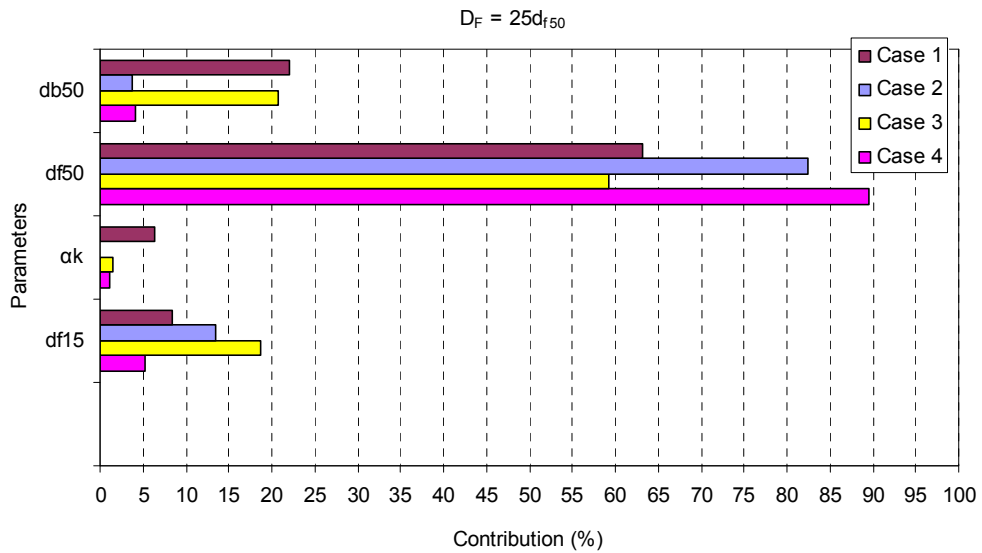


Figure 1.3 Contribution of parameters for different cases ( $D_F = 25d_{f50}$ )

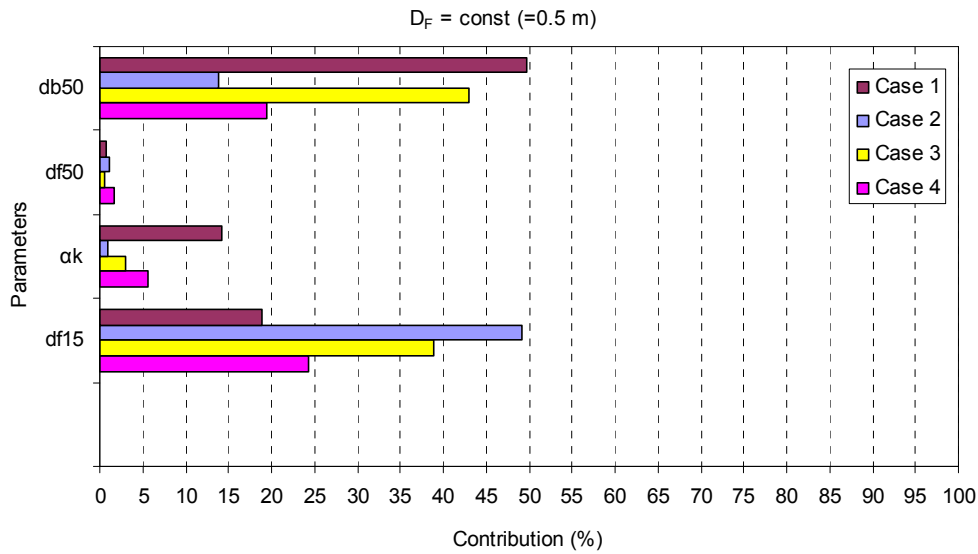


Figure 1.4 Contribution of parameters for different cases (constant  $D_F = 0.5 \text{ m}$ )

Also, we analysed the case with graded sediment for two different values of  $\alpha_k$  and different layer thickness (3 and 10 times  $d_{f50}$  respectively). The result is shown in Figure 1.5-1.6, which shows that all parameters except for  $d_{f50}$  are insensitive. This appears to be mainly due to the graded sediment filter material which is much finer than generally used filter material.

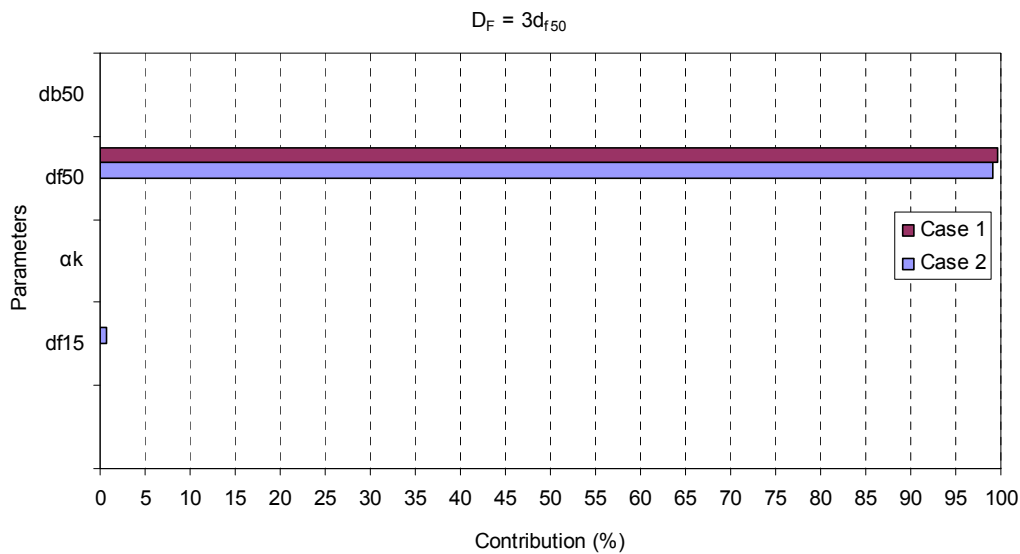


Figure 1.5 Contribution of parameters for filter layer with graded material ( $D_F = 3d_{f50}$ )

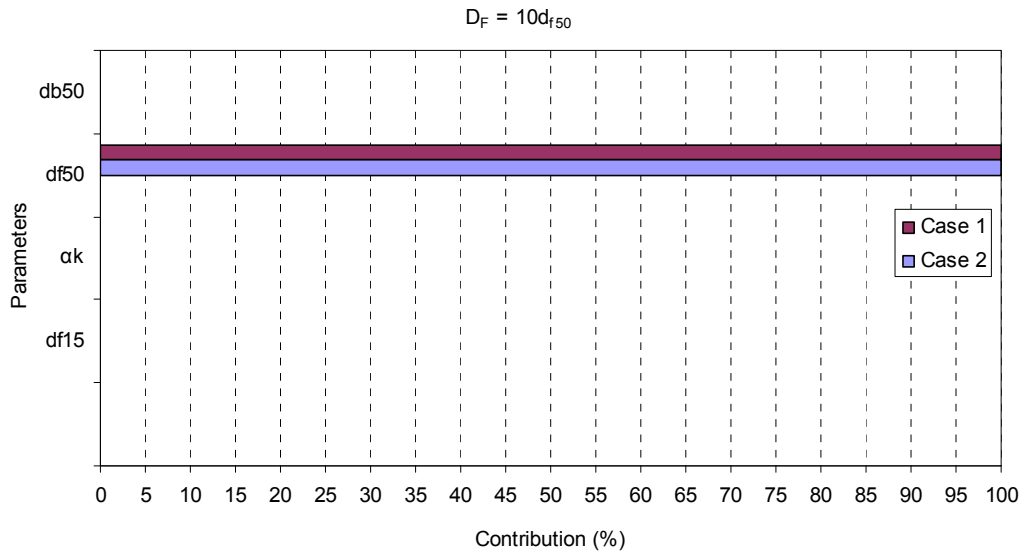


Figure 1.6 Contribution of parameters for filter layer with graded material ( $D_F = 10d_{f50}$ )

### 3.5 Conclusions and recommendations

For horizontal geometrically open filters without bed turbulence, equations that are based on Darcy’s law, the Forchheimer equation and the Chézy equation are deduced and validated using flume experiments. Equations 3.19 and 3.20 are valid for laminar and turbulent flow respectively.

Although the exact relationship between the inverse of the damping coefficient  $\xi$  in a filter material and its material properties is questionable, the type of relationship between characteristic length scale and particle size will hold (Equation 2.8), in spite of the fact that the assumptions for a continuum approach are violated. The practical considerations (Pilarczyk 1990, 1998) regarding the thickness of a filter layer ensure that fluctuations, as generated in open channel flow, are sufficiently damped.

For horizontal geometrically open filters with an open channel flow above the filter structure a new criterion for the interface stability of granular filters has been derived, based on accepted theories – Equation 3.31. The influence of the grading effects of grading and gradation of the filter and base materials has been discussed and illustrated qualitatively. Although Equation 3.31 has been validated using uniform flow tests, no validation has been carried out for non-uniform flow conditions. Wörman has validated his design method (Equation 2.9) using experimental data from filter layers around bridge piers where the flow is highly turbulent. However, the horseshoe vortices and the Kármán vortex streets are not representative for all types of non-uniform flow. It is recommended to verify Equation 3.31 for non-uniform flow and for graded materials to investigate the effects of armouring. Moreover, Deltares advises to check the validity of the decrease of turbulence (Equations 2.12 and 3.34) in thick filter layers by carrying out sufficient experiments.

## 4 Overview of knowledge gaps and quick wins

In Chapters 2 and 3 design formulas for granular filters are summarised. In this chapter knowledge gaps will be presented including a priority for possible research in the (near) future. Separately quick wins are mentioned.

However, first the relevant equations are summarised:

### 4.1 Summary of design methods

The following methods can be applied for the design of geometrically open sand-tight granular filters:

*Questions 1: filter layer thickness, and Question 2: wide-graded gravel mixtures*

- A new formula also taking into account the layer thickness reads as follows:

$$\frac{D_F}{d_{f50}} = 1.6 \ln \left( \frac{\alpha_k d_{f50}}{d_{b50}} \right) \quad (3.37)$$

Note: this formula has not been validated.

The following assumptions have been made:

- theoretical relationship for the relative turbulence in the filter (Equation 2.12) including the value of the damping factor  $\chi$ :

$$r_{0,f}^2 = r_0^2 \exp \left( - \frac{\chi D_F}{d_{f15}} \right) \quad (2.12)$$

- the value of the allowable transport is:  $\gamma = 0.625$

*Question 1: filter layer thickness at bridge piers*

- The Wörman formula can be applied for bridge pier protections although the equation is rather conservative (due to high turbulence resulting from the horseshoe vortices and the Kármán vortex streets and a value of 2 times the approach velocity):

$$\frac{D_F}{d_{f15}} = 0.16 \frac{\Delta_f}{\Delta_b} \frac{n_f}{1 - n_f} \frac{d_{f85}}{d_{b85}} \quad (2.9)$$

Equation 2.9 is applicable for:

- $d_{b85}/d_{b50} = d_{f85}/d_{f50} = d_{f50}/d_{f15} \approx 1.25$
- water depth - pier width ratios of 1.05 to 2.6, and
- filter thickness – pier width ratios of 0.15 to 0.28.

Question 2: wide-graded gravel mixtures

- Simplified Bakker/Konter-formula (CUR, 1993):

$$\frac{d_{f15}}{d_{b50}} = \frac{\alpha}{C_0} \frac{R_h}{d_{f50}} \quad (2.7)$$

where  $\alpha = 9.5$  for base material with a  $d_{b50}$  in the range of 0.15 to 5 mm and  $\alpha = 19$  for base material larger than 5 mm, and  $C_0 \sim 15$ .

The equation can be applied although it needs additional validation and another complication is the presence of the hydraulic radius  $R_h$  (in practice equal to the water depth). Probably  $R_h$  is not the most appropriate parameter; a local vertical length may be a better parameter.

The applicability of Equation 2.7 is limited to values of  $R_h$  smaller than 10 m.

- New formula based on a theoretical approach and taking into account the gradation of filter material via  $V_{Gf}$  and base material via  $V_{Gb}$ :

$$\frac{d_{f50}}{d_{b50}} = \frac{1}{\eta} \frac{1 - \gamma V_{Gb} \Psi_{cb} \Delta_b}{1 - \gamma V_{Gf} \Psi_{cf} \Delta_f} \quad (3.31)$$

where  $\eta$  represents the relative turbulence in the filter layer and reads:

$$\eta = \frac{\tau_{bf}}{\tau_0} = \left( \frac{r_{0,f} u_*}{r_0 U_0} \right)^2 = 0.7 r_{0,f}^2 \quad (3.8)$$

with

$$r_{0,f}^2 = r_0^2 \exp\left(-\frac{\chi D_F}{d_{f15}}\right) \quad (2.12)$$

Note: Equation 3.31 has been validated for uniform flow only; see Figure 3.11.

The following assumptions have been made:

- relative turbulence in the filter is linearly related to the relative turbulence in the flow (Equation 3.8)
- theoretical relationship for the relative turbulence in the filter (Equation 2.12) including the value of the damping factor  $\chi$ .

In principle, Equation 3.34 is valid for thin and thick filter layers.

Up to now, Equation 3.34 is applicable for:

- uniform flow conditions
- $D_F/d_{f50}$  in the range of 1.5 to 4.5
- $d_{f50}/d_{b50}$  ranged between 40 to 415.

A simplified version of Equation 3.31 reads:

$$\frac{d_{f50}}{d_{b50}} = \frac{1}{\eta} = \frac{1}{0.7 r_0^2} \quad (3.34)$$

Assumption: the relative turbulence in the filter equals the relative turbulence in the flow:  $r_{0,f} = r_0$

Equation 3.34 is only valid for thin filter layers.

- For wide-graded mixtures also the design method proposed by Cistin and Ziems (Heibaum, 2004) can be applied; see Figure 2.4.

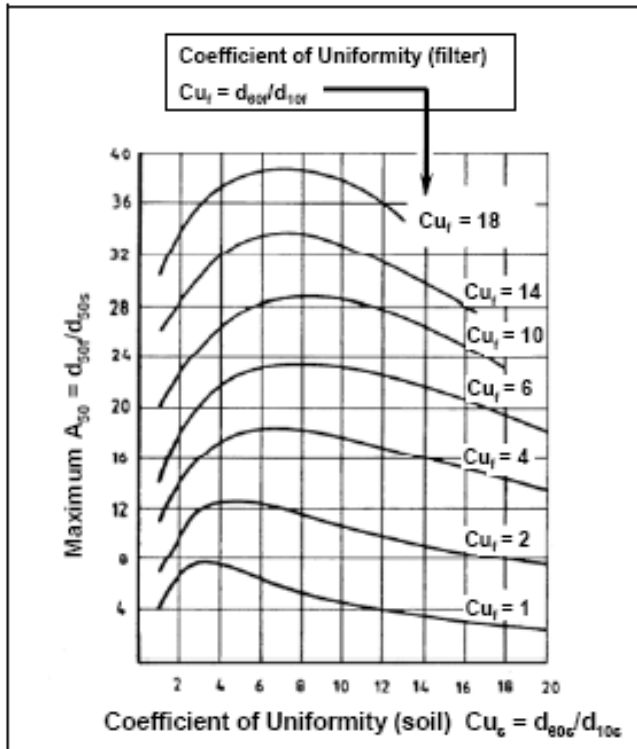


Figure 2.4 Granular filter design chart according to Cistin and Ziems (Heibaum, 2004)

**Note:** Not yet solved is the question how much wide-graded filter material has to be applied to create a stable filter structure, with stability at the interfaces water-filter material and filter material-base material. This aspect will be addressed more in detail in section 4.6.

#### 4.2 Knowledge gaps

The knowledge gaps are summarised in Table 4.1 and discussed shortly in the next sections. The intention is to carry out specific research to these aspects.

The priority of each knowledge gap has been mentioned as well as the option to obtain a quick win. The quick wins are discussed more in detail in section 4.3. Regarding the priority the following distinction has been considered:

- I knowledge gap resulting in “profit” by doing research
- II knowledge gap for which it is not clear whether research will give “profits”
- III knowledge gap for which research will not result in any “profit”

In order to avoid misunderstanding: “profit” means better knowledge enabling a better and more reliable design and application of granular filters. Obviously, this may result in safer and cheaper structures and probably shorter construction time.

Table 4.1 Overview of knowledge gaps and assumptions

No	Name knowledge gap	Priority	Quick win
1	Sensitivity analysis of Equations 3.31 and 3.37	I	yes
2	Validation Equation 3.31 for wide-graded material	I	no
3	Validation Equation 3.31 for non-uniform flow	I	no
4	Damping turbulence acc. to Equation 2.12 and 3.8 (inclusive order of magnitude of $\chi$ )	I	yes
5	Validation Equation 3.34 for thin filters	III	yes
6	Validation Equation 2.7 for non-uniform flow	- )	no
7	Validation Equation 3.37 for uniform and non-uniform flow	I	no
8	Equations for short hydraulic loads are missing	I	no
9	Adaptation of the Wörman equation 2.9	II	yes
10	Design method for armouring of a filter structure (armouring)	I	yes/no

) Equation 3.31 is more important than Equation 2.7 because the perspectives are better.

Although not the scope of this study, the literature review made clear that there is hardly information on the interface stability of granular filter structures in conditions with wave attack. From that point of view it obviously is a knowledge gap; it is, however, not a quick win. It is recommended to carry out a study similar to the present one, e.g. literature search resulting in an overview of knowledge gaps with respect to interface stability under wave attack.

#### 4.2.1 Non-uniform flow

The knowledge gaps 3, 5, 6, 7 and 8 address non-uniform and/or non-permanent flow conditions. Non-uniform is defined here as rapidly changing flow. Gradually changing flow is for this study assumed to be 'part' of the uniform flow conditions.

Equation 3.31 (knowledge gap 3, priority I) addresses the influence of the grading width and has already been validated for uniform flow using the Van Huystee et al (1991) test results.

The same holds for equation 2.7 (knowledge gap 6, no priority). However, since Equation 3.31 offers more perspectives than Equation 2.7 the last one will not be considered from hereon.

Equation 3.37 (knowledge gap 7, priority I) has not been tested for uniform flow conditions either.

Validation of the Equations 2.7, 3.31 and 3.37 requires physical model tests. These tests are time consuming and costly, and consequently no quick wins. Nevertheless, it is recommended to carry out these tests because of the high priority to have available validated relationships.

Relationships for non-permanent and short hydraulic loads are missing (knowledge gap 8, priority I). A short literature search did not provide relationships for the interface stability for this type of flow conditions. It is recommended to carry out a more intensive literature search and, in addition, a theoretical study in which a method will be developed. Obviously, this is not a quick win.

#### 4.2.2 Wide-graded material

The knowledge gaps 2, 5 and 10 deal with wide-graded filter materials.

Equation 3.31 (knowledge gap 2, priority I) has been derived for wide-graded filters and validated for uniform flow conditions. Further validation requires physical model tests and consequently, this is not a quick win.

Equation 3.34 (knowledge gap 5, priority III) is valid for thin wide-graded filters. Although the priority is low, this relationship can be validated quickly with available data.

Knowledge gap 10 (armouring) refers to the required minimum thickness of a filter structure of which the material in the upper part will become stable due to armouring (after preceding erosion of fines), while it complies with the requirement of interface stability with the base material.

#### 4.2.3 Damping of turbulence

Knowledge gaps 4 and 9 address the damping of the relative turbulence in the filter layer due to the layer thickness. The damping is assumed to follow the relationship according to Equation 2.12 (knowledge gap 4, priority I) with the damping factor  $\chi$ .

It is recommended to carry out a desk study to the value of  $\chi$ .

Equation 2.9 (knowledge gap 9, priority II) is the Wörman formula for bed protections around bridge piers. This formula implicitly contains a damping factor for the turbulence. It can be interesting to adapt the Wörman formula to conditions comparable with a bed protection downstream of a hydraulic structure.

### 4.3 Quick wins

Quick wins are defined as research that is highly effective in terms of research investments and practical applications (when successful).

The present review of the state-of-the-art of design of filter layers as an effective measure for scour erosion shows that different formulae are derived that take into account the complex flow structure above the filter (including high turbulence), in the filter(s) and at the interface between the (lowest) filter and the base material.

Hence, the effects of non-uniform flow and high turbulence may be incorporated well in filter layer design.

At the other hand, some inconsistencies are still present between the different formulae. In addition, the complex and empirical nature of many of the formulas often requires a large number of parameters to be assumed in order to arrive at useful answers.

Based on this observation, the following quick-wins are identified:

- Knowledge gap 1: A sensitivity study can give insight into the limitations of Equations 3.31 and 3.37. This makes the setup of model tests easier.
- Knowledge gaps 4: Measurements are available of Wenka et al (2007). These measurements can be used easily for increasing the applicability of Equation 3.31 as well as 2.12 for the influence of layer thickness and damping of turbulence respectively. A limited desk study will already give proper results.

- Knowledge gap 9: The Wörman equation can be improved (viz making it less conservative) by using available bridge pier data.
- Knowledge gap 5: Equation 3.34 can be easily checked with available data, although its priority is low.
- Knowledge gap 10: Development of a design method for the required thickness of a filter structure of which the upper part becomes stable due to armouring.

#### 4.4 Hydraulic modelling

Not a quick win, but a phased hydraulic modelling program may underline and extent the data of Van Huijstee et al (1991). As proper data are scarce, especially related to systematically varied turbulence intensities, filter thicknesses and filter gradings, experiments are necessary for further calibration, tuning and refinement of the formulae as proposed in this report. The phasing of these tests may be such that maximum practical spin-off is gained in the earliest stages. As an example: it seems to be worthwhile to start with tests that demonstrate (practical) maximum layer thicknesses and practical limits of filter gradation first. Next, further tests can be carried out that satisfy more scientific goals, based on expectations of practical spin-off. This step-by-step approach will strongly lean on progressive practical and scientific knowledge.

Furthermore, from a practical point-of-view it is important to verify the sensitivity of the interface stability for increasing the number of layers. E.g.: when increasing a bed protection by one or two layers to ascertain the stability, this may be practical. However, increasing the number of layers by 5 to 10 layers will usually not be practical.

#### 4.5 Evaluation

In the preceding sections the knowledge gaps and quick wins are discussed as well as the required efforts to validate the derived equations for non-uniform flow conditions. However, one practical design idea for upgrading a present filter protection (that is not sufficient as regards the stability of the interface) has not been mentioned yet. This idea is to feed ('sprinkle') fine materials in the top layer, provided that this top layer is rather coarse and narrow-graded. When carefully dimensioned, these fine materials will not decrease the stability of the top layer and will be stable themselves (by hiding effects). These fine materials, however, may significantly increase the stability of the interface below the top layer and probably also the lower interfaces in case of multiple layers. The outcome of the white spot research as mentioned above, may indicate the usefulness of such a promising application. As an advantage above increasing the number of top layers, the flow blocking effect will not change and we anticipate that this application will be much more cost effective. When the above research shows positive results, some pilot testing may be required to explore and demonstrate this application in practice.

#### 4.6 Possible approach to estimate the thickness (reduction) of wide-graded layers

Finally, the question: is it possible at this point in time to make a design of a bed protection that consists of wide-graded material?

Based on the foregoing section the answer should be: No. An accepted proven method for the assessment of transport of fines and the subsequent armouring process of wide-

graded gravel mixtures is not available. That is also the reason why ‘armouring’ is included in the list of the knowledge gaps (see Table 4.1).

However, some promising results and proposed approaches can be found in literature, for instance the results of Sumer et al (2001) and Dixen et al (2008). Their method has, however, not been verified yet. Furthermore, results of the studies within the framework of the design and construction of the Deltaworks indicated that the thickness of wide-graded gravel mixtures with  $d_{85}/d_{15} \approx 10$  could reduce by 4 to  $5d_{85}$ . In a subsequent quick win study these methods will be discussed in more detail.

Until further guidance is published, the alternative is to follow a pragmatic approach. Suppose the boundary conditions are known, i.e. the hydraulic load  $U_0$ , the characteristics of the wide-graded gravel mixture ( $d_{15f}$ ,  $d_{50f}$  and  $d_{85f}$ ) and the characteristics of the base material,  $d_{15b}$ ,  $d_{50b}$  and  $d_{85b}$ . The following procedure is proposed:

- 1 Determine with Shields the median size of the material of the top layer of the bed protection required to ensure stability against current attack,  $d_{50a}$ ; this is the characteristic size of the top layer after washing out of the fine material, i.e. after ‘armouring’.
- 2 Assume that all particles larger than this required median size,  $d_{50a}$ , are stable and that finer particles will erode until a top layer mixture results with a median particle size equal to  $d_{50a} = d_{i\%,f}$ , where  $d_{i\%,f}$  is the size below which  $i\%$  of the mass of the parent wide-graded filter material is falling. Usually, a secondary layer, consisting of parent material characterised by  $d_{50f}$ , will remain; an extreme situation may, however, occur in the case that no parent material remains.
- 3 The amount of material that has been washed out from the (top part of the) wide-graded mixture can be assessed as follows: the amount of particles in the armoured layer larger than  $d_{50a}$  is equal to the amount smaller than  $d_{50a}$  ( $= d_{i\%,f}$ ). Hence, the total amount of top layer material is:  $2(100 - i)\%$  of the original amount of wide-graded material. The amount washed out is then:  $100 - 2(100 - i)\% = (2i - 100)\%$ .
- 4 The ratio  $d_{50a}/d_{50f}$  is in most cases  $\ll 20$  (the criterion for geometrically closed filters), which means that the thickness of the top layer cannot be evaluated using Equation 3.37. The required thickness of the top layer to guarantee stability can be assessed at  $D_a = 2d_{50a}$ , which is a safe and reasonable assumption in the case of a remaining secondary layer of parent wide-graded material. The amount of wide-graded material to be placed before armouring is taking place,  $D_0$ , can be calculated as the thickness of the (remaining) underlayer,  $D_u$ , plus the initial thickness of the top layer subject to ‘armouring’,  $D_{0,a} = 100/[2(100 - i)]D_a$ .

**Note:** To assume a linear relationship between volume (or mass) and thickness is quite conservative, as part of the relative fine material that is washed out, originates from the voids between the coarser particles.

- 5 For the extreme situation – no parent wide-graded material left between armoured top layer and base material – the interface stability should be evaluated with Equation 3.37. If not meeting this criterion, the layer thickness has to be larger than the minimum of  $2d_{50a}$ . For the usual situation – with a remaining layer of parent material between base and top layer, the interface stability has also to be evaluated. The first check is the geometrical sand tightness (e.g.  $d_{15f} < 5d_{85b}$  or

$d_{50f} < 20d_{50b}$ ); if this criterion is satisfied, that interface is stable. If it is not geometrically sand-tight, the same Equation 3.37 can be used for this purpose. Note that the relative turbulence intensity of the underlayer should be used instead of the usual parameter,  $r_0$ . As the 'armoured' top layer is relatively thin, the turbulence intensity in both flows is assumed to have the same order of magnitude.

6 Finally, the internal stability and the permeability should be checked.

The following example may illustrate the procedure.

Ad 1: Suppose that the wide-graded mixture can be characterised by:  $d_{50f} = 0.15$  m and that the top part has to consist of stones with a median size of  $d_{50a} = 0.30$  m to be stable (based on Shields or another accepted method).

Ad 2: Use the cumulative distribution curve of the mixture to assess which  $d_{i\%,f}$  value corresponds to  $d_{50a}$ . In this example, this median size is equal to  $d_{80f}$  ( $i = 80$ ) of the parent wide-graded material.

Ad 3: Part of the fine material of the parent wide-graded mixture will erode until a mixture results with  $d_{50a} = 0.30$  m. The amount of material of the new armoured top layer larger than 0.30 m equals the amount smaller than 0.30 m. Both represent 20% of the top part of the original wide-graded mixture, because  $d_{50a} = d_{80f} = 0.30$  m. The amount of eroded material is then: 60%, =  $(2 \cdot 80 - 100)\%$ .

Ad 4: The filter layer is geometrically closed, as the ratio  $d_{50a}/d_{50f}$  is  $\ll 20$ . Hence the thickness of the armoured layer can be assumed to be  $D_a = 2d_{50a} = 0.60$  m, which is regarded to be the minimum. The required initial thickness of the top part of wide-graded material amounts to:  $D_{0,a} = 100/[2(100 - i)]D_a = 5/2 \cdot 0.60$  m = 1.50 m. The minimum thickness of the underlayer,  $D_u$ , is  $2d_{50f} = 0.30$  m. The total thickness initially required amounts to:  $D_0 = 1.80$  m, which is equal to  $12d_{50f}$ .

Note that the reduction of the thickness using this approach is not much different from the results of the Deltaworks studies as mentioned above.

Ad 5: For the extreme situation – no intermediate layer of parent material – the interface stability at the base layer can be evaluated using Equation 3.37 (assuming that  $V_{Gb} = V_{Ga}$ ,  $A_a = A_b$  and  $\Psi_{ca} = \Psi_{cb}$ ). To this end the values of the turbulence intensity,  $r_0$ , the damping factor,  $\chi$ , the median size of the base material,  $d_{50b}$ , and  $d_{15a}$  have to be estimated: assume  $r_0 = 0.2$ ,  $\chi = 0.2$ ,  $d_{50b} = 500$   $\mu$ m and  $d_{15a} = 0.20$  m. Using Equation 3.37 gives:  $D_F = D_a = 2.90$  m. Such a large thickness (5 times as much as the minimum of  $D_a = 0.60$  m) could be expected in view of the large ratio of  $d_{50a}$  to  $d_{50b}$  (= 600). Alternatively, the maximum value of  $d_{15a}$  could be calculated given the minimum thickness of  $D_F = 0.60$  m. The result would be:  $d_{15a,max} \leq 40$  mm, which is  $\ll d_{15a}$  ( $\approx 200$  mm). This means that the total layer thickness after armouring must be larger than  $2d_{50a}$ , so that a double layer system can develop; or, in other words, the original layer thickness should be  $D_0 = D_{0,a} + D_u = 1.80$  m.

The interface between parent wide-graded material and base layer: As  $d_{50f}/d_{50b}$  (= 300)  $\gg 20$ , this is a geometrically open filter. The thickness and maximum value of  $d_{15f}$  have to be evaluated using Equation 3.37. Assuming the same values of the parameters as used above and  $d_{15f} = 40$  to 50 mm), the minimum thickness is:  $D_F = 0.4$  m; this is a conservative approach, because damping of turbulence in the top armoured layer is neglected. The thickness applied (0.3 m) should therefore be slightly increased. Note, however, that the assumption  $r_{0,f} \cong r_0$  still has to be validated for such filters.

Ad 6: Subsequently, the internal stability and the permeability can be evaluated.

An alternative for the procedure described above might be to compute the amount of transport of filter material with the use of an appropriate sediment transport formula or

filter transport model, for instance the Egiazaroff formula (Equation 2.10), followed by a computation of the reduction in thickness and the new grading width of the filter material.

It is recommended to carry out a desk study to see whether the procedure can be used.

## 5 QW-3: Adjustment of Wörman for a bed protection

The Wörman formula is derived for the bed protection around bridge piers. This quick win is to see whether it would be possible to adjust Wörman formula for the conditions of bed protection under low turbulence.

The Wörman formula reads as follows:

$$\frac{D_F}{d_{f15}} = 0.16 \frac{\Delta_f}{\Delta_b} \frac{n_f}{1-n_f} \frac{d_{f85}}{d_{b85}} \quad (3.1)$$

where,  $\Delta_f$  and  $\Delta_b$  = relative density of filter and bed material respectively;  $n_f$  = porosity of filter material,  $d_{f85}$  and  $d_{b85}$  = grain diameter (finer of which is 85%) for filter and the base material respectively.

Formula (3.1) was developed for riprap protection (without filter layer) around the bridge pier. The turbulence around the structure is considerably high due to the structure-induced non-uniform flow. For the case of bed protection, only near-bed turbulence should be considered. Wörman formula, however, does not consider turbulence explicitly. He used a simple approach for the pressure gradient inside riprap layer (he found a linear relation) and parameterized it in the form of a non-dimensional parameter based on his experiments.

In his derivation (Worman, 1989), he used following non-dimensional incipient erosion criterion for base material through riprap:

$$\left( \frac{U^2}{g\Delta L} \right)_{cr} \sim \frac{\beta}{C_D} \frac{d_{b85}}{d_{f15}} \frac{1-n_f}{n_f} (S_s - 1) \quad (3.2)$$

In which,  $U$  = mean velocity of undisturbed flow;  $S_s$  = specific grain density ( $= \rho_s / \rho_w$ );  $\Delta L$  = infinitesimal distance over which a pressure gradient in the riprap layer is defined (which was found to be proportional to riprap thickness,  $D_F$ );  $\beta$  = friction factor for turbulent flow, and  $C_D$  = drag coefficient for the grain.

So, the variable  $\beta$  appears to include turbulence effect, which was found to be constant from his experiments. He fitted the critical value of this parameter with relative material property (Figure 1). So, the region below this threshold line is stable. However, it can be seen that the equation is valid only for the range  $0 < d_{b85}/d_{f85} < 0.1$  as in case  $d_{b85}/d_{f85} > 0.1$ , the value of  $U^2/gD_F$  is significantly large. Worman has recommended to restrict the generalization of this equation for the base material size larger than in his experiment.

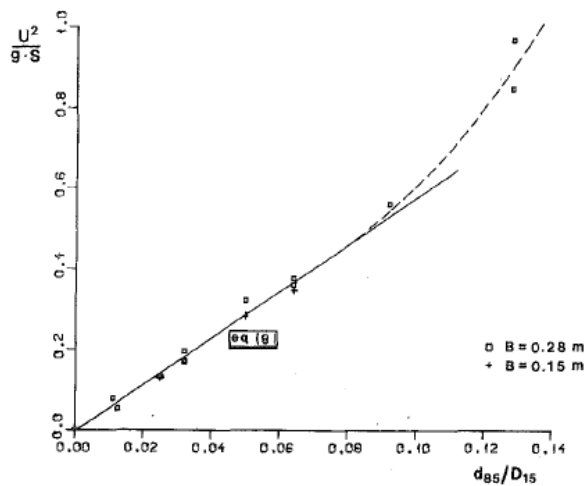


Figure 1: Fitting curve for non-dimensional parameters considering initiation of erosion of base material on upstream side of the pier (After Worman, 1989;  $D_{15}$  is  $d_{f15}$  and  $S$  is  $D_F$  in our notation).

Furthermore, he used Izbash formula for determining grain size of riprap material based on critical velocity as follows:

$$u_{cr} = 0.85\sqrt{2g(S_s - 1)D} \tag{3.3}$$

where,  $D$  = grain size of filter material (Worman assumed  $D = d_{f85}$ ).

As per suggestion by Breusers et al. (1977), he chose the value of twice the mean velocity of undisturbed flow (i.e.  $u_{cr} = 2U$ ), and also evaluating  $\beta/C_D$  from their experiments he reached to his original formula (3.1).

Worman did not mention the value of  $\beta/C_D$  in the paper. Based on his relation, we found following:

$$0.361 \frac{C_D}{\beta} = 0.16 \tag{3.4}$$

This implies that the effect of turbulence is incorporated implicitly.

We can rewrite equation (3.1) with a new coefficient of proportionality ( $\alpha$ , which is equal to 0.16 for the original equation (3.1)), and try to evaluate comparing with the available experiments:

$$\frac{D_F}{d_{f15}} = \alpha \frac{\Delta_f}{\Delta_b} \frac{n_f}{1 - n_f} \frac{d_{f85}}{d_{b85}} \tag{3.5}$$

For his own data, it can be seen that the prediction by the equation does not fit as an envelop curve for his experimental data (Figure 2). Also, it shows rather high filter layer thickness for the cases with low turbulence.

The Worman equation tends to be near the data of Van Huijstee and Verhij with considerably low value of  $\alpha$  ( $<0.04$ ; not shown here). Moreover, it cannot be used as an envelop curve as it is a linear function.

So, improvement is necessary considering the turbulence under uniform flow, and the damping of turbulence in filter layer. For this, we can refer to the recent work of Hoffmans et al. (2009).

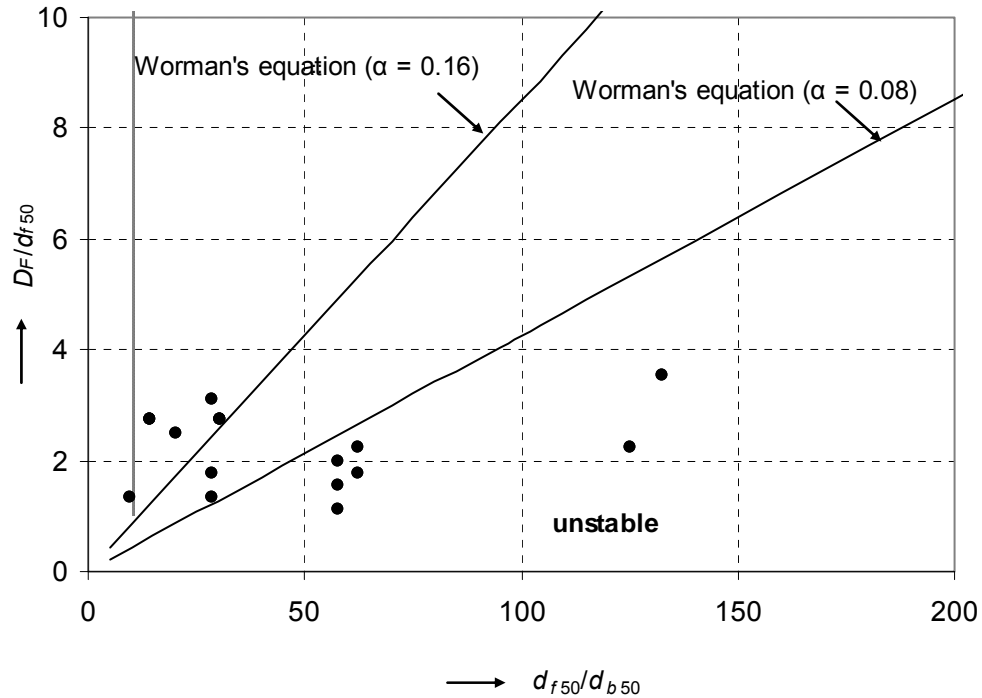


Figure 2: Prediction using Wörman formula (lines) for his experiments (dots)

We have attempted to linearise our previously proposed equation (Verheij et al., 2008) in order to make a fair comparison with Wörman formula. Based on the experiments of Klar (2005), Hoffmans et al. (2009) derived the following relationship for the relative load ( $\eta$ ) for  $D_F > 2d_{f15}$ :

$$\eta = \tau_{bf} / \tau_0 = \alpha_k \exp\left(-\frac{1}{2} D_F / d_{f15}\right) \tag{3.6}$$

Combining equation (3.6) with an approximated relationship,

$$\frac{d_{f50}}{d_{b50}} = \frac{1}{\eta} \tag{3.7}$$

and assuming  $d_{f50}/d_{f15} \approx 1.25$ , we get:

$$\frac{D_F}{d_{f50}} = 1.6 \ln\left(\frac{\alpha_k d_{f50}}{d_{b50}}\right) \tag{3.8}$$

Basically, this formula is identical to Wörman's relation, but it considers the turbulence damping. Also, formula works for both low and high turbulent flow with different coefficient  $\alpha_v$  (which is proposed to be varied from 0.05 to 0.5 depending on the flow condition (uniform or non-uniform with high turbulence)).

Now, we simply consider a linear approach as:

$$\eta = \alpha_v \left( \chi_l^{-1} \frac{d_{f15}}{D_F} \right) \tag{3.9}$$

This gives us a linear relationship identical to Wörman equation as follows:

$$\frac{D_F}{d_{f15}} = \alpha_v \chi_l^{-1} \frac{d_{f50}}{d_{b50}} \tag{3.10}$$

$d_{f50} \approx 1.25d_{f15}$ . Comparison for different cases can be seen in Figure 3 below. This figure shows the comparison between predictions by using Wörman formula and new formula considering turbulence damping. Also, the prediction of a linear formula. From the result it can be seen that with highest value of  $\alpha_v$ , an envelop curve can be obtained that covers both cases with high (structure-induced) and low turbulence, whereas lower value appears to be appropriate for the uniform flow with low turbulence (as in experiments of Huijstee and Verheij, 1991). For the linear formula, we use  $\alpha_v = 0.05$  (for low turbulence as in non-linear case), and  $\chi_l = 1.2$ . For the high turbulence, coefficient  $\chi_l$  will be higher. One can see from the figure (and from the relationship) that for some specific combination of coefficient for high turbulence, our linear relationship (Eq.(3.10)) would give similar result as Wörman's equation.

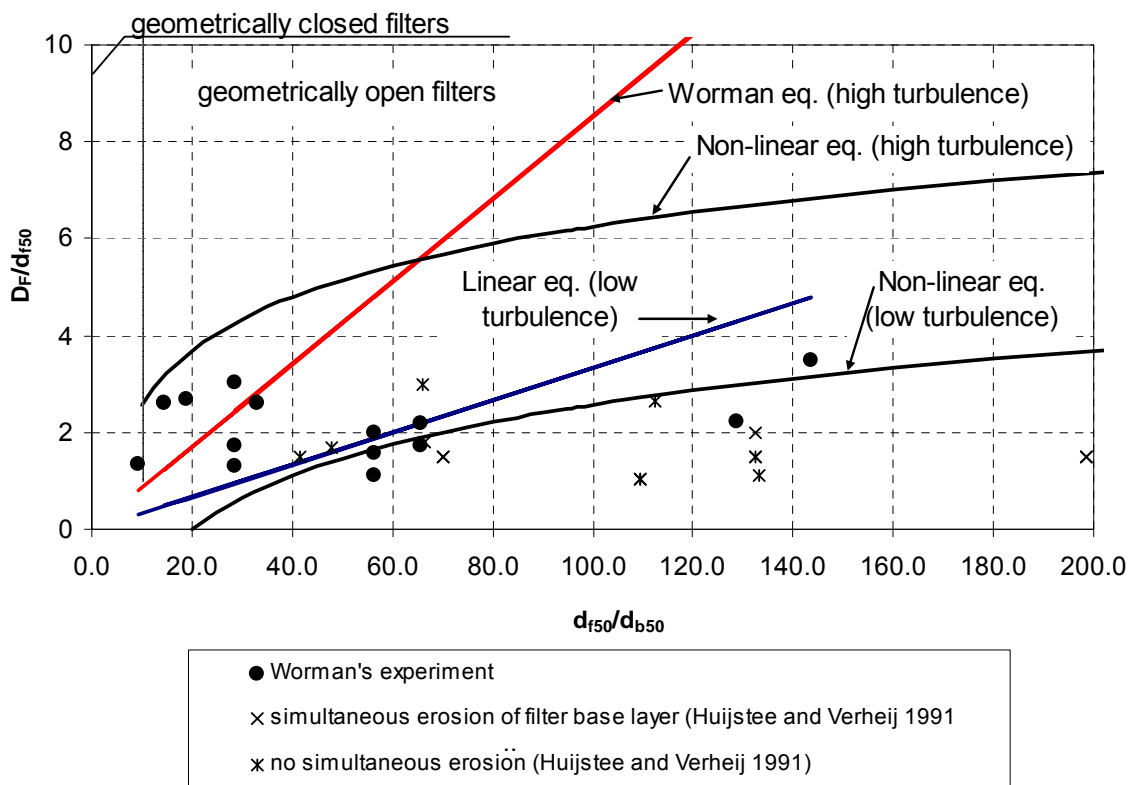


Figure 3: Comparison of different approach with experiments

Conclusions

- 1- In order to implement Wörman equation for low turbulence, the parameter  $(U^2/gD_F)_{cr}$  should be defined for the case of filter layer without presence of

structure. For this purpose, relevant experimental data is necessary (with respect to the condition of initiation of erosion of base material).

- 2- The linear function presented here (Eq.(3.10)) which is identical to Wörman equation can be regarded as a version of Wörman equation for low turbulence case (or simply use Wörman equation with low coefficient  $\sim 0.08$ , which gives almost similar result as this linear equation).
- 3- The equation with non-linear damping proposed in our previous study can be regarded as an improvement over Wörman's equation, and can be used for low turbulence situation (normal situation without structure).

## 6 QW-5: Design of a thick bed protection consisting of wide-graded material

In Section 4.6 a procedure has been presented for designing the thickness of wide/graded layers. Here the transport of wide-graded sand-gravel sediment will be considered which is applied as bed protection. Transport of graded sediment is a dynamic and complicated process to be described in a simple manner. Nevertheless, number of works have been conducted so far to describe the graded sediment as well as gravel bed transport processes.

In general, two basic approaches of graded sediment transport can be considered:

- 1 by using a conventional approach of bed load transport (basically used for uniform sediment) to compute fractional transport of sediment mixture considering hiding and exposure effect (as proposed by Ashida-Michiue with modified Egiazaroff approach, 1972; Wu et al., 2000 with Van Rijn's transport equation), and
- 2 the surface-based fractional transport of gravel by renormalizing sediment mixture removing fine sediment from it (as proposed by Parker, 1990), and later on modified by Wilcock and Crowe (2003) to include fine sediment and its effect on the mobility of gravels.

We recommend the latter approach, since the former one produces complexity due to the uncertainty on hiding-exposure function and armouring effect. Latter approach is more reliable and straightforward as it is based on observations on graded sediment transport.

The formula of Wilcock-Crowe (2003) will be used which allows to include the finer sediment as well (unlike Parker's relation) as well as exposure effect of sand content through a correction to Shields number (it is postulated that sand content up to 30% causes the higher mobility of surface gravel fractions).

This approach is similar to Parker's approach (1990), but includes sand fraction as well as reduction of critical shear stress (precisely saying, reference shear stress for geometric mean size,  $\tau_{ssrg}^*$ ) with respect to the sand content (which is considered to be less than 30% of the total mixture). They proposed an exponential function for reduction of reference shear stress.

The relations read as follows:

$$W_i^* = G(\phi_i) \quad (2.1)$$

with

$$G(\phi) = \begin{cases} 0.002\phi^{7.5} & \text{for } \phi < 1.35 \\ 14 \left( 1 - \frac{0.894}{\phi^{0.5}} \right)^{4.5} & \text{for } \phi \geq 1.35 \end{cases} \quad (2.2)$$

Where  $W_i^*$  = the dimensionless bed load transport parameter (for i-th fraction); and defined by:

$$W_i^* = \frac{(s-1)gq_{bi}}{F_i u_*^3} \quad (2.3)$$

where  $s$  = ratio of sediment to water density;  $q_{bi}$  = volumetric transport rate per unit width (for  $i$ -th fraction);  $F_i$  = proportion of  $i$ -th fraction in filter material;  $u_*$  = shear velocity.

$\phi$  is defined as follows:

$$\phi_i = \frac{\tau_{sm}^*}{\tau_{ssrm}^*} \left( \frac{D_i}{D_{sm}} \right)^{-b} \quad \text{with } b = \frac{0.67}{1 + \exp(1.5 - D_i / D_{sm})} \quad (2.4)$$

where,  $\tau_{sm}^*$  = Dimensionless bed shear stress;  $\tau_{ssrm}^*$  = Dimensionless reference shear stress; and  $D_{sm}$  = mean diameter

$D_{sm}$  is defined as arithmetic mean  $D_{sm} = \sum D_i F_i$ , where  $D_i$  is  $i$ -th particle diameter and  $F_i$  is proportion of  $i$ -th fraction (Parker proposed to use geometric mean; however herein we used arithmetic mean).

Dimensionless bed shear stress can be calculated as:

$$\tau_{sm}^* = \frac{u_*^2}{(s-1)gD_{sm}} \quad (2.5)$$

The reference shear stress is calculated as:

$$\tau_{ssrm}^* = 0.021 + 0.015 \exp(-20F_s) \quad (2.6)$$

where  $F_s$  denotes the sand fraction in gravel mixture.

### Calculation procedure with example

#### Step 1

Grain-size characteristic of filter material: Calculation of fractional size ( $D_i$ ) and proportion ( $F_i$ )

Graded sediment characteristics, i.e. sieve analysis or fractional content should be given. A brief grain characteristic is given in Table:

Table 2.1 Grain characteristics

Range, mm	$\mu (D_{bi}), mm$	% finer
0.25~0.6	0.4	15
10~20	15	50
60~150	100	85

However, for a proper consideration we expand this data in a wider range by linearly interpolating/extrapolating the given values (Table 2.2 and Figure 2.1):

Table 2.2 Extended grain-size distribution characteristics

$D_{bi}$ , mm	% finer
0.25	0
0.4	15
1	17
2	19
10	38
15	50
40	60
60	68
75	75
100	85
150	100

For the reasons of comparison, we use two approaches: the first approach is to exclude the fine sediment ( $d < 2$  mm) and renormalize the grain-size distribution and fractional content as proposed by Parker (1990), and the second approach is to include all sediment size.

In case of renormalization, the fraction content increases depending upon the proportion of gravel fraction ( $F_g$ ), i.e. renormalized  $F_i = F_i/F_g$ . On the basis of increased fraction content, grain-size curve can be modified (this leads to the increment of median grain size of the mixture).

Calculation result of fractional diameter and fractional content (proportion) for both cases is presented in Table 2.3 and 2.4 respectively. Both initial and renormalized grain-size distribution curve is shown in Figure 2.1.

Table 2.3 Calculation of fractional diameter and proportion considering all sediment fraction

$D_{bi}$ , mm	$D_i$	% finer	$F_i$
150		100	
	122.47		0.15
100		85	
	86.60		0.1
75		75	
	67.08		0.07
60		68	
	48.99		0.08
40		60	
	24.49		0.1
15		50	
	12.25		0.12
10		38	
	4.47		0.19
2		19	
	1.41		0.02
1		17	
	0.63		0.02
0.4		15	
	0.32		0.15
0.25		0	

		Fraction gravel ( $F_g$ ) =	0.81
		Fraction sand ( $F_s$ ) =	0.19

Table 2.4 Calculation of fractional diameter and proportion excluding finer fraction (<2 mm)

$D_{bi}$ , mm	% finer	$F_i$
2	0	
10	23.5	0.23
15	38.3	0.15
40	50.6	0.12
60	60.5	0.10
75	69.1	0.09
100	81.5	0.12
150	100.0	0.19

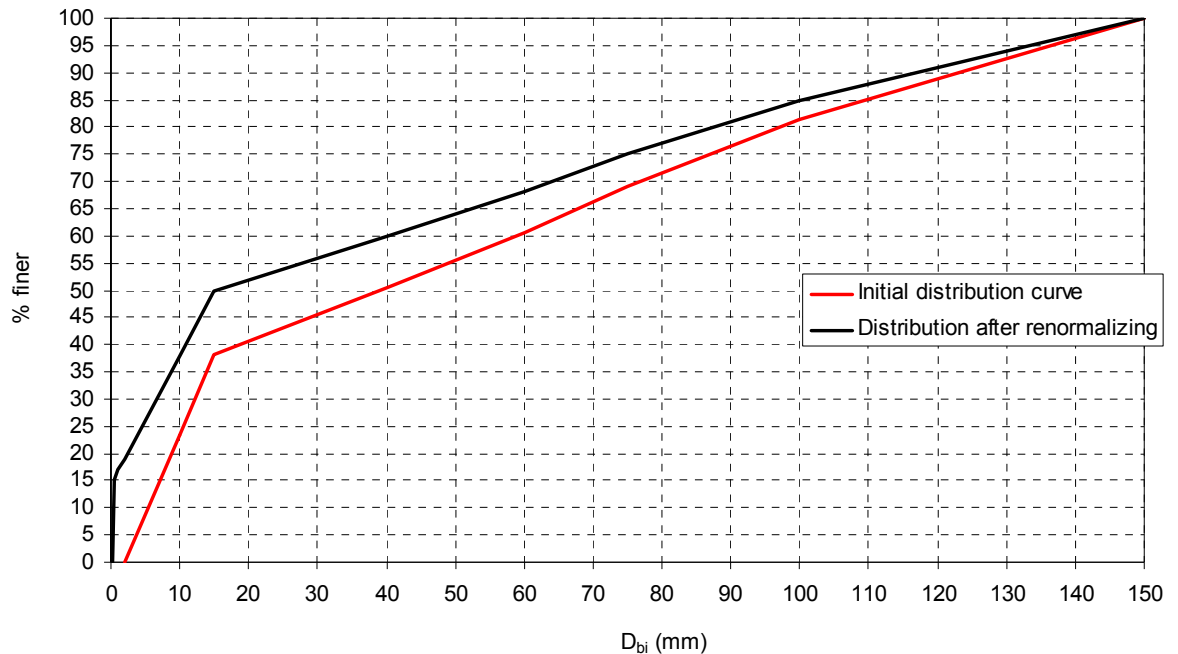


Figure 2.1 Grain size distribution including and excluding finer sediment

**Step 2**

Calculation of fractional transport

- For the example given here, we assume  $u^* = 0.15$  m/s (which is a characteristic value for a Dutch river during high flow). Otherwise, this can be calculated for the given flow condition.
- $D_{sm}$  ( $= \sum D_i F_i$ ) is equal to 40.5 and 49.9 mm for the cases of including and excluding finer sediment respectively.
- For comparison, we considered the sand content  $F_s$  to be 0 and 0.2 (as shown by grain characteristics). Using Eq. (2.6) results in the following values of dimensionless reference shear stress ( $\tau_{ssrm}^*$ ):  
 $\tau_{ssrm}^* = 0.036$  (if  $F_s = 0$ ), and  $\tau_{ssrm}^* = 0.021$  (if  $F_s = 0.2$ )
- Having known  $D_{sm}$  and  $u^*$ ,  $\tau_{sm}^*$  can be calculated using Eq. (2.5):  $\tau_{sm}^* = 0.034$  (same for both cases).

- Calculate  $b$  and  $\phi_i$  using Eq. (2.4) and then  $W_i^*$  for each (i-th) fraction can be calculated by using Eq. (2.1).
- Knowing  $W_i^*$ , bed load transport rate for each fraction ( $q_{bi}$ ) can be calculated using Eq. (2.3).
- From  $q_{bi}$ , daily transport per unit width for each fraction ( $Q_{bi}$ ) can be calculated:  
 $Q_{bdi} = q_{bi} * 3600 * 24$

A comparison on daily transport rate of each fraction is given in Figure 2.2 to Figure 2.4. Figure 2.2 and 2.3 show that the effect of sand content on the mobility of gravel fraction leads to the increased transport rate for all fraction for both cases (with and without finer sand). From Figure 2.4, it is evident that the consideration of all fraction gives higher transport than the case of excluding the finer sediment (i.e. after renormalization). Consequently, to be in the safe side, it is better to consider all sediment size (i.e., without excluding finer sand size < 2 mm) and also the effect of fine sand on gravel transport rate as it gives higher transport.

Knowing the total volume of filter material per width and the transport rate of each fraction, total period for the removal of certain fraction from the mixture can easily be calculated.

Let's assume that the total volume of filter material per unit width ( $V$ ) is  $100 \text{ m}^3/\text{m}$ . Then the volume of each fraction ( $V_{fi}$ ) can be calculated by multiplying total volume to the proportion of each fraction (i.e.,  $V_{fi} = V * F_i$ ). Knowing the daily transport rate of each fraction, time to erode ( $T_{edi}$ ) each fraction can be calculated (i.e.,  $E_{di} = V_{fi} / Q_{bdi}$ ). Results for both cases are depicted in the Table 2.5 and 2.6. Results are shown for all cases mentioned above.

If we consider the worst case, we can see that the 85% of the filter layer mixture of  $100 \text{ m}^3/\text{m}$  will be eroded in less than 3 days. Increment of coarser fraction leads to the stability of the filter material (as can be seen from the result with excluding finer sediment and renormalizing gravel content).

Table 2.5 Calculation result of transport rate and eroding time (case with all farctions)

$D_i$ (mm)	$F_i$	$q_{bi} \text{ (m}^3/\text{s/m)}$		$Q_{bdi} \text{ (m}^3/\text{day/m)}$		$V_{fi}$ ( $\text{m}^3/\text{m}$ )	$T_{E_{di}} \text{ (days)}$	
		$F_s = 0$	$F_s = 0.2$	$F_s = 0$	$F_s = 0.2$		$F_s = 0$	$F_s = 0.2$
0.3	0.15	2.62E-06	1.58E-05	82.64	497.19	15.00	0.18	0.03
0.6	0.02	2.30E-07	1.70E-06	7.26	53.70	2.00	0.28	0.04
1.4	0.02	1.33E-07	1.31E-06	4.18	41.27	2.00	0.48	0.05
4.5	0.19	5.04E-07	8.25E-06	15.89	260.04	19.00	1.20	0.07
12.2	0.12	1.41E-07	3.47E-06	4.44	109.35	12.00	2.70	0.11
24.5	0.1	6.06E-08	1.98E-06	1.91	62.44	10.00	5.23	0.16
49.0	0.08	1.55E-08	7.20E-07	0.49	22.69	8.00	16.38	0.35
67.1	0.07	5.20E-09	2.69E-07	0.16	8.48	7.00	42.68	0.83
86.6	0.1	2.39E-09	1.24E-07	0.08	3.90	10.00	132.42	2.56
122.5	0.15	4.55E-10	2.35E-08	0.01	0.74	15.00	1046.05	20.24

Table 2.6 Calculation result of transport rate and eroding time (case with excluding finer fraction)

$D_i$ (mm)	$F_i$	$q_{bi} \text{ (m}^3/\text{s/m)}$		$Q_{bdi} \text{ (m}^3/\text{day/m)}$		$V_f$ ( $\text{m}^3/\text{m}$ )	$T_{E_{di}} \text{ (days)}$	
		$F_s = 0$	$F_s = 0.2$	$F_s = 0$	$F_s = 0.2$		$F_s = 0$	$F_s = 0.2$
4.5	0.23	1.5E-07	4.9E-06	0.0133	0.42	23.5	1760.7	55.7

12.2	0.15	4.3E-08	1.8E-06	0.0037	0.16	14.8	3963.6	94.6
24.5	0.12	2.0E-08	9.5E-07	0.0017	0.08	12.3	7303.4	151.1
49.0	0.10	6.2E-09	3.2E-07	0.0005	0.03	9.9	18340.6	354.9
67.1	0.09	2.7E-09	1.4E-07	0.0002	0.01	8.6	37691.0	729.4
86.6	0.12	1.6E-09	8.3E-08	0.0001	0.01	12.3	89243.9	1727.0
122.5	0.19	4.3E-10	2.2E-08	0.0000	0.00	18.5	493523.8	9550.4

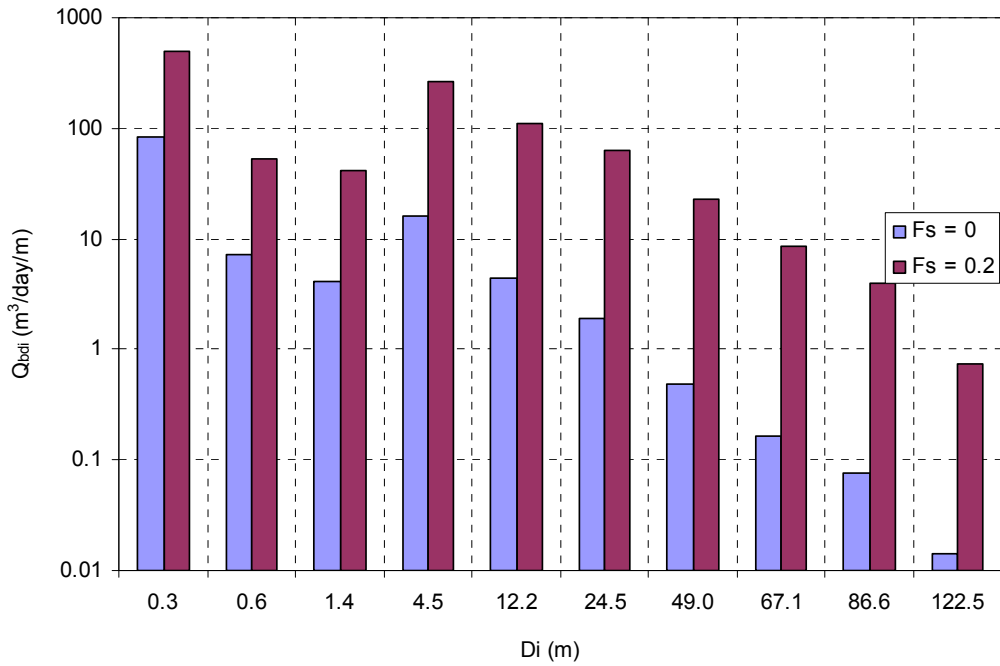


Figure 2.2 Comparison of daily transport of each fraction with and without effect of sand content (case including all fractions)

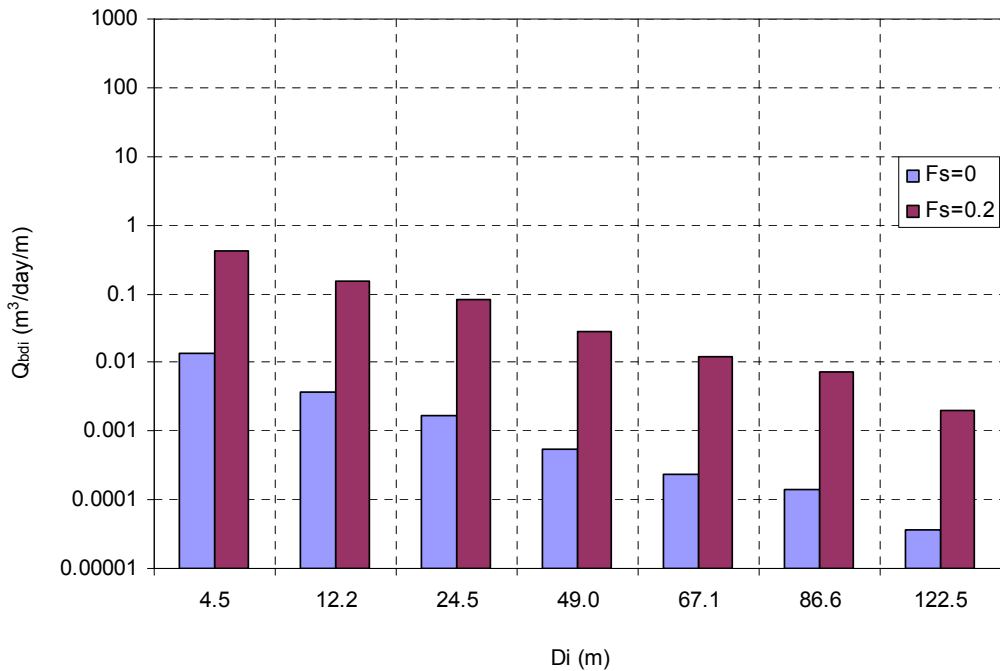


Figure 2.3 Comparison of daily transport of each fraction with and without effect of sand content (case exclusive finer fraction, i.e. < 2 mm)

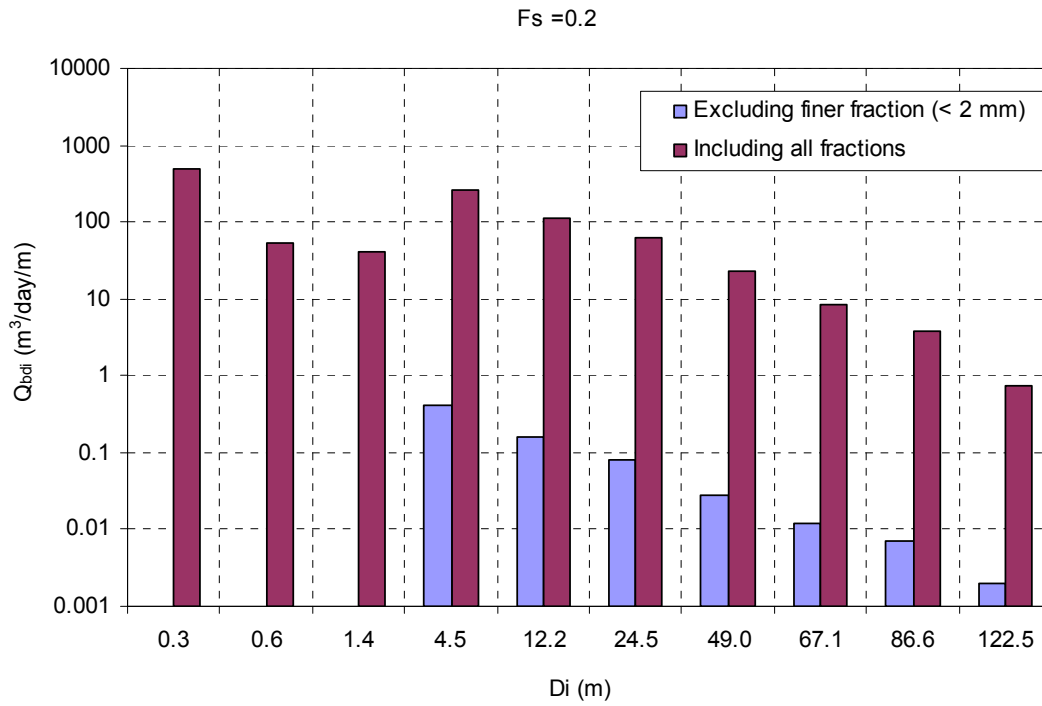


Figure 2.3 Comparison of daily transport of each fraction with and without finer fractions (For  $F_s = 0.2$ ).

## 7 Conclusions and recommendations

A desk study has been carried out to present the state-of-the-art of criteria for the interface stability of granular filter structures. In addition, the practicability of the criteria has been indicated and knowledge gaps and quick wins have been identified. Actually, the project focuses on two particular aspects:

1. interface stability as function of the thickness of the filter layer consisting of standard armourstone grading, and
2. Interface stability of mixtures with a wide gradation.

The study has brought an overview of the existing design formulas for interface stability for the above mentioned two aspects, including remarks which formulas need improvement or are even missing.

The study has resulted in a new filter criterion for geometrically-open sand-tight filter structures in a flow channel:

$$\frac{D_F}{d_{f50}} = 1.6 \ln \left( \frac{\alpha_k d_{f50}}{d_{b50}} \right) \quad (3.37)$$

The formula includes grading effects (parameters  $V_{Gf}$  and  $V_{Gb}$  for filter and base material respectively) as well as interface stability as a function of filter layer thickness (parameter  $D_F$ ).

It is recommended to validate the new filter design formula in a hydraulic model.

Moreover, knowledge gaps have been defined and prioritized. An assessment of quick wins has been made in order to define short and long term research. Short term research, a desk study, may give quick wins for the hydraulic gaps 1, 4, 5 and 9 (see Table 4.1). Long term research, physical model tests, is needed for the high priority knowledge gaps 2, 3, 7 and 10. Furthermore, it is recommended to carry out a literature inventory to knowledge gaps with respect to interface stability under wave attack.



## 8 Literature

- Adel, den H., 1986. *Analysis of permeability measurements using Forchheimer's equation (in Dutch)*, Report CO-272550/6, GeoDelft, Delft.
- Adel, den H., M.A. Koenders and K.J. Bakker, 1994. *The analysis of relaxed criteria for erosion-control filters*. J. of Canadian Geotech. 31
- Bakker, K.J., Verheij, H.J., and Groot, de M.B., 1994. *Design relationship for filters in bed protection*, J. of Hydraulic Engineering, 120(9), 1083-1088.
- Bezuijen, A., and Köhler, H.-J., 1998. *Filter and revetment design of water imposed embankments induced by wave and draw-down loadings*, in: K.W. Pilarczyk (Ed.) *Dikes and Revetments*, Balkema, Rotterdam.
- Broekens, R.D., 1991. *Transport of base material in granular filter, influence of side slopes on filter material (in Dutch)*, Report H869, Delft Hydraulics, Delft.
- Chin, C.O., B.W. Melville and A.J. Raudkivi, 1994. *Streambed Armoring*. J. of Hydraulic Engineering, Vol 120, no 8, ASCE, August 1994
- CUR, 1993. *Filters in de waterbouw*. Report 161, Gouda (in Dutch)
- Dixen, F.H., Sumer, B.M. and Fredsoe, J., 2008: *Suction removal of sediment from between armor blocks. II: waves*. J. of Hydraulic Engineering, Vol 134, no 10, October 2008, ASCE.
- Egiazaroff, I.V., 1965. *Calculation of non-uniform sediment concentrations*, Proc. ASCE, 91(HY4), pp 225-247.
- Emmerling, A., 1973, *The instantaneous structure of the wall pressure under a turbulent boundary layer flow (in German)*, Max-Planck-Institut für Strömungsforschung, Bericht 9, Göttingen, Germany
- Graauw, de A., Meulen, van der T., Does de Bye, van der M., 1983. *Design criteria for granular filters*, Publication No. 287, Delft Hydraulics, Delft.
- Graf, W.H., 1998. *Fluvial Hydraulics, Flow and transport processes in channels of simple geometry*, Wiley, Chichester, England.
- Grass, A.J., 1970. *Initial instability of fine bed sand*, Hydraulic Division, Proc. of the ASCE, 96, (HY3), 619-632.
- Heibaum, M. H., 2002. *Geotechnical Parameters of Scouring and Scour counter measures*. Mitteilungsblatt der Bundesanstalt für Wasserbau nr. 85, Karlsruhe

- Heibaum, M.H., 2004. *Geotechnical filters – The important link in scour protection*, Proc. of 2<sup>nd</sup> ICSE, Singapore.
- Hoffmans, G.J.C.M., 1993. *A study concerning the influence of the relative turbulence intensity on local-scour holes*, Rep. W-DWW-93-251, Ministry of Transport, Public Works and Water Management, Rijkswaterstaat, Delft.
- Hoffmans, G.J.C.M., Adel, den H., Verheij, H., 2000. *Shear stress concept in granular filters*, Proc. of an Int. Symp. organised by TC 33 of ISSMGE, Melbourne.
- Hoffmans, G.J.C.M., 2006. *Stability of stones under non-uniform flow*, Rep. DWW-2006-085, Ministry of Transport, Public Works and Water Management, Rijkswaterstaat, Delft.
- Huijstee, van, J.J.A., and Verheij, H.J., 1991. *Design relations for granular filters in bed protections (in Dutch)*, Report Q572, Delft Hydraulics, Delft.
- Kenney, T.C. and Lau, D., 1985. *Internal stability of granular filters*, Canadian Geotechnical Journal 22, 215-255.
- Klein Breteler M., 1989. *Sand transport in granular filters, horizontal and steady flow (in Dutch)*, Report H869, Delft Hydraulics, Delft.
- Klein Breteler, M., 1992. *Talusbekledingen van gezette steen, ontwerpregels voor het filter (in Dutch)* Delft Hydraulics, Rapport M1795;/H195;CO287270/30, deel XXI, June 1992, Delft.
- Koenders, M.A., 1985. *Hydraulic criteria for filters*, Estuary Physics, Physical modelling consultants, Surrey, UK.
- Köhler, H.J and A. Bezuyen, 1994. *Permeability of filter layers on stability of riprap revetments under wave attack*. 5<sup>th</sup> Intern. Conf. on Geotextiles, Geomembranes and Related Products, Singapore, 5-9 September 1994
- Lauchlan, C.S. and B.W. Melville, 2001. *Riprap protection at Bridge Piers*. J. of Hydraulic Engineering Vol 127 no 5, May 2001, ASCE
- Locke, M., B. Indraratna and G. Adikari, 2001 *Time-dependent particle transport through granular filters*. J. of Geotechnical and Geoenvironmental Engineering 127 (6)
- Lu, S.S., Willmarth, W.W., 1973. *Measurements of the structure of the Reynolds stress in a turbulent boundary layer*, J. of Fluid Mechanics, 60(3), 481-511.
- Meulen, van der, T., 1983. *Granular filters, Flow perpendicular to the interface (in Dutch)*

---

Report M898 part 3, Delft Hydraulics, Delft.

Meulen, van der, T., 1984. *Granular filters, Flow parallel to the interface (in Dutch)*,  
Report M898 part 4, Delft Hydraulics, Delft.

Ockeloen, W.J., 2007. *Open filters in breakwaters with a sand core*  
Delft University of Technology, MSc thesis, Delft

PIANC, 1987. *Guidelines for the design and construction of flexible revetments  
incorporating geotextiles for inland waterways*,  
Report WG 4, PTC I, Supplement to Bulletin No. 57, Brussels, Belgium.

PIANC, 1992. *Guidelines for the design and construction of flexible revetments  
incorporating geotextiles in marine environment*,  
Report WG 21, PTC II, Supplement to Bulletin No. 78/79, Brussels, Belgium.

Pilarczyk, K.W. (editor), 1990. *Coastal Protection*  
Balkema, Rotterdam.

Pilarczyk, K.W. (editor), 1998. *Dikes and revetments*  
Balkema, Rotterdam.

Rodi, W., 1984. *Turbulence models and their application in hydraulics, A state of the art  
review*,  
IAHR monograph, Balkema, Rotterdam.

Sellmeijer, J.B., 1988. *On the mechanism of piping under impervious structures*,  
Publication No. 96, GeoDelft, Delft.

Sherard, J.L. and L.P. Dunnigan, 1989. *Critical filters for impervious soils*.  
J. of Geotechnical Engineering, Vol 115, No 7, July 1998, ASCE

Shields, A., 1936. *Anwendung der Aehnlichkeitsmechanik und der Turbulenzforschung  
auf die Geschiebebewegung (in German)*,  
Mitteilungen der Preussischen Versuchsanstalt für Wasser-bau und Schiffbau, Heft  
26, Berlin NW 87.

Shimizu, Y., Tsujimoto T., Nakawaga, H., 1990. *Experiment and macroscopic  
modelling of flow in highly permeable porous medium under free surface flow*,  
J. of Hydrosience and Hydr. Engineering, 8(1), 69-78.

Silveira, A., 1965. *An analysis of the problem of washing through in protective filters*.  
Proc. 6<sup>th</sup> Int. Conf. Soil Mechanics and Found. Engrg, ICSMFE, Montreal, Canada,  
Vol. 2, pp 551-555 (1965).

Sumer, B.M., Cokgor, S. and Fredsoe, J., 2001: *Suction removal of sediment from  
between armor blocks*.  
J. of Hydraulic Engineering, Vol. 127, No 4, April 2001, ASCE.

Terzaghi, K., and Peck, R., 1948. *Soil mechanics in engineering practice*, Wiley & Sons,  
New York.

- 
- Uelman, E.F., 2006. *Geometrically open filters in breakwaters*  
Delft University of Technology, MSc thesis, Delft
- Verheij, 1999. *Analysis and prediction potential of new design formulas for granular filters*  
Delft Hydraulics, report Q2506, Delft.
- Verheij, H.J., Adel, den, H., and Petit, H., 2000. *Design formulas for granular filters*,  
Delft Hydraulics, Report Q2629, Delft.
- Verheij, H.J. 2003. *Stroming in granulaire filters (in Dutch)*  
Delft Hydraulics, report Q2331, Delft
- Wenka, T. and H.J.Köhler, 2007. *Simultane Druck- und 3D-Geschwindigkeitsmessungen im Porenraum einer Kiessohle.*  
Mitteilungsblatt der Bundesanstalt für Wasserbau nr. 90, Karlsruhe.
- Wörman, A., 1989. *Riprap protection without filters*,  
J. of Hydraulic Engineering, 115 (12), p. 1615-1630.
- Wörman, A., 2001. *Stochastic analysis of internal erosion in soil structures – Implications for risk assessments.*  
J. of Hydraulic Engineering, 127 (5), May 2001, ASCE.

**Paper presented at the Fourth International Conference  
on Scour and Erosion, ICSE-4, Tokyo, 5-7<sup>th</sup> November  
2008**

# HORIZONTAL GRANULAR FILTERS

Gijs HOFFMANS<sup>1</sup>, Henk den ADEL<sup>2</sup> and Henk VERHEIJ<sup>3</sup>

<sup>1</sup>Member of ISSMGE, Hydraulic Specialist, Deltares  
(P.O. Box 177, 2600 MH Delft, The Netherlands)  
E-mail: gijs.hoffmans@deltares.nl

<sup>2</sup>Geotechnical Specialist, Deltares  
E-mail: henk.denadel@deltares.nl

<sup>3</sup>Lecturer, Delft University of Technology & Deltares  
E-mail: henk.verheij@deltares.nl

This study investigate s the stability of horizontal granular filters which protect the underlying soil, i.e., the base layer, from erosion by static and fluctuating loads. The head usually characterizes the static load over hydraulic structures, whereas the fluctuating load represents turbulence caused by the geometry of hydraulic structures or by the roughness of the top layer. The erosion resistance or strength of granular filters is mainly characterised by the geometrical properties of the materials used. In general, two types of granular filters can be distinguished, namely geometrically closed and geometrically open filters. Here filter equations based on accepted theories are discussed for laminar and turbulent flow in horizontal filters. When the top layer is influenced by bed turbulence generated in open channel flow, also filter equations are derived.

*Key Words : Granular Filters, Laminar Flow, Open Channel Flow, Turbulence, Turbulent Flow*

## 1. INTRODUCTION

Typically, granular filter elements (stone, gravel and sand) are robust and give a good contact inter- face between the filter and base layers. Granular fil- ters could smoothen bed irregularities and thus pro- vide a more uniform construction base. Moreover, they are easy to repair and sometimes they may be self-healing. The major disadvantage of granular fil- ters is the difficulty of assuring uniform construction underwater to obtain the required thickness of the filter layers.

Granular filters protect the underlying soil, i.e. the base layer, from erosion by static or mean hydraulic load and fluctuating loads. The head usually char- acterizes the static load over hydraulic structures, whereas the fluctuating load represents turbulence caused by the geometry of hydraulic structures or by the roughness of the top layer.

The erosion resistance or strength of granular filters is mainly characterised by the geometrical properties of the materials used. In a geometrically closed filter, the ratio between the largest and smallest particles is so small that the bigger particles block the

smaller ones. Geometrically open filters are characterised by particles that can erode through the filter layer.

Here equations are discussed for designing and testing horizontal filters, which are influenced by laminar or turbulent flow. Moreover, this study examines the effects of bed turbulence in filter layers.

## 2. HYDRAULIC MODELLING

To model static and fluctuating (hydraulic) loads various parameters can be used, for example, energy slope (or filter velocity), shear velocity (or shear stress), pressure fluctuations (or turbulent kinetic energy) and drag, lift and shear forces. The energy slope, shear velocity and pressure fluctuations can all be related to forces acting on particles.

Turbulence in open channel flow is generated close to the bed and in non-uniform flow turbulence is also caused by the geometry of hydraulic structures. The blunter the hydraulic structure and the rougher the bed, the higher the bed turbulence is. In granular filters water flows through open spaces and when the flow reattaches, small mixing layers occur generating turbulence. The vortices in these open spaces are much smaller than the vortices in open channel flow and thus contain less energy. The depth-averaged relative turbulence intensity ( $r_0$ ) in channel flow and the mean relative turbulence intensity ( $r_{0,f}$ ) in the filter layer are defined as

$$r_0 = \sqrt{k_0} / U_0 \quad \text{and} \quad r_{0,f} = \sqrt{k_{0,f}} / u_f \quad \text{with} \quad k_0 = \frac{1}{h} \int_0^h \frac{1}{2} (\sigma_u^2 + \sigma_v^2 + \sigma_w^2) dz \quad (1)$$

where  $h$  is the flow depth,  $k_0$  is the depth-averaged turbulent kinetic energy in open channel flow,  $k_{0,f}$  is the mean turbulent kinetic energy in the filter layer,  $u_f$  is the filter velocity,  $U_0$  is the depth-averaged flow velocity in open channel flow and  $\sigma_u$ ,  $\sigma_v$  and  $\sigma_w$  are the standard deviations of the fluctuating flow velocities in the  $x$  (= longitudinal),  $y$  (= transverse) and  $z$  (= vertical) direction respectively. For uniform flow  $r_0 = 1.21g^{0.5}/C$  where  $C$  is the Chézy coefficient and  $g$  is the acceleration due to gravity.

To determine  $u_f$  and its critical value ( $u_{c,f}$ ), the Forchheimer equation and an equation similar to Chézy are applied. When granular filters are influenced by bed turbulence from channel flow the load is described using the shear stress approach of Grass (1970) and an equation for the decrease of the pressure in the filter layer as proposed by Bezuijen and Köhler (1998).

Forchheimer found a relation between the mean energy slope ( $S$ ) and  $u_f$  which is non-linear at sufficiently high velocities. This non-linearity increases with  $u_f$  and is caused by turbulent effects of the flow in the filter

$$S = au_f + bu_f^2 \quad (2)$$

in which  $a$  [s/m] and  $b$  [s<sup>2</sup>/m<sup>2</sup>] are dimensional coefficients. The Forchheimer equation assumes that Darcy's law is still valid. However, an additional term is added to account for the increased  $S$ . Based on permeability measurements, Den Adel (1986) found for the coefficients  $a$  and  $b$

$$a = 160 \frac{\nu (1 - n_f)^2}{g n_f^3 d_{f15}^2} \quad \text{and} \quad b = \frac{2.2}{gn_f^2 d_{f15}} \quad (3)$$

where  $d_{f15}$  is the particle (or grain) diameter in the filter layer for which 15% of the particles is finer than  $d_{f15}$ ,  $n_f$  is the porosity of the filter and  $\nu$  is the kinematic viscosity. The predictability of  $S$  in Eq. 2 applying  $a$  and  $b$ , lies in the range of  $1/3 < \zeta < 3$  where  $\zeta$  is the ratio of the measured and calculated  $S$ .

### 3. INCIPIENT MOTION

Particle transport occurs when there is no balance between load and strength. When the load is less than some critical value, particles remain motionless and can be considered as fully stable. But when load exceeds its critical value, particle motion begins. The initiation of motion is difficult to define, which can mainly be ascribed to phenomena that are random in time and space.

When dealing with particle stability in granular filters, the exact shape of the distribution of both load and strength are irrelevant because a characteristic load<sup>1</sup> ( $\tau_{0,k}$ ) and a characteristic strength<sup>1</sup> ( $\tau_{G,k}$ ) can be defined. A characteristic value is a value that is higher or lower than the mean value. Usually characteristic values are expressed as a mean value and a fraction or manifold of the standard deviation. Consequently, the problem of particle stability could be transferred to the magnitude of this fluctuation. Using the hypothesis of Grass (1970), which is based on statistical assumptions for both  $\tau_{0,k}$  and  $\tau_{G,k}$  read (Fig. 1)

$$\text{characteristic load: } \tau_{0,k} = \tau_0 + \gamma\sigma_0 \tag{4}$$

$$\text{characteristic strength: } \tau_{G,k} = \tau_G - \gamma\sigma_G \tag{5}$$

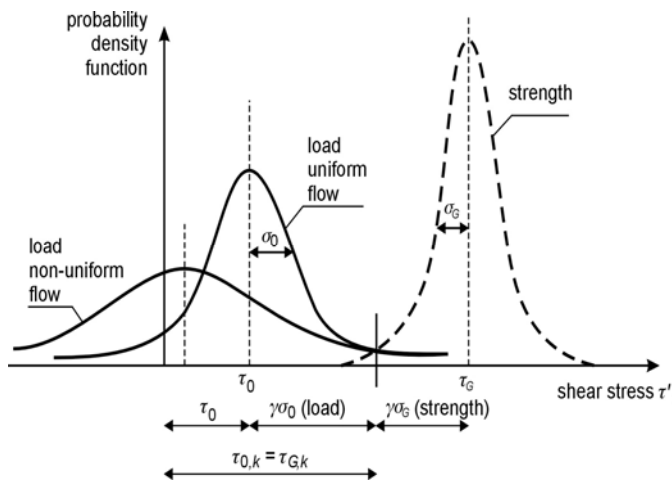


**Fig. 1** Probability functions of load and strength (Grass 1970)

where  $\gamma$  is determined by an allowable transport of the bed material,  $\sigma_0$  is the standard deviation of  $\tau_{0,k}$ ,  $\sigma_G$  is the standard deviation of  $\tau_{G,k}$ ,  $\tau_0$  is the mean load (or mean bed shear stress) and  $\tau_G$  is the mean strength (or critical mean bed shear stress) as given by Grass.

If  $\tau_{0,k} = \tau_{G,k}$  and  $\sigma_G = V_G \tau_G$  with  $\tau_G = \Psi_G \Delta \rho g d_{50}$  (analogous to Shields), a general equation for the filter layer (or top layer) follows

$$\Delta_f d_{f50} = \frac{\tau_0 + \gamma\sigma_0}{\Psi_{Gf} \rho g (1 - V_{Gf} \gamma)} \tag{6}$$

where  $d_{f50}$  is the mean particle diameter of the filter layer,  $V_{Gf}$  is the variation coefficient that represents the influence of the non uniformity of the filter layer,  $\Delta_f (= \rho_s/\rho - 1)$  is the relative density of the filter material,  $\rho$  is the density of the water,  $\rho_s$  is the density of the filter material and  $\Psi_{Gf}$  is related to the critical Shields parameter ( $\Psi_c$ ).

<sup>1</sup> Under channel flow conditions,  $\tau_{0,k}$  and  $\tau_{G,k}$  are the instantaneous bed shear stress and the critical instantaneous bed shear stress respectively.

A specific transport will occur if  $\tau_{0,k} = \tau_{G,k}$ . For uniform flow,  $\sigma_0 \approx 0.4\tau_0$ , Grass found that a bed of nearly uniform sand,  $V_{Gf} \approx 0.3$ , was completely stable for  $\gamma = 1$  and for  $\gamma = 0$  a significant transport of sediment particles was observed. Based on his tests, he reported that for  $\gamma = 0.625$  and using  $\Psi_{Gf} = 1.5\Psi_c$  the criterion of Shields (or Rouse curve) was met for the initial movement of sands up to a size of 250  $\mu\text{m}$ .

#### 4. HORIZONTAL FILTERS WITHOUT BED TURBULENCE

When the water flows parallel to the interface, the gradient in both layers is about the same, causing  $u_f$  in the filter layer to be much higher than in the base layer, because of the greater hydraulic conductivity. At the interface there will be a velocity gradient, inducing a shear stress at the upper fines in the base layer. Van der Meulen (1984), Klein Breteler (1989) and Broekens (1991) conducted flume experiments in which the flow was parallel to the filter and base layer. In these tests the flow was laminar as well as turbulent and no open channel flow above the filter was considered.

The critical filter velocity ( $u_{c,f}$ ) is a function of filter characteristics on the one hand and the critical bed shear velocity ( $u_{*c,bf}$ ) at the interface of filter and base layer on the other hand. Analogous to channel flow, i.e., using Chézy's equation,  $u_{c,f}$  could be written as

$$u_{c,f} = \frac{C_f}{\sqrt{g}} u_{*c,bf} \quad \text{with} \quad C_f = \alpha_{15} \sqrt{g} \left( \frac{d_{f15}}{d_{b50}} \right)^{1/6} \quad \text{and} \quad u_{*c,bf} = \sqrt{\Psi_{c,b} \Delta_b g d_{b50}} \quad (7)$$

where  $C_f$  is a coefficient [ $\text{m}^{0.5}/\text{s}$ ] representing the resistance in the filter layer,  $\alpha_{15}$  is a coefficient,  $\Delta_b$  is the relative density related to the base layer and  $\Psi_{c,b}$  is the critical Shields parameter related to  $d_{b50}$ . Combining Eqs. 2, 3 and 7 and considering laminar flow (thus  $\text{Re}_f = d_{f15} u_f / \nu < 1000$  and  $b = 0$  in Eq. 2) yields (Fig. 2)

$$S_{c,lam} = \alpha_L \frac{(1 - n_f)^2 \nu \sqrt{\Delta_b} (d_{b50})^{1/3}}{n_f^3 \sqrt{g} (d_{f15})^{5/6}} \quad \text{with} \quad \alpha_L = 160 \alpha_{15} \sqrt{\Psi_{c,b,lam}} \approx 65 \quad (8)$$

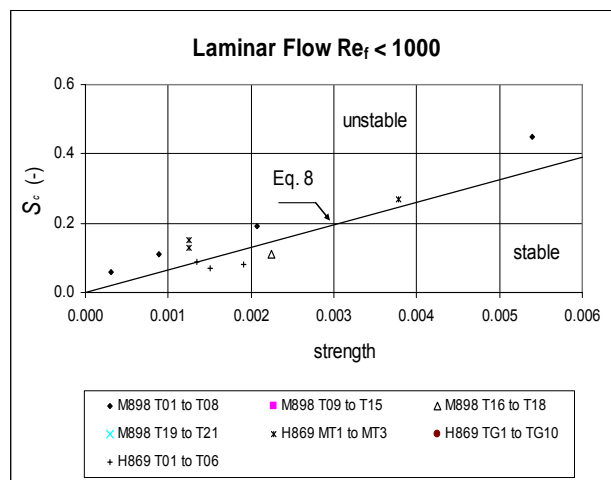


**Fig. 2**  $S_c$  as function of strength:  $\frac{(1 - n_f)^2 \nu \sqrt{\Delta_b} (d_{b50})^{1/3}}{n_f^3 \sqrt{g} (d_{f15})^{5/6}}$

Substitution of Eq. 7 in Eq. 2 with  $a = 0$ , Eq. 2 reads for turbulent flow, thus  $\text{Re}_f > 1000$  (Fig. 3)

$$S_{c,tur} = \alpha_T \frac{\Delta_b}{n_f^2} \left( \frac{d_{b50}}{d_{f15}} \right)^{2/3} \quad \text{with} \quad \alpha_T = 2.2\alpha_{15}^2 \Psi_{c,b,tur} \approx 0.1 \quad (9)$$

The Shields diagram shows that for laminar flow or for fines smaller than 0.1 mm,  $\Psi_{c,b,lam}$  could reach values up to 0.1. Assuming that  $\Psi_{c,b,lam} = 0.1$  and using Eq. 8,  $\alpha_{15} = 65/(160 \cdot 0.1^{0.5}) = 1.28$ . Substitution of  $\alpha_{15} = 1.28$  into Eq. 9,  $\Psi_{c,b,tur} = 0.1/(2.2 \cdot 1.28^2) = 0.03$ , which is in agreement with turbulent flow measurements.

According to Aguirre Pe (see Hoffmans 2006), who investigated the incipient motion of gravel ( $d_{f50} = 0.05$  m) under steep channel flow conditions ( $0.01 < S_c < 0.1$ ),  $r_0$  lies in the range of 0.3 to 0.6. In the tests carried out by Deltares,  $d_{f15}/d_{b50}$  varied from 50 to 300 giving  $8 < C_f < 10$  and  $0.4 < r_{0,f} (= 1.21g^{0.5}/C_f) < 0.5$ , so the order of magnitudes of  $r_{0,f}$  and  $r_0$  are the same, thus  $O(r_{0,f}) = O(r_0)$ .

As given by Koenders (1985), who used a fully different approach of solving the equilibrium of particles in granular filters,  $S_c$  is in the low and high gradient limit proportional to

$$S_{c,lam} \equiv \frac{(d_{b50})^{2/3}}{(d_{f15})^{2/3}} \quad \text{and} \quad S_{c,tur} \equiv \frac{d_{b50}}{(d_{f15})^{1/2}} \quad (10)$$

whence follows that Koenders results show similar proportions as in the proposed Eqs. 8 and 9.

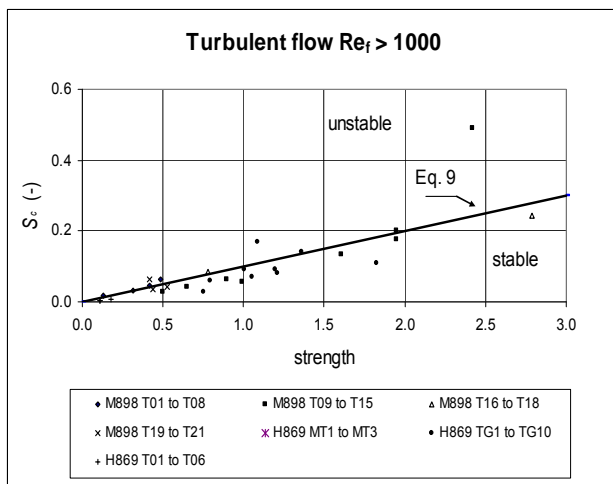


Fig. 3  $S_c$  as function of strength:  $\frac{\Delta_b}{n_f^2} \left( \frac{d_{b50}}{d_{f15}} \right)^{2/3}$

### 5. HORIZONTAL FILTERS INFLUENCED BY BED TURBULENCE

Hoffmans et al. (2000) discussed load in a horizontal one-layer filter with a thickness ( $D_F$ ) above the base material in open channel flow (Fig. 4). Equations for granular filters based on the Navier Stokes equation for uniform flow, Forchheimer’s equation and the hypothesis of Boussinesq are deduced and validated.

The distribution of  $\tau$  being defined as load in a one- layered filter is

$$\tau(z) = \tau_{bf} e^{-\zeta z} + \tau_0 e^{\zeta(z-D_F)} \quad \text{with} \quad \zeta = \sqrt{\frac{2gb}{\alpha_v d_{f15}}} \approx \frac{5.5}{d_{f15}} \quad (11)$$

where  $\zeta$  is a damping parameter and  $\tau_{bf}$  is the mean load at the interface of the filter-base layer. Similar to channel flow  $\tau_{bf}$  could be related to  $\tau_0$  as follows (see also Appendix A)

$$\tau_{bf} = \eta\tau_0 \quad \text{with} \quad \eta = 0.7r_{0,f}^2 \quad (12)$$

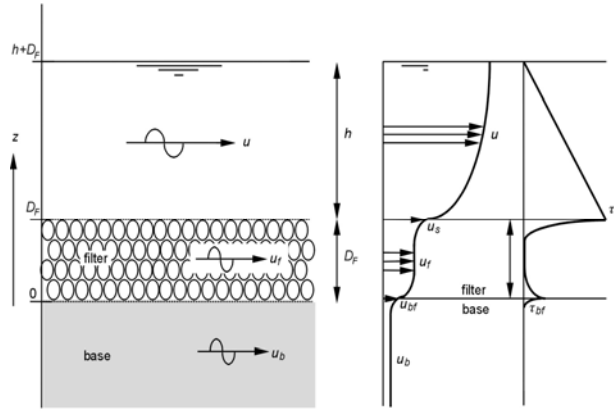


**Fig. 4** Overview of definitions for a one-layer filter

If either  $\tau_0$  or  $r_{0,f}$  increases,  $\tau_{bf}$  also increases which is in agreement with observations.

In a similar way equations can be derived for filters at the interface of the filter-base layer. Applying the hypothesis of Grass, the characteristic load ( $\tau_{bf,k}$ ) and the characteristic strength ( $\tau_{c,bf,k}$ ) of the base material at  $z = 0$  are

$$\tau_{bf,k} = \eta(\tau_0 + \gamma\sigma_0) \quad (13)$$

$$\tau_{c,bf,k} = \tau_{Gb} - \gamma\sigma_{cb} = \Psi_{Gb}\Delta_b\rho g d_{b50}(1 - \gamma V_{Gb}) \quad (14)$$

By combining Eqs. (6), (13) and (14), gives for geometrically open filters

$$\frac{d_{f50}}{d_{b50}} = \frac{1}{\eta} \frac{1 - \gamma V_{Gb}}{1 - \gamma V_{Gf}} \frac{\Psi_{Gb}}{\Psi_{Gf}} \frac{\Delta_b}{\Delta_f} \quad (15)$$

With Eq. (15) the influence of particle gradation on the stability of the base material can be explained in a qualitative way. For example, when the base material is more graded than the filter material, thus  $V_{Gb} > V_{Gf}$ , the required ratio  $d_f/d_b$  is less than the value in situations where base and filter materials do have the same gradation. If only the filter material is broadly graded, thus  $V_{Gb} < V_{Gf}$ , the maximum value of  $d_f/d_b$  is higher than for similarly graded materials. These predictions correspond with observations in flume experiments.

A widely graded base material has more fines than a more uniform material. The material in the filter layer has to prevent the erosion of the fines. This can only be achieved by reducing  $u_f$  or by putting more fines into the filter layers. A widely graded material in the filter layer has relatively more fines, which reduces  $u_f$  and so  $\tau_{bf}$ . Hence, the widely graded filter material is allowed to have a  $d_{f50}$  that is larger than for uniform material.

Van Huijstee and Verheij (1991) conducted tests where bed turbulence was generated under uniform flow. In addition, a distinction was made between simultaneous instability of base and top layer and instability of either top or base layer. In all these tests  $D_F/d_{f50}$  varied from 1.5 to 4.5 and the critical  $d_{f50}/d_{b50}$  obtained from tests ranged from 40 to 415. Figure 5

shows the critical  $[d_{f50}/d_{b50}]_{\text{measured}}$  when erosion occurs versus the critical  $[d_{f50}/d_{b50}]_{\text{computed}}$  assuming that  $\eta = 0.7(r_0)^2$  (or  $r_{0,f} = r_0$  see also section 4),  $V_{Gb} = V_{Gf}$  and  $\Delta_b = \Delta_f$

$$\left[ \frac{d_{f50}}{d_{b50}} \right]_{\text{computed}} = \frac{1}{0.7r_0^2} \frac{\Psi_{cb}}{\Psi_{cf}} \quad \text{with} \quad r_0 = 1.21\kappa \left( \ln \frac{6R_h}{d_{f50}} \right)^{-1} \quad (16)$$

where  $R_h$  is the hydraulic radius and  $\kappa$  ( $= 0.4$ ) is the constant of Von Kármán. Since most of the experiments consists of a thin filter layer, 100% of the measurements lie in the range of  $0.5 < \zeta < 2$ , where  $\zeta$  is the ratio between the measured and computed  $d_{f50}/d_{b50}$ .

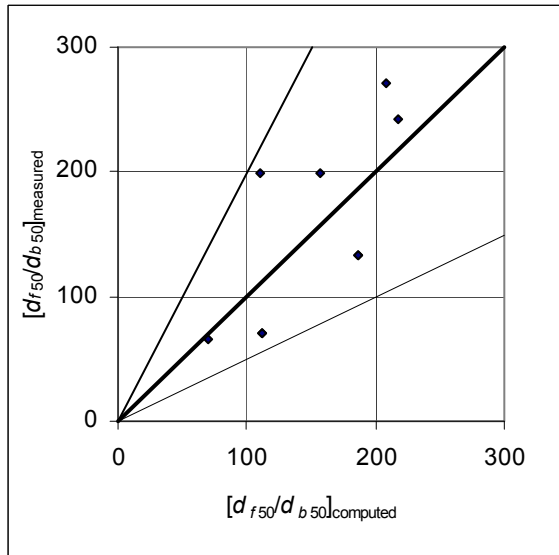


**Fig. 5**  $[d_{f50}/d_{b50}]_{\text{measured}}$  versus  $[d_{f50}/d_{b50}]_{\text{computed}}$   
Experiments in which simultaneous erosion occurs in filter and base layer (Van Huijstee and Verheij 1991)

For uniform equilibrium and non-uniform gradually varied flows,  $r_0$  ranges typically from  $r_0 = 0.042$  (or  $\eta = 0.0013$  for large smooth channel) up to  $r_0 = 0.126$  (or  $\eta = 0.0113$  for small rough channel). For steep channel flow and non-uniform flow when  $0.2 < r_0 < 0.5$ ,  $\eta$  lies in the range of 0.028 to 0.18. Hence, for very high turbulence intensities, say  $r_0 > 0.25$  geometrically closed filters are required, that is  $d_{f50}/d_{b50} < 25$  or  $\eta > 0.04$ .

Bezuijen and Köhler (1998) examined the stability of revetment structures, which is governed by the interaction between pore water on the one hand, and the top layer, filter layer and base layer on the other hand. Based on theoretical considerations they deduced an exponential equation for the pressure decrease, which is here expressed in terms of mean relative turbulence intensities

$$r_{0,f}^2 = r_0^2 \exp\left(-\frac{\chi D_F}{d_{f15}}\right) \quad (17)$$

where the order of magnitude of  $\chi$  is  $O(\chi) = 0.1$ . Hence,  $r_{0,f}$  not only depends on  $r_0$  but also on  $D_F$  and  $d_{f15}$ . Combining Eqs. 15 and 17 gives

$$\frac{D_F}{d_{f15}} = \chi^{-1} \ln\left(0.7r_0^2 \frac{d_{f50}}{d_{b50}} \frac{1-\gamma V_{Gf}}{1-\gamma V_{Gb}} \frac{\Psi_{cf}}{\Psi_{cb}} \frac{\Delta_f}{\Delta_b}\right) \approx \chi^{-1} \ln\left(0.7r_0^2 \frac{d_{f50}}{d_{b50}}\right) \quad (18)$$

Wörman (1989) investigated granular filters at bridge piers. Based on accepted theories he arrived at the following relation for one-single layer bed

$$D_F = 0.16 \frac{\Delta_f}{\Delta_b} \frac{n_f}{1-n_f} \frac{d_{f85}d_{f15}}{d_{b85}} \quad (19)$$

For nearly uniform-graded materials when  $d_{b85}/d_{b50} = d_{f50}/d_{f15} \approx 1.25$ ,  $n_f = 0.4$ , and  $\Delta_b = \Delta_f$ , Eq. 19 can be rewritten as

$$\frac{d_{f50}}{d_{b50}} = 11.7 \frac{D_F}{d_{f50}} \quad (20)$$

Figure 6 shows Wörman’s equation (Eq. 20), Eq. 18 as an envelop curve using  $\chi = 0.3$  and  $r_0 = 0.25$  as first approximations and experimental data from Van Huijstee and Verheij (1991), which all lie in the un- stable part of the diagram. The interesting section for designing and testing geometrically open filters in non-uniform flow is the stable part that lies above Wörman’s equation or above Eq. 18 and adjacent to the zone representing geometrically closed filters ( $d_{f50}/d_{b50} = 25$  or  $\eta = 0.04$ ).

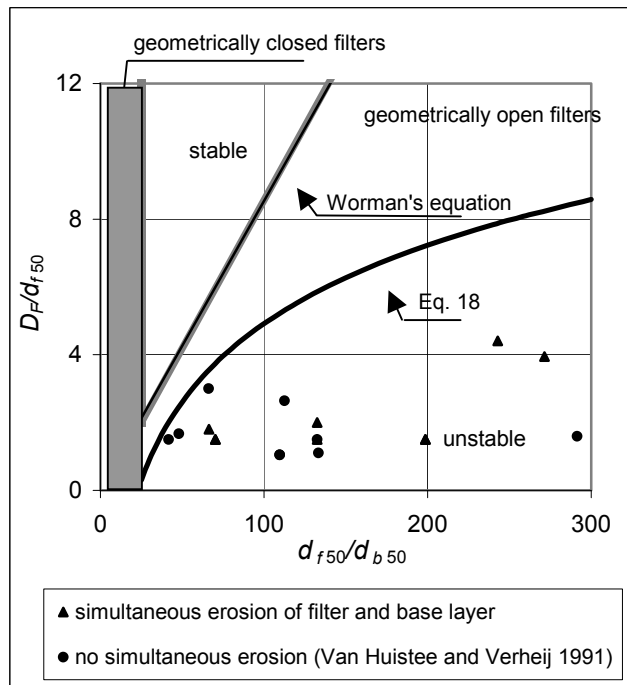


Fig. 6  $D_F/d_{f50}$  versus the critical  $[d_{f50}/d_{b50}]$ . In Eq. 18  $\chi = 0.3$  and  $r_0 = 0.25$  are first estimations.

## 6. CONCLUSIONS

For horizontal geometrically open filters without bed turbulence, equations that are based on the Forchheimer and Chézy equations are deduced and validated using flume experiments. The best guess predictors, Eqs. 8 and 9, are valid for laminar and turbulent flow respectively.

For horizontal geometrically open filters in which open channel flow is considered a filter equation is derived which is based on the shear stress approach as proposed by Grass. The influence of both the thickness of the filter layer (Eq. 17) and grading effects of the filter and base materials have been shown qualitatively. Although Eqs. 15 and 18 are validated using uniform flow tests, no validation has been carried out for non-uniform flow conditions.

Wörman's equation is validated applying data from filter layers around bridge piers where the flow is highly turbulent. However, the horseshoe vortices and the Kármán vortex streets are not representative for all types of non-uniform flow.

## APPENDIX A

The mean load at the interface of the filter-base layer and the mean bed shear stress are defined as

$$\tau_{bf} = \rho u_{*bf}^2 \quad \text{and} \quad \tau_0 = \rho u_*^2 \quad (\text{A1})$$

For open channel flow, Chézy's equation reads

$$u_* = U_0 \sqrt{g} / C = 0.83 r_0 U_0 \quad (\text{A2})$$

In the present study, Eq. A2 is used to model the resistance in the filter layer as

$$u_{*bf} = u_f \sqrt{g} / C_f = 0.83 r_{0,f} u_f \quad (\text{A3})$$

Substitution of Eqs. A2 and A3 in A1 gives

$$\tau_{bf} = \rho (r_{0,f} u_f)^2 \quad \text{and} \quad \tau_0 = 0.7 \rho (r_0 U_0)^2 \quad (\text{A4})$$

Assuming that  $u_* = u_f$ ,  $\eta$  is

$$\eta = \tau_{bf} / \tau_0 = 0.7 r_{0,f}^2 \quad (\text{A5})$$

## REFERENCES

1. Adel, den, H.: Analyse of permeable measurements using Forchheimer's equation, Report CO 272550/6 (in Dutch), Deltares, Delft, 1986.
2. Bezuijen, A., and Köhler, H.-J.: Filter and revetment design of water imposed embankments induced by wave and draw-down loadings. in: Dikes and Revetments, Edt. K.W. Pilarczyk, Balkema, Rotterdam, 1998.
3. Broekens, R.D.: Transport of base material in granular filter, influence of side slopes on filter material (in Dutch), Report H869, Deltares, Delft, 1991.
4. Grass, A.J.: Initial instability of fine bed sand, *Hydraulic Division, Proc. of the ASCE*, Vol. 96, HY3, pp. 619-632, 1970.
5. Hoffmans, G.J.C.M., Adel, den, H., Verheij, H.: Shear stress concept in granular filters, Proc. of an Int. Symp. Organised by TC 33 of ISSMGE, Melbourne, 2000.
6. Hoffmans, G.J.C.M.: Stability of stones under non-uniform flow, Rep. DWW-2006-085, Ministry of Transport, Public Works and Water Management, Rijkswaterstaat, Delft, 2006.
7. Huijstee, van, J.J.A., and Verheij, H.J.: Design relations for granular filters in bed protections (in Dutch), Report Q572, Deltares, Delft, 1991.
8. Klein Breteler, M.: Sand transport in granular filters, horizontal and steady flow (in Dutch), Report H869, Deltares, Delft, 1989.
9. Koenders, M.A.: Hydraulic criteria for filters, Estuary Physics, Physical modelling consultants, Surrey, UK, 1985.
10. Meulen, van der T.: Granular filters, Flow parallel to the interface (in Dutch), Report M898 part 4, Deltares, Delft, 1984.
11. Wörman, A.: Riprap protection without filters, *J. Hydraulic Engineering*, Vol. 115, No. 12, pp.1615-1630, 1989.